Dissertation

submitted to the

Combined Faculties for the Natural Sciences and for Mathematics

of the Ruperto-Carola University of Heidelberg, Germany

for the degree of

Doctor of Natural Sciences

presented by

Dipl.-Biol. Madeleine Meusburger

born in Innsbruck in 1980

Oral examination: 01. 09. 2008

Characterization of the Substrate Specificity of the Dnmt2 Methyltransferase

Referees: Prof. Dr. Harald Herrmann-Lerdon

Prof. Dr. Frank Lyko

List of Abbreviations

A	adenine
aa	amino acid
AdoHcy	S-adenosyl-homocysteine
Arg	arginine
Asp	aspartate
ATP	adenosine triphosphate
bp	base pair
BSA	bovine serum albumin
BWS	Beckwith-Wiedemann syndrome
C	cytosine
CpG	cytosine-phosphatidyl-guanosine
CE	Capillary Electrophoresis
cpm	counts per minute
d	deoxy
D.m.	*Drosophila melanogaster*
DNA	deoxyribonucleic acid
Dnmt	DNA methyltransferase
DEPC	di-ethyl-propyl carbonate
DTT	dithiothreitol
dNTP	deoxynucleotide triphosphate
ES	embryonic stem (cells)
FCS	Fetal Calf Serum
G	guanine
HEPES	4-(2-hydroxyethyl)-1-piperazineethanesulfonic acid
His	histidine
HPLC	High Performance Liquid Chromatography
H.s.	*Homo sapiens*
Hsp	heat shock protein
I	inosine
IAP	intracisternal A-particle
ICR	imprinting control region

Igf2	insulin-like growth factor 2
IP	immunoprecipitation
IPTG	isopropyl β-D-1-thiogalactopyranoside
kDa	kilo Dalton
LTR	long terminal repeat
mA	milli-Ampere
MBD 2/3	methylated CpG binding protein 2/3
m^5C	5-methyl-cytosine
mM	millimolar
M.m.	*Mus musculus*
MTase	methyltransferase
m^5U	5-methyl-uridine
Mg	Magnesium
MOPS	3-(N-morpholino)-propanesulfonic acid
miRNA	micro RNA
mRNA	messenger RNA
N	nitrogen
NLS	nuclear localisation signal
NTP	nucleotide-triphosphate
OrR	Oregon R
P.a.	*Pyrococcus abyssi*
PAGE	polyacrylamide-gel-electrophoresis
PBHD	polybromo homology domain
PC	proline-cysteine motif
PCNA	proliferating cell nuclear antigen
PCR	Polymerase Chain Reaction
piRNA	piwi-interacting RNA
PNK	Polynucleotide Kinase
Q	queuosine
RNA	ribonucleic acid
rpm	rounds per minute
rRNA	ribosomal RNA
RT-PCR	Reverse-Transcription-Polymerase-Chain-Reaction
s	seconds

S	Sulfur
SAH	S-adenosyl-homocysteine
SAM	S-adenosyl-methionine
S.c.	*Saccharomyces cerevisiae*
snoRNA	small nucleolar RNA
SRS	Silver-Russell syndrome
T	thymine
TEMED	N, N, N´, N´-tetramethylenediamine
Thr	threonine
TRD	target recognition domain
Tris	tris(hydroxymethyl)aminomethane
tRNA	transfer-RNA
Tyr	tyrosine
U	uridine
wt	wildtype

Zusammenfassung

Die Methylierung von Cytosin zu 5-methyl-Cytosin in DNA spielt eine wichtige Rolle in zahlreichen epigenetischen Regulationsprozessen. In Eukaryoten wird die Methylierungsreaktion von der Familie der DNA-Methyltransferasen (Dnmts) katalysiert. Das Dnmt2-Protein ist das am höchsten konservierte und das am weitesten verbreitete Mitglied dieser Enzymfamilie; jedoch blieb seine katalytische Funktion lange rätselhaft. Aufgrund von Strukturanalysen wurde die Vorhersage getroffen, dass Dnmt2 eine *bona fide* DNA-Methyltransferase sein sollte; jedoch konnte nur eine sehr geringe katalytische Aktivität von Dnmt2 in einem *in vitro* Methylierungsexperiment nachgewiesen werden. Kürzlich wurde allerdings entdeckt, dass Dnmt2 eine tRNA-Methyltransferase ist, welche die Position C38 in dem Anticodon-Loop von $tRNA^{Asp}$ methyliert.

Die vorliegende Arbeit trug zu der weiteren Charakterisierung des Enzyms in dem Modellorganismus *Drosophila melanogaster* bei. Eine Dnmt2-Nullmutante wurde charakterisiert und in DNA-Methylierungsanalysen mit Wildtyp-Fliegen verglichen. Dnmt2-abhängige DNA-Methylierung wurde an einer definierten Stelle im Fliegengenom gefunden: in der 3´-Region des *mini-white*-Markergens eines mobilen Elements, welches in das Retrotransposon Invader 4 gesprungen war.

In weiteren Experimenten konnte gezeigt werden, dass *in vitro* transkribierte, nicht modifizierte tRNAs als Substrate von Dnmt2 aus Mensch und Fliege akzeptiert werden, und dass demnach andere Modifikationen keine Voraussetzung für die Substraterkennung durch Dnmt2 darstellen. Neben $tRNA^{Asp}$ wurde $tRNA^{Val}$ als neues *in vivo* und *in vitro* Substrat von *Drosophila* Dnmt2 identifiziert. Die Optimierung und die vielseitige Anwendung der DNAzym-Methode ermöglichte die Quantifizierung des Methylierungssignals. Darüber hinaus konnten mehrere nicht-C38-enthaltende tRNAs aus verschiedenen Organismen von Dnmt2 *in vitro* methyliert werden. Als neue Methylierungsstellen wurden C40 in $tRNA^{Phe}$ aus *Saccharomyces cerevisiae* und C40 und C42 in $tRNA^{Lys}$ aus *Drosophila melanogaster* identifiziert. Die Analyse mehrerer katalytischer Mutanten von humanem Dnmt2 unter Verwendung verschiedener tRNA-Substrate zeigte zwei unterschiedliche katalytische Mechanismen auf.

Summary

The modification of cytosine to 5-methyl-cytosine within DNA plays an important role in epigenetic processes. In eukaryotes, the methylation reaction is catalyzed by the family of DNA methyltransferases (Dnmts). The Dnmt2 protein is the most conserved and most widely distributed member of the Dnmt family, however, its catalytic function has been an enigma. Structural analysis predicts the enzyme to be a *bona fide* DNA methyltransferase, though it exhibits only marginal DNA methylating activity *in vitro*. Recently, however, Dnmt2 was discovered to be a tRNA methyltransferase, catalyzing the formation of 5-methyl-cytosine at position 38 of $tRNA^{Asp}$ within the anticodon stem-loop.

This work contributed to the further characterization of the enzyme in the model organism *Drosophila melanogaster*. A null mutant was characterized and used for further DNA methylation analysis in comparison to Dnmt2-containing wildtype flies. Dnmt2-dependent DNA methylation was discovered at one defined locus in the fly genome: within the 3´-region of the *mini-white* marker gene of a mobile element which had inserted into the retrotransposon invader 4.

Further experiments could show that unmodified, *in vitro* transcribed tRNAs are targets of the Dnmt2 enzyme derived from fly and human, and that other modifications are not a prerequisite for Dnmt2 target recognition. Besides $tRNA^{Asp}$, $tRNA^{Val}$ was identified as a new target of Dnmt2 *in vitro* and *in vivo*. The optimization and versatile application of the DNAzyme technique allowed the quantification of the methylation signal. Furthermore, non-C38 containing tRNAs from various organisms were also found to be methylated by Dnmt2 *in vitro*. The new methylation site could be mapped to C40 in $tRNA^{Phe}$ from *Saccharomyces cerevisiae,* and to C40 and C42 in $tRNA^{Lys}$ from *Drosophila melanogaster*. The analysis of several catalytic Dnmt2 mutants of human Dnmt2 in combination with various tRNA substrates revealed two different catalytic mechanisms.

1 Introduction

1.1 DNA and RNA Modifications

The presence of non-canonical nucleotides in DNA was reported 60 years ago by Hotchkiss (Hotchkiss, 1948). Two years later, they were identified as 5-methyl-cytidine (Wyatt, 1950). Not long after, pseudouridine was detected as the "fifth ribonucleoside" in RNA (Cohn & Volkin, 1951; Davis & Allen, 1957; Cohn, 1960). In the following decades, the discovery rate of new modified nucleotides increased rapidly, culminating in presently more than 100 different modified nucleotides reported in RNA and four in DNA (Grosjean & Benne, 1998). By far the most nucleotide modifications have been identified in tRNA.

1.2 DNA Methylation

Methylation of DNA can occur at C5 and N4 of cytosine and N6 of adenine. N^4-methylcytosine is restricted to bacteria, and N^6-methyladenine can be found in bacteria, fungi, and simple eukaryotes such as green algae and ciliates. Only 5-methylcytosine (m^5C; see Fig. 1.1) is present in all three domains of life (reviewed in Cheng, 1995 and Wion & Casadesus, 2006). The functions of the methylation signal in DNA are diverse. In bacteria, for example, DNA adenine and cytosine methylation play an important role in the genome defense against bacteriophages. Hereby, methylation of the bacterial DNA is the crucial signal for genome identity or "self" (Murray, 2002). Unmethylated DNA will be recognized as an intruder and destroyed by endonucleolytic digestion. This interplay of a DNA methyltransferase conferring "self" and a restriction endonuclease recognizing and eliminating the unmethylated "non-self" DNA has been described as restriction-methylation system(s) (Murray, 2002). Other functions of bacterial methylation include for example methylation-guided mismatch-repair, chromosome replication and segregation (reviewed in Wion & Casadesus, 2006).

The role of m^5C DNA methylation in higher eukaryotes is much more complex and will be described in the following.

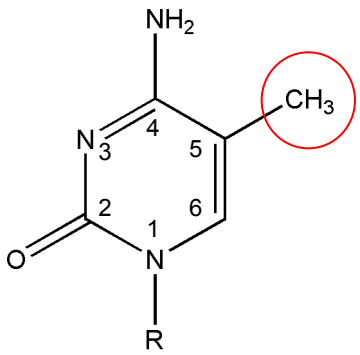

Fig. 1.1: Chemical structure of 5-methyl-cytosine (m^5C)
5-methyl-cytosine differs from canonical cytosine by the addition of a methyl group to the C5 atom of the pyrimidine ring (red circle). R stands for the hydrogen atom in 5-methyl-cytosine, and for the (deoxy)ribosyl-moiety in 5-methyl-cytidine.

1.3 Definition of Epigenetics

In higher eukaryotes, the presence of 5-methyl-cytidine in DNA is closely linked to epigenetic processes. The term epigenetics describes the phenomenon and the analysis of heritable changes in gene function that occur without a change in the DNA sequence. “Epi” is a prefix of greek origin meaning “upon” or “above”. Epigenetic research encompasses for example the state of modification of DNA and its degree of packaging in the context of chromatin. DNA is the information coding molecule of the cell, but besides the information itself, it is the accessibility of this information which is inherited and contributes to the regulation of gene expression. DNA methylation at the position 5 of cytosine in a CpG context and modification of histone tail residues by e.g. methylation, acetylation, and ubiquitinylation are the two key players which take part in the generation of epigenetic signals. The interplay between m^5C methylation of genomic DNA and a combination of histone tail modifications leads to loose or tight packaging of the nucleosomes, thereby creating transcription competent (euchromatin) or transcription incompetent chromatin (heterochromatin).

1.4 The Role of m^5C Methylation in Epigenetic Regulatory Processes in Higher Eukaryotes

m^5C methylation plays an important role throughout the development of an organism. Main functions of DNA methylation in higher eukaryotes are the silencing of retrotransposons and genes (reviewed in Bird, 2002; Yoder et al., 1997). The methylation of satellite sequences in pericentric regions contributes to heterochromatin formation and structural stabilization of the chromosomes. Furthermore, DNA methylation is involved in imprinting and X-chromosome inactivation in the process of dosage compensation in female mammals (Panning & Jaenisch, 1998; Feil & Khosla, 1999).

In animals, methylation occurs usually in the context of CpG dinucleotides. The term CpG islands was first mentioned in 1987 (Gardiner-Garden & Frommer, 1987) and was later refined to describe regions larger than 500 bp with a GC content equal to or greater than 55 % (Takai & Jones, 2002). CpG islands can be found in the promoter and exonic regions of about 40 % of all genes (Larsen et al., 1992) where they are usually unmethylated. However, in numerous cancers, the methylation of CpG islands in the promoters of tumor suppressor genes has been observed (Esteller & Herman, 2002). Therefore, aberrant DNA methylation has an important impact on cancer development.

1.5 RNA Modification

The number of observed RNA modifications is much higher compared to DNA. The most abundantly modified RNA species is transfer RNA (tRNA). RNA modifications have also been detected in ribosomal RNA (rRNA), messenger RNA (mRNA), and small RNAs like piwi-interacting RNAs (piRNAs), microRNAs (miRNAs), and small nucleolar RNAs (snoRNAs). The cellular function of RNA modifications still remains to be determined in many cases. So far, it is largely unclear why many modifications are so conserved yet lead to no obvious phenotype when absent.

1.5.1 Modifications in rRNA, mRNA and Small RNAs

In ribosomal RNA of higher eukaryotes, three different types of modification at over 200 sites have been reported: largely 2-O-methylation of the ribose ring, pseudouridine, and a few methyl groups at heterocyclic bases (reviewed in Maden et al., 1995). Especially the 2-O-methyl groups reside in regions conserved between several species and are – like pseudouridine – introduced by snoRNA-dependent mechanisms (Maden & Hughes, 1997; Decatur et al., 2007).

Besides the m^7G cap, modified nucleotides found within mRNA are the product of the RNA-editing process. In mammals, this is mainly limited to the exchange of adenine for inosine. The so-called A-to-I-editing was for example identified in the mRNA of mammalian glutamate receptor subunits (Simpson & Emeson, 1996). The exchange of adenine for inosine is mediated by an adenosine deaminase. Failure of A-to-I editing has been linked to neurological diseases such as amyotrophic lateral sclerosis, epilepsy, depression and schizophrenia (reviewed in Maas et al., 2006). In addition to inosine, the presence of 6-methyladenine (m^6A) in eukaryotic mRNA has also been reported (Tuck, 1992; Rottman et al., 1994). 30 – 50 % of all incorporated methyl groups into RNA have been attributed to m^6A. The majority of analyzed mRNAs carries at least one m^6A residue, with the exception of histone and globin transcripts (Tuck, 1992).

Even in small RNAs such as snoRNAs and piRNAs, modifications have been detected. snoRNAs and piRNAs harbour 2-O-methylated nucleotides, and small nuclear RNAs carry pseudouridine (Patton, 1994; Rozenski et al., 1999; Kirino & Mourelatos, 2007). piRNAs are modified specifically at their 3´ends (Horwich et al., 2007). Micro-RNA precursors (pri-miRNAs) are subject to A-to-I editing by adenosine deaminases acting on RNA (Luciano et al., 2004; Yang et al., 2006).

1.5.2 tRNA Modification

Transfer RNAs are adaptor molecules which are crucial for translation of messenger RNA into protein. tRNAs bind with their anticodon to defined codon triplets and carry the codon-specific amino acid, which is attached to the emerging peptide chain in the ribosome. Of all RNA species, tRNA is by far the most heavily and most diversely modified. Presently, around 100 different tRNA modifications have been reported in all three domains of life (Fig. 1.2). Some modifications are common to bacteria, archaea and eukaryotes – such as inosine, pseudouridine, m^1G, m^1A, m^5U – while others are unique and can only be found in bacteria, such as $m^3\Psi$, m^4Cm, and m^2A (Grosjean & Benne, 1998).

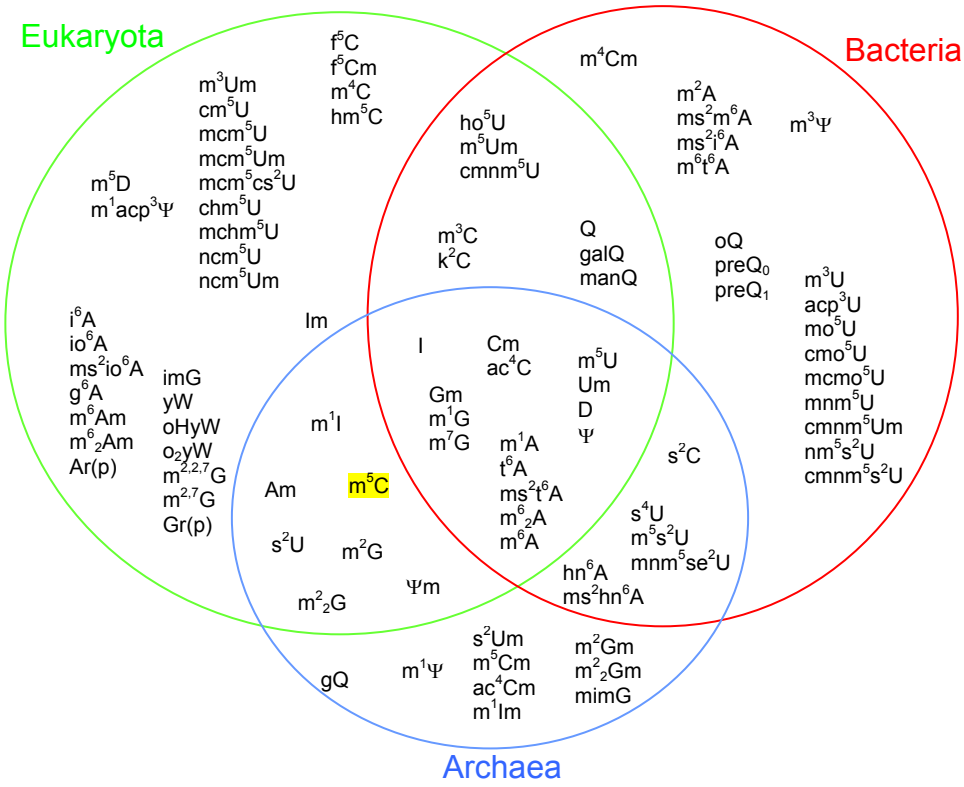

Fig. 1.2: tRNA modifications of all three kingdoms
Green circle: eukaryotic tRNA modifications; red circle: tRNA modifications found in bacteria; blue circle: tRNA modifications present in archaea. Overlap: common tRNA modifications found in two or all three kingdoms. m^5C is marked in yellow. Adapted from Grosjean & Benne, 1998.

tRNA molecules adapt a cloverleaf structure in the secondary structure, with D-loop, anticodon-loop and T-loop forming its leaves, with short stems that allow Watson-Crick pairing for stabilization. The tertiary structure of a tRNA-molecule is L-shaped. Modifications are found in all parts of a tRNA molecule, both within the stems and loops. An example of modifications that were identified within total tRNA of one species is given in Fig 1.3, using *S. cerevisiae* as a model organism.

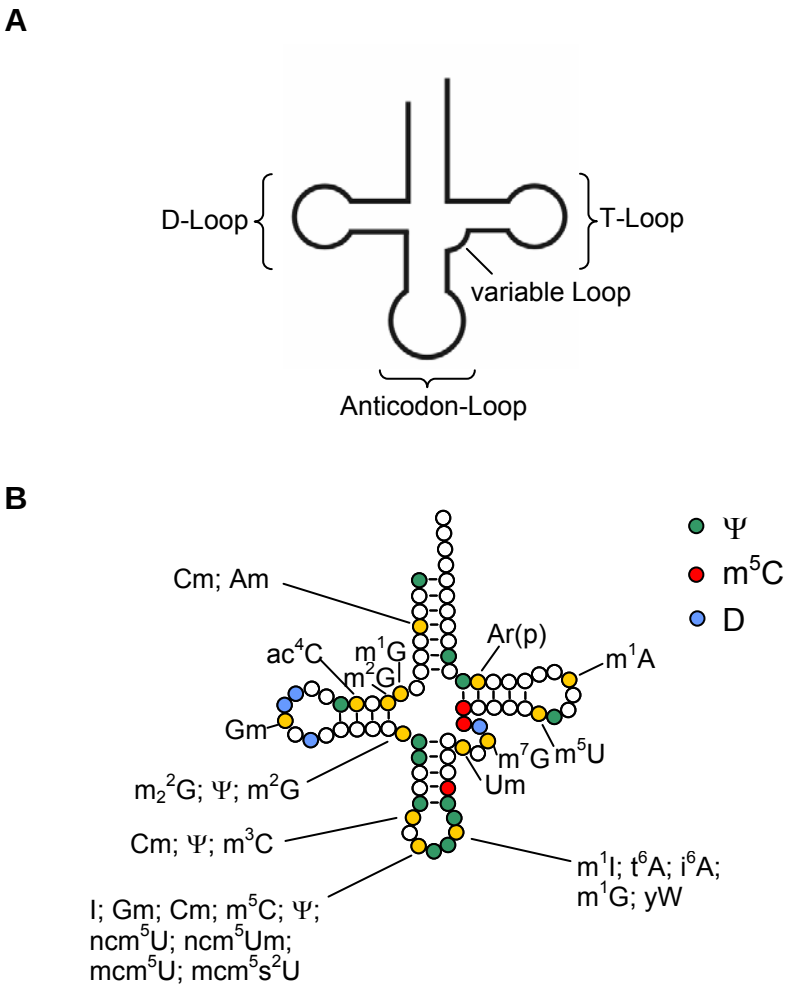

Fig. 1.3: Possible sites of tRNA modification in *S. cerevisiae*
A) Two-dimensional structure of a tRNA molecule (scheme). B) Reported tRNA modification sites in *S. cerevisiae* (adapted from Grosjean, 2005).

It is important to note that sites of a certain modification can differ between species. Fig 1.4 shows a comparison of the m^5C modification sites in *S. cerevisiae* and higher eukaryotes. While m^5C occurs in *S. cerevisiae* at positions 34, 40, 48, and 49, it has been reported at positions 38, 48, 49, 50, and 72 in animals (tRNA sequence database; Sprinzl & Vassilenko, 2005).

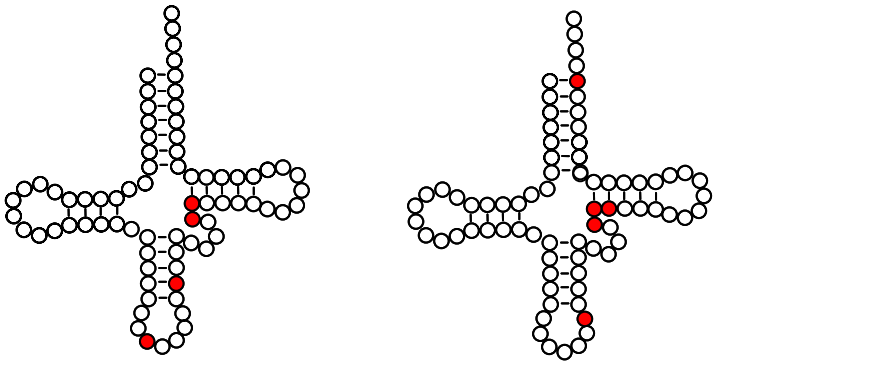

m^5C modification sites in *S. cerevisiae* tRNA

m^5C modification sites in tRNA of higher eukaryotes

Fig. 1.4: m^5C tRNA modification sites in *S. cerevisiae* and higher eukaryotes
Left: tRNA molecule with m^5C modification sites found in *S. cerevisiae* marked in red. Right: m^5C modification sites in higher eukaryotes (red circles). Common is m^5C modification at C48 and C49. m^5C methylation at positions 34 and 40 has not been reported in animals. There, however, m^5C modification can also be found at C38, C50, and C72, which is not the case for tRNA of *S. cerevisiae*.

1.5.3 Function of tRNA Modifications

tRNA modifications can be classified in several ways, including the chemical complexity of modifications, their degree of conservation, as well as their localization within the tRNA molecule. The latter allows drawing conclusions about its function.
Modifications within the anticodon loop are by far the most frequent and are crucial to ensure proper translation and correct codon recognition; they are involved in reading frame maintenance and show a positive influence on the processivity of translation (reviewed in Bjork et al., 1987). Especially positions 34 and 37 within the anticodon

loop are usually hypermodified and contribute to the fine-tuning of codon reading. The position 37 is located 3´ to the anticodon and contains very often bulky modifications in eukaryotes and eubacteria, especially in the context UNN and ANN, where N can be any nucleotide (Bjork et al., 1987). In *E.coli*, 2-methyl-thio-N6-isopentenyl-adenosine at position 37 has been found to exert a stabilizing effect on the anticodon-anticodon interaction of $tRNA^{Pro}$ and $tRNA^{Trp}$ (Vacher et al., 1984). The lack of this modification in *S. typhimurium* results in 20 – 50 % reduction in growth rate as well as in a reduction of translational chain elongation rate from 16 amino acids per second (aa/ s) to 11 aa/ s (Ericson & Bjork, 1986). The direct influence of a bulky modification present at position 37 on ribosome binding could be demonstrated with yW37 of yeast $tRNA^{Phe}$. Its absence led to reduced binding to ribosomes and inefficient *in vitro* translation performance (Thiebe & Zachau, 1968; Bjork et al., 1987). Of all the smaller modifications present at position 37, the presence of m^1G after an anticodon starting with C is very frequent.

To ensure the decoding of 61 amino acid codons by the ~ 40 tRNAs, some tRNAs must recognize more than one codon. This can be explained by the wobble hypothesis. The nucleotide at position 34 in the anticodon of a tRNA binds to the third base of the mRNA codon triplet with relaxed affinity and enables non-canonical (non-Watson-Crick) base pairing, which increases the number of recognizable codons for one tRNA (reviewed in Agris et al., 2007).

Therefore, the important role of these modifications lies primarily in the expansion and regulation of codon reading and improvement of translation fidelity. Several examples exist in bacteria and eukaryotes where the presence of a modification at position 34 leads to the preferred and more efficient binding of one codon over the other, which differ only in the third letter of the to-be-read codon sequence (Lustig et al., 1981; Hagervall & Bjork, 1984). The modification of position 34 with queuosine (Q) can be found in $tRNA^{Tyr}$, $tRNA^{His}$, $tRNA^{Arg}$, and $tRNA^{Asp}$. In *Drosophila melanogaster*, the presence of Q in $tRNA^{His}$ also has an influence on codon choice: when $tRNA^{His}$ carrying either GUG or QUG in the anticodon was analyzed for the acceptance of the codons CAC and CAU, unmodified $tRNA^{His}$ displayed a clear preference for CAC over CAU, whereas the queuosine-carrying $tRNA^{His}$ accepted both codons equally well (Meier et al., 1985). This finding points to a role of queuosine modification in translational regulation, with a possible impact on gene expression depending on codon usage and frequency.

Other modifications within the anticodon loop have been reported at positions 32, 35, 38, 39 and 40, and consist mainly of Ψ and m^5C (Bjork et al., 1987; Grosjean, 2005). Especially for m^5C and pseudouridine, the stabilization of nucleic acid structure by increased base stacking has been described (Agris et al., 1995; Helm, 2006).
The structural stabilization of the tRNA and facilitated Mg^{2+} binding is also the main function of modifications outside the anticodon loop. Studies using tRNA of hyperthermophile organisms such as *Thermus thermophilus* identified modifications at position 54 (2-thioribothymidine) and 58 (m^1A) in the T-Loop, which are important for tRNA stability at high temperatures (up to 80 °C). The absence of these modifications is associated with a thermosensitive phenotype (Kowalak et al., 1994; Shigi et al., 2002; Droogmans et al., 2003). Melting curve analyses revealed that the absence of 2-thioribothymidine at position 54 lowers the melting point of $tRNA^{Ile}$ by three degrees compared to wildtype, 2-thioribothymidine containing $tRNA^{Ile}$ (Horie et al., 1985).

1.6 Nucleotide Modification Associated Diseases

1.6.1 DNA Methyltransferases and Cancer

The role of dysregulated DNA methylation and other epigenetic mechanisms in cancer development becomes evident in the large number of studies and reviews published on this topic. Concerning DNA methylation within tumors, two general features are observed which differ from healthy cells: First, the hypomethylation of pericentromeric satellites and other repeat sequences such as retrotransposons, and second, the hypermethylation and silencing of normally unmethylated and active tumor suppressor genes. The occurrence of hypomethylation in tumors was first observed 25 years ago (Feinberg & Vogelstein, 1983). The reduction in methylation levels can vary greatly between tumor types and is most evident in colon and breast cancers (reviewed in Wilson et al., 2007). Possible causes for the decrease in m^5C content are altered activities of methyltransferases and histone modification enzymes, but also dietary factors, infection and environmental influences. Detrimental carcinogenic consequences for the affected cell are loss of imprinting,

microsatellite instability, activation of retrotransposons, and chromosomal instabilities (Wilson et al., 2007).

The inactivation of tumor suppressor genes on both alleles by mutation or loss of heterozygosity is a crucial step in carcinogenesis. Similarly, the silencing of one allele by promoter CpG island methylation is a possibility to eliminate tumor suppressor gene function (Jones & Laird, 1999). Epigenetically silenced tumor suppressor genes include $p16^{ink4A}$, p53, MLH1, BRCA1, VHL, TIMP3, ATM, and APC (reviewed in Baylin & Herman, 2000; Jones & Baylin, 2002). Many studies have reported an upregulation of one or more DNA methyltransferases in tumor tissues. In a study including ten matched sets of tumor and healthy tissue derived from bladder, colon, kidney and pancreas, overexpression of the Dnmt1, 3a and 3b was seen in at least 50% of all cases. In some tumor samples, a simultaneous upregulation of all three Dnmts could be observed (Robertson et al., 1999).

1.6.2 Imprinting disorders

Imprinted genes are expressed in a parent-of-origin-specific manner. Only the allele coming either from the mother or the father is expressed while the other is epigenetically silenced. Many of the imprinted genes play an important role in embryonic growth regulation. Usually the paternally expressed genes support fetal growth, while the maternally expressed genes exert a growth-limiting effect. The disturbance of the carefully regulated expression pattern of these imprinted genes leads to their bi-allelic expression and manifests in imprinting disorders such as Angelman syndrome, Prader-Willi syndrome, Silver-Russell syndrome (SRS), and Beckwith-Wiedemann syndrome (BWS). Hypo- and hypermethylation of imprinting control regions (ICR) can also play a substantial role (reviewed in Eggermann et al., 2008). While SRS is characterized by severe growth retardation, BWS is associated with overgrowth. This contrasting phenotype is mirrored in the epigenetic status of two imprinting control regions. While ICR1 on 11p15 is hypermethylated in BWS, it is hypomethylated in SRS. ICR2, on the other hand, is hypomethylated in BWS and hypermethylated in SRS (Eggermann et al., 2008).

1.6.3 tRNA point mutations and mitochondrial diseases

High concentrations of reactive oxygen species within mitochondria render the mitochondrial genome especially sensitive to DNA damage. Point mutations within the mitochondrially encoded tRNA genes have been shown to contribute to a number of mitochondrial diseases with complex symptoms. The mutation A3243G within the $tRNA^{Leu(UUR)}$ gene, for example, contributes to the MELAS (*mitochondrial encephalomyopathy, lactic acidosis and stroke-like episodes*) and MIDD (*maternally inherited diabetes and deafness*) syndromes (Goto et al., 1990; van den Ouweland et al., 1992). Several mutations within mitochondrial $tRNA^{Lys}$ and $tRNA^{Leu(UUR)}$ are implicated in MERRF (*myoclonic epilepsy associated with ragged red fibers*) (Shoffner et al., 1990 ; Zeviani et al., 1993). In these mutant tRNAs, the modification taurine (2-aminoethanesulphonic acid) is missing at the wobble position 34 (Suzuki et al., 2002). The phenotypes and onset of the multisystem disorders MELAS and MERRF are very diverse. Myopathies, seizures and deafness are among the most frequently observed features, which correlates with a very high number of mitochondria in muscle and brain tissue (Finsterer, 2007).

1.6.4 tRNA modifications and cancer

Fluctuations in tRNA modification status occur between different organs, and can be induced by hormones or drug treatment. Variation in modification content is also observed during ageing and differentiation (reviewed in Dirheimer et al., 1995). Over the last fifty years, many laboratories have searched for a possible link between hypo- or hypermodified tRNAs and cancer development. The comparison of Morris hepatoma cells to hepatocytes revealed less m^5U, m^3C, m^5C in cancer versus healthy tissue, as well as a hypermodification of m^1G (Randerath et al., 1974). Using mainly mouse and rat as experimental systems, changes of multiple modifications were detected in several tRNAs in various tumor types (summarized in Dirheimer et al., 1995). However, tRNA modification differences were also found in human cancers. Emmerich and colleagues analyzed the queuosine content (usually found at position 34 in $tRNA^{Asp}$, $tRNA^{Asn}$, $tRNA^{His}$, and $tRNA^{Tyr}$) in human lymphomas and leukemias and found that queuosine is underrepresented in these cancer cells. Moreover, the degree of underrepresentation correlated with the malignancy of the

disease (Emmerich et al., 1985). Similar results were achieved with solid lung tumors, where a high correlation between lack of Q (and replacement by G) and the histopathological classification was demonstrated (Huang et al., 1992). These data are further supported by a study of ovarian cancers, which shows a link between queuosine deficiency and differentiation state of the tumor (Baranowski et al., 1994).

1.7 Structural Motifs of DNA and RNA Methyltransferases – Similar yet Different

Common to DNA m^5C methyltransferases are ten conserved motifs, numbered I to X, which can usually be found arranged in strict order and form two domains (see Fig. 1.5). The large domain consists of the motifs I to VIII and X, while the small domain comprises motif IX and a variable region with very low sequence conservation and great variation in length. Motif I is the cofactor binding site; additionally, motifs II-V and X also play an important role in the formation of a binding pocket for the cofactor and methyl-group donor S-adenosyl-methionine (SAM). The catalytic site (consisting of an invariant Pro-Cys dipeptide) resides in motif IV (Kumar et al., 1994). The target recognition domain is situated in a loop region between motif VIII and IX in the small domain. These ten important signature motifs are also present in RNA m^5C methyltransferases. However, the sequence context as well as the degree of conservation can vary, and sometimes the motifs can only be identified by structural homology. Usually, the order of the ten motifs is X-I-II-III-IV-V-VI-VII-VIII-IX, while in DNA m^5C methyltransferases, motif X is C-terminal. In some cases, the order of the motifs has been found rearranged. Nevertheless, the presence of the structural motifs in DNA and RNA m^5C methyltransferases predicts their function: the transfer of methyl groups onto nucleic acids (Reid et al., 1999; Bujnicki et al., 2004).

Despite the similar structural outline that is necessary for substrate recognition, SAM-binding and catalysis, striking differences regarding the catalytic residue have been reported. Both DNA and RNA m^5C methyltransferases use a highly conserved cysteine as the catalytic residue. The catalytic cysteine of DNA m^5C methyltransferases lies in motif IV, whereas RNA m^5C methyltransferases use two conserved cysteines in motifs IV and VI. After mutational studies of the two conserved cysteines, the cysteine in motif VI was proposed to be responsible for the actual formation of the enzyme-RNA intermediate (see below), and the cysteine in

motif IV to be involved in the reversal of the covalent intermediate (King & Redman, 2002; Walbott et al., 2007b). Sequence analysis of RNA and DNA m^5C methyltransferases revealed that while both possess the highly conserved cysteine in the proline-cysteine-context in motif IV, only RNA m^5C methyltransferases harbour the second conserved cysteine in motif VI (Bujnicki et al., 2004).

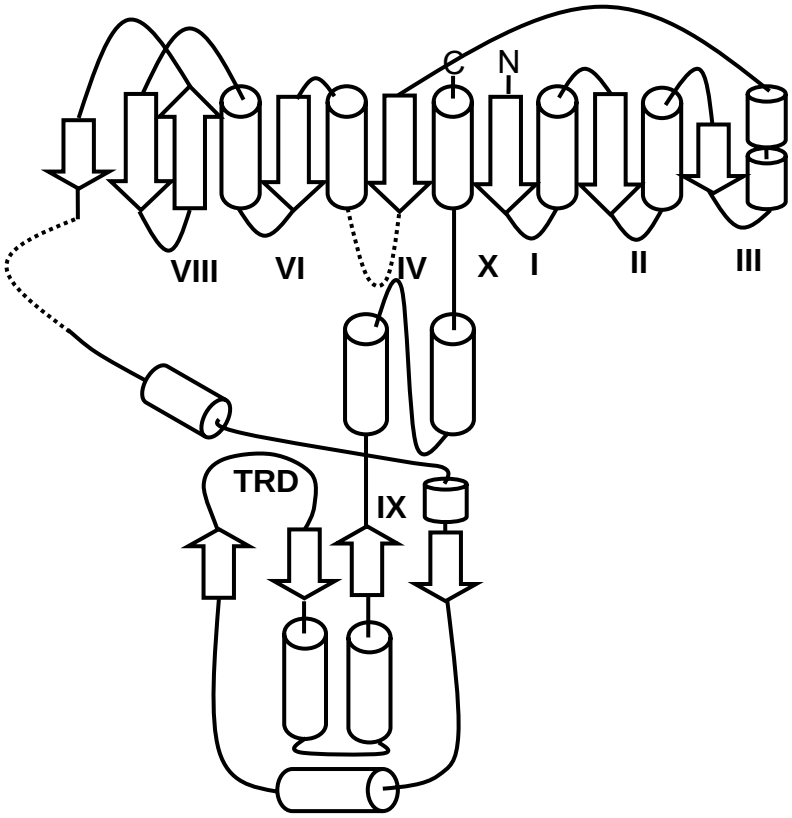

Fig. 1.5: Conserved motifs within the catalytic domain of DNA methyltransferases
The catalytic domain consists of two subdomains. The large subdomain contains motifs I, II, III, IV, V, VI, VIII and X. The small domain encompasses motif IX and the target recognition domain (TRD). Motif I, II-V and X participate in cofactor binding. Motif IV carries the catalytic site, an invariant PC dipeptide. (Adapted from Dong et al., 2001)

1.8 Common Mechanism of DNA and RNA Methyltransferases

1.8.1 Base Flipping and SAM binding

Surprisingly, the core structure encompassing the SAM-dependent MTase fold is similar for all methyltransferases, regardless of their targets ranging from small molecules such as glycine to macromolecules such as DNA or tRNA. The question arises how an enzyme that methylates deoxycytosine in a DNA template can access its target base if it is hidden within the double helix (Cheng & Roberts, 2001). In 1994, Klimasauskas and colleagues analyzed the crystal structure of the bacterial methyltransferase MHhaI from *Haemophilus haemolyticus* together with S-adenosyl-L-homocysteine and a duplex 13mer DNA oligonucleotide (Klimasauskas et al., 1994). In the resolved structure, the authors were able to show that the target base is flipped out of the helix by a rotation on its flanking sugar-phosphate bonds by an angle of 180°. This enables the easy projection of the target base into the concave catalytic pocket of the methyltransferase without the cleavage of covalent bonds (Cheng & Roberts, 2001; Klimasauskas et al., 1994).
S-adenosyl-L-methionine (SAM) is the cofactor common to all methyltransferases. Its chemical properties make this molecule a good methyl group donor. The attachment of the methyl group to the sulphur atom adds a positive charge to the sulfur and leads to thermodynamic destabilization and increased reactivity of the usually inert methylthiol towards nucleophiles such as N, O, S and carbanions (Cheng & Roberts, 2001; Hermann et al., 2004; Fontecave et al., 2004).

1.8.2 Catalytic mechanism

The catalytic mechanism of methyl group transfer to position 5 of cytosine was first proposed for the bacterial DNA methyltransferase MHhaI by (Wu & Santi, 1987). Detailed kinetic analysis revealed a sequential order of DNA binding to the enzyme, followed by the binding of the cofactor S-adenosyl-methionine. After methyl group transfer and conversion of S-adenosyl-methionine to S-adenosyl-homocysteine (SAH), the cofactor is released from the enzyme-DNA-cofactor complex prior to the dissociation of the DNA from the enzyme. SAH is then further hydrolyzed to adenosine and homocysteine by AdoHcy hydrolase (Chiang et al., 1996).

The actual methylation step comprises the attack of an invariant cysteine residue of the enzyme as a nucleophile to the C6 atom of the target cytosine ring, thereby creating a covalent intermediate: a dihydropyrimidine with carbanion character at C5. This renders the C5 atom sufficiently nucleophilic to accept the methyl group from its donor, S-adenosyl-methionine (Wu & Santi, 1987 and Fig. 1.6). The catalytic center in motif IV, which comprises the proline-cysteine (PC) dipeptide, is found in all DNA methyltransferases. Due to the high conservation of the structured catalytic motifs, the above described catalytic mechanism is not limited to prokaryotic methyltransferases but also holds true for the DNA methyltransferases of higher eukaryotes. Additionally, a conserved glutamic acid residue within the amino acid sequence ENV in motif VI plays an important role in the stabilization of the DNA-enzyme complex through contact of N3 in the pyrimidine ring (Jeltsch et al., 2006).
As mentioned above, for RNA m^5C methyltransferases, another conserved cysteine residing in motif VI has been suggested to be the site of catalysis. Its inactivation abolished all enzymatic activity, whereas the mutation of the cysteine in motif IV showed no effect (Walbott et al., 2007b; Liu & Santi, 2000).

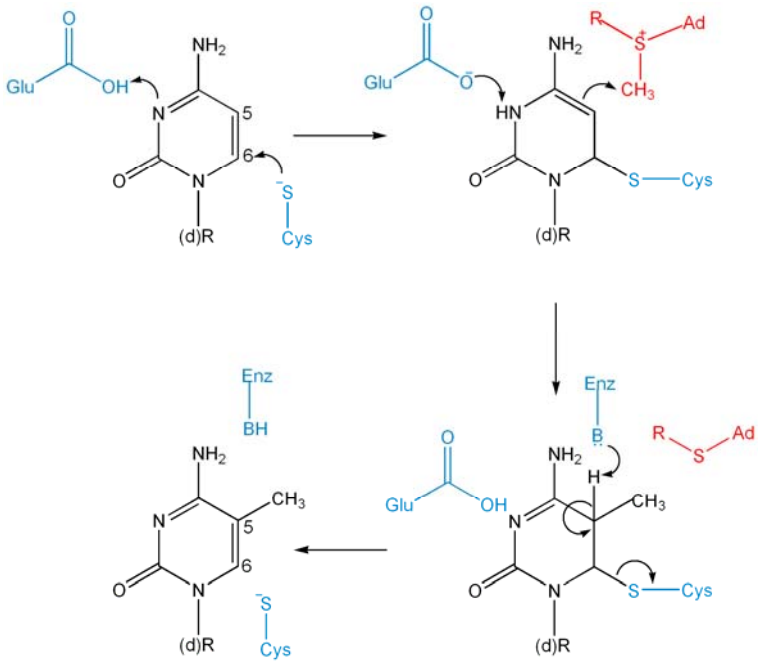

Fig. 1.6: The catalytic mechanism of DNA and RNA methyltransferases
The nucleophilic attack of the invariant cysteine at position 6 of the pyrimidine ring is facilitated by a glutamatic residue interacting with N3. After the formation of the dihydropyrimidine covalent intermediate, the nucleophilic C5 accepts the methyl group from its donor, SAM. Figure modified after Jeltsch et al., 2006.

1.9 Eukaryotic DNA Methyltransferases

The methylation mark at position 5 of cytosine is catalyzed by DNA methyltransferases. In the eukaryotic kingdom, these enzymes can be divided into three classes according to sequence and structure, namely the Dnmt1, Dnmt2, and Dnmt3 families (Fig. 1.7). Not all organisms possess DNA methyltransferases of every family, and there are even organisms without any DNA methyltransferase, such as *Caenorhabditis elegans* and *Saccharomyces cerevisiae*.

1.9.1 The Dnmt1 Family of DNA Methyltransferases

The first mammalian DNA methyltransferase was cloned in 1988 (Bestor, 1988) and was later named Dnmt1. Murine Dnmt1 comprises 1620 amino acids, with a long N-terminal region containing regulatory domains of partly unknown function. Among them are a nuclear localisation signal domain (NLS-domain), a domain which targets replication foci via PCNA (proliferating cell nuclear antigen) interaction (PCNA binding domain, PBD domain), a zinc binding domain (Zn-domain), a cysteine-rich region and a polybromo homology domain (PBHD) (Fatemi et al., 2001; Margot et al., 2003). Only the C-terminal part displays high homology to bacterial methyltransferases, which led to the conclusion that mammalian and prokaryotic DNA methyltransferases share a common evolutionary origin (Bestor, 1988). A schematic overview of the domains of DNA methyltransferases is given in Fig. 1.7.
In vitro methylation assays using various substrates showed a clear preference of human Dnmt1 for hemimethylated DNA (Gruenbaum et al., 1983; Pradhan et al., 1999; Fatemi et al., 2001), which led to the conclusion that Dnmt1 is a maintenance methyltransferase. During replication, methylation of the unmethylated daughter strand is re-established using the parental DNA strand as a template. Support for this theory comes from the observation that Dnmt1 is recruited to DNA repair sites (Mortusewicz et al., 2005) and interacts with PCNA via its PBD domain also at replication foci. The PCNA interaction leads to a two-fold increase in methylation efficiency (Schermelleh et al., 2007). The targeted mutation of both Dnmt1 alleles in murine embryonic stem cells resulted in a decrease of m^5C content in the DNA by two thirds, with no effect on the growth rate and morphology. However, homozygous mutant mouse embryos display a recessive lethal phenotype and die around mid-

gestation. Earlier stages appear stunted and delayed in development (Li et al., 1992). A similar effect was observed upon the injection of Dnmt1-overexpressing embryonic stem cells into early blastocysts: these embryos die as well (Biniszkiewicz et al., 2002). One major cause for the embryonic lethality is the loss of imprinting due to disruption of allele-specific methylation signals. Loss of methylation signal due to absence of Dnmt1 or hypermethylation due to Dnmt1 overexpression leads to biallelic gene expression e.g. of the important growth factor Igf2 (Li et al., 1992; Biniszkiewicz et al., 2002).

1.9.2 The Dnmt3 Family of DNA Methyltransferases

The presence of a *de novo* DNA methyltransferase activity in mammalian cells became evident in 1996. Looking closely at Dnmt1 null mutant mouse embryonic stem cells, Lei and coworkers observed stable levels of m^5C and low *de novo* methyltransferase activity independent of Dnmt1 (Lei et al., 1996). Three years later, two members of this new family of *de novo* methyltransferases – called Dnmt3 – were cloned and characterized in detail. The human Dnmt3a and 3b proteins were shown to be highly homologous to the murine Dnmt3 enzymes, especially in the C-terminal catalytic domain and in a cysteine-rich region (Xie et al., 1999). Expression studies revealed Dnmt3a mRNA transcripts throughout most tissues. Dnmt3b is expressed at much lower levels. Both enzymes are of essential importance for proper *de novo* methylation and mammalian development (Okano et al., 1998a). The generation of homozygous mouse mutants lead to the observation that $Dnmt3a^{-/-}$ mice die 4 weeks after birth, whereas $Dnmt3b^{-/-}$ mice do not develop further than E9.5 (embryonic day 9.5). Homozygous $Dnmt3a^{-/-}$ $Dnmt3b^{-/-}$ double mutants are smaller and display abnormal morphology as early as E 8.5 and die before E11.5 (Okano et al., 1998a). A conditional, germ-line-specific knockout of Dnmt3a and 3b allowed the study of their impact on imprinting. Embryos derived from their conditional knockout mothers died early and showed absence of methylation at maternally imprinted loci (Kaneda et al., 2004). The conditional knockout males had defective spermatogenesis. However, Dnmt3b conditional knockouts had apparently healthy offspring and showed no observable phenotype.

1.9.3 The Dnmt2 Family of DNA Methyltransferases

Dnmt2 is the most highly conserved and most widely distributed DNA methyltransferase (Dong et al., 2001). With the notable exception of C*aenorhabditis elegans* and *Saccharomyces cerevisiae*, this protein has been reported in many model organisms such as *Drosophila melanogaster, Bombyx mori, Arabidopsis thaliana, Xenopus laevis*, *Danio rerio*, *Mus musculus*, and *Homo sapiens*. It is also present in simple eukaryotes such as *Dictyostelium discoideum* and *Entamoeba histolytica*. Compared to the Dnmt1 and Dnmt3 enzymes, Dnmt2 is rather small and consists only of the catalytic domain. Additional N-terminal regulatory domains are absent. The structure of the catalytic domain of human Dnmt2 is nearly superimposable on the structure of the bacterial DNA methyltransferase MHhaI (Dong et al., 2001), and carries the ten catalytic motifs in the correct order. The target recognition domain is surrounded by a 41 amino acid stretch of highly conserved residues (Dong et al., 2001). Structural analysis clearly allows the prediction that Dnmt2 is a *bona fide* DNA methyltransferase. Surprisingly, this enzyme failed to show DNA methylating activity in the classical *in vitro* methylation assays (Okano et al., 1998b). Nevertheless, denaturing-resistant binding of Dnmt2 to DNA was reported *in vitro* (Dong et al., 2001). Others were able to detect residual methylating activity, however at a much lower level than Dnmt1 and Dnmt3a and b. An m^5C spot resulting from Dnmt2 enzymatic activity on λ-DNA or PCR-amplified plasmid DNA in an *in vitro* methylation assay could be detected by two-dimensional thin-layer chromatography (Hermann et al., 2003). In mouse and human, Dnmt2 is expressed in various presumable splice forms in all tissues at low levels; with highest transcription rates in testis, ovary and thymus (Yoder & Bestor, 1998). Dnmt2 knockout mice show no obvious phenotype and are viable and fertile. Despite the high degree of conservation, this enzyme is therefore not essential for development (Goll et al., 2006). The targeted deletion of the catalytic motif crucial for Dnmt2 function in murine embryonic stem (ES) cells had no effect on global methylation levels or *de novo* methylation of newly integrated retroviruses (Okano et al., 1998b).
In vivo data supporting a DNA methylating function of the enzyme Dnmt2 has been reported in three model organisms: the slime mold *Dictyostelium discoideum*, the amoeba *Entamoeba histolytica* and the fruit fly *Drosophila melanogaster* (see below). Ribosomal DNA circles from *Entamoeba histolytica* were enriched via m^5C-binding

antibodies, and their methylation status was confirmed by bisulfite sequencing (Fisher et al., 2004). In addition, the m^5C methyltransferase Ehmeth was described, which bears high homology to human Dnmt2 and was shown to (weakly) methylate genomic DNA of *Entamoeba* (Banerjee et al., 2005). Further analysis revealed that Ehmeth is a nuclear matrix binding protein which binds to a DNA region that includes a scaffold/matrix attachment region. The overexpression of Ehmeth leads to a complex phenoptype, with resistance to oxidative stress, upregulation of the heat shock protein HSP70, and the accumulation of multinucleated cells (Fisher et al., 2006). In *Dictyostelium discoideum*, only one DNA methyltransferase has been identified: DnmA, which belongs to the Dnmt2 family. Despite the very low genome-wide methylation content of 0.2 % of all cytosines (Kuhlmann et al., 2005), two methylated regions could be identified. The retrotransposons DIRS-1 and Skipper carry mostly asymmetric m^5C methylation (in a non-CpG context), which is lost upon disruption of DnmA. A developmental role of DnmA has been suggested, but is discussed controversially. While Kuhlmann et al. reported a downregulation of DnmA throughout the developmental cycle, Katoh et al. observed an increase of methylation during development and described morphological defects of DnmA mutants in late developmental stages (Katoh et al., 2006).

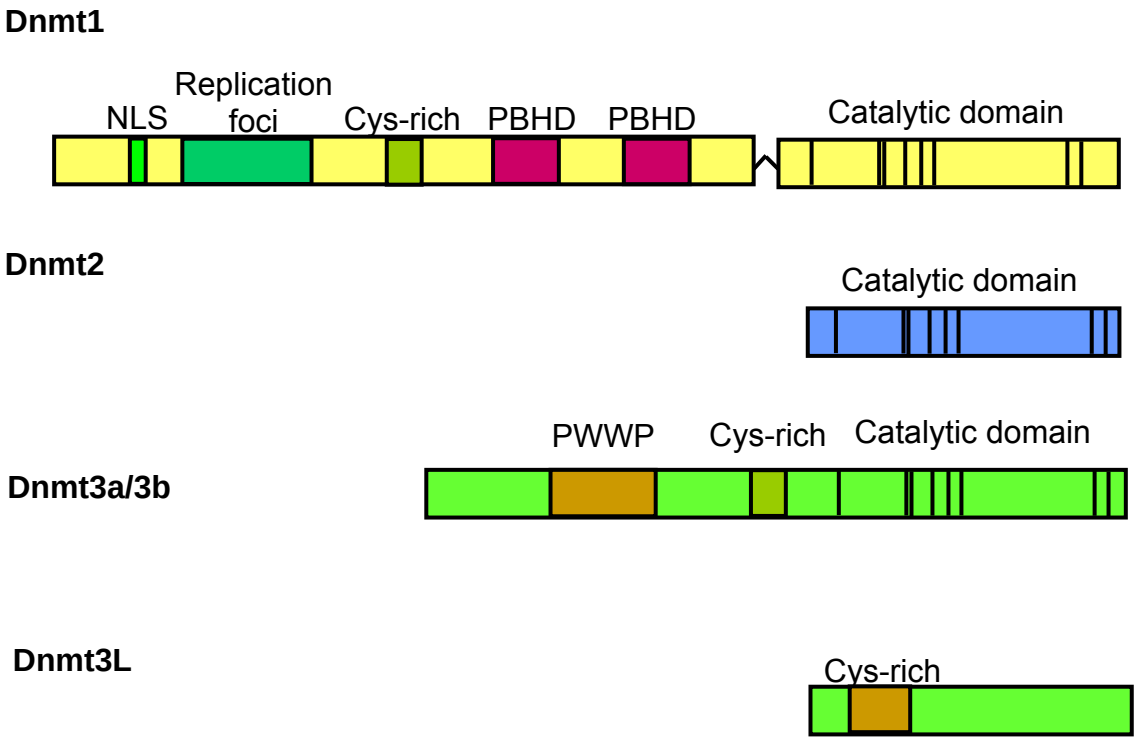

Fig. 1.7: Structural comparison of DNA methyltransferase families of the animal kingdom
Dnmt1 has the largest N-terminal regulatory domain consisting of a nuclear localization signal (NLS), the replication foci-localization domain, a cysteine-rich region, and a large polybromo homology domain (PBHD). Dnmt2 is the smallest enzyme and consists only of the catalytic region and has no N-terminal regulatory domain. The *de novo* methyltransferases Dnmt3a and 3b carry a PWWP domain and a cysteine-rich region. Dnmt3L misses the complete catalytic region and shows homology to the Dnmt3a and 3b proteins via its conserved cysteine-rich region. Adapted from (Goll & Bestor, 2005).

1.9.4 A Methylation System in Drosophila Mediated by Dnmt2

The first finding of a potential DNA methylation system in *Drosophila melanogaster*, consisting of the m^5C methyltransferase Dnmt2 and a methyl-CpG-binding-domain protein (MBD2/3), was reported by Tweedie and colleagues (Tweedie et al., 1999). Sequence comparison with yeast (*S. pombe*) and mouse DNA methyltransferases led to the classification of Dnmt2 as a member of the Dnmt2 family of m^5C methyltransferases, with a reported sequence homology to both mammalian Dnmt2

and pmt1 of 50 % (Hung et al., 1999). Dnmt2 transcript was found throughout all developmental stages. Further studies of expression revealed predominant expression of Dnmt2 transcript in ovarian nurse cells and through early embryonic development (Lyko et al., 2000b). The occurrence of endogenous m^5C DNA methylation in young embryos of *D. melanogaster* was reported using sensitive methods such as HPLC and nearest neighbour analysis (Lyko et al., 2000a). Interestingly, m^5C methylation appeared mainly in a CpT context, as opposed to the CpG context reported for mammals. Later, additional expression studies demonstrated the expression of Dnmt2 throughout embryonic and larval development, although slightly reduced in second and third instar larvae. Gowher and colleagues demonstrated the presence of m^5C in genomic DNA of all developmental stages using a combinatorial approach of nucleoside purification by HPLC, radioactive labelling, and one- or two-dimensional thin-layer-chromatography (Gowher et al., 2000). Dnmt2 protein was detected in all developmental stages of Drosophila, albeit to a lower extent in somatic tissue of adult flies (Schaefer et al., 2008). Biochemical analysis of cellular Dnmt2 localization revealed that Dnmt2 is mainly cytoplasmic (as has also been reported by Goll et al., 2006), but in addition, a significant nuclear fraction could be detected. Throughout the cell cycle, Dnmt2 accumulated in mitotic cells and localized to mitotic nuclei in a dynamic fashion (Schaefer et al., 2008).

1.10 RNA m^5C Methyltransferases

1.10.1 Trm4

A well characterized m^5C methyltransferase acting on tRNA is the Trm4 enzyme of *S. cerevisiae*. Originally identified by homology search using the bacterial ribosomal m^5C methyltransferase SUN for comparison, this multisite-specific enzyme was found to methylate cytosines at positions 34, 40, 48 and 49 (Motorin & Grosjean, 1999). The actual site of methylation was mapped by nearest neighbour analysis. The occurrence of m^5C at positions 48 or 49 is quite frequent and does not require any pre-modifications, as *in vitro* transcribed tRNA and total tRNA of *E.coli* are accepted as substrates for Trm4. However, the methylation at positions 34 and 40 was

identified in only two tRNA species, $tRNA^{Leu(CUA)}$ and $tRNA^{Phe(GAA)}$, and the presence of an intron is absolutely mandatory for correct target recognition of these two pre-tRNAs. The methylating activity was measured by ^{3}H incorporation into tRNA, using radioactive *S*-adenosyl-methionine as the methyl-group donor. Comparison of several tRNA targets revealed differing turnover rates. Apparently, the methylation at C48 or 49 is slightly faster than the methylation of the intron-containing pre-tRNAs. Deletion of the Trm4 gene abolished all detectable m^5C methylation within yeast tRNA. Therefore, in *S. cerevisiae*, Trm4 can be considered the only m^5C tRNA methyltransferase. The human orthologue of yeast Trm4 was identified in 2006, albeit with limited substrate recognition ability. Only the intron-dependent methylation of C34 could be demonstrated for hTrm4; whereas no methylation of positions 48 and 49 was detected in both human and yeast tRNA precursors. hTrm4 is encoded as a single-copy gene on chromosome 5 and the protein was found to be localized in the nucleoplasm and nucleolus (Brzezicha et al., 2006).

1.10.2 Dnmt2 as a tRNA m^5C Methyltransferase

The enzymatic activity of Dnmt2 was further characterized in 2006, when Goll et al. reported that recombinant, his-tagged hDnmt2 enzyme was able to methylate $tRNA^{Asp}$ derived from homozygous Dnmt2 mutants of *Mus musculus*, *Arabidopsis thaliana* and *Drosophila melanogaster*. RNA samples from the respective wildtype organisms could not be modified, arguing for the presence of an endogenous methylation signal which blocks additional methylation by the recombinant enzyme (Goll et al., 2006). Mass spectrometry analysis led to the identification of $tRNA^{Asp}$ as the target molecule, and the site of methylation was narrowed down to C38 in the anticodon loop. The authors did not observe methylation of *in vitro* transcribed, unmodified $tRNA^{Asp}$, which led to their hypothesis that methylation by Dnmt2 depends on other tRNA modifications. One year later, the first severe phenotype in a Dnmt2 null mutant was reported in the zebrafish *Danio rerio* (Rai et al., 2007). Previous mutants in mouse and fruitfly had not shown any deviation from wildtype behaviour and development.

In *Danio rerio*, the morpholino knockdown of the Dnmt2 enzyme led to severe differentiation defects in retina, liver and brain, which became evident at 80 hours post fertilization. Rescue experiments using Dnmt2 targeted either exclusively to the

nucleus or the cytoplasm revealed that the phenotype can only be reversed if Dnmt2 localizes to the cytoplasm. Furthermore, immunopurified Dnmt2 of zebrafish was incubated with morphant-derived or wt-derived RNA and radioactive SAM, which resulted in 7.5 fold increase in tritium-incorporation in the 80 base species of morphant-RNA (where endogenous Dnmt2 had been knocked down) compared to the wildtype situation. In summary, the data obtained in zebrafish support the hypothesis that the Dnmt2 enzyme is a cytosolic tRNA methyltransferase.

1.11 Aim of this work

Dnmt2 is an enigmatic enzyme which was assigned to the family of DNA m^5C methyltransferases based on sequence homology to the other family members Dnmt1, Dnmt3a/b, and its nearly superimposable structure onto the bacterial methyltransferase MHhaI (Dong et al., 2001). However, the extremely weak catalytic activity on DNA raises questions about its target preference. Two years ago, Goll and co-workers found that Dnmt2 is able to exclusively methylate position C38 in $tRNA^{Asp}$, which was derived from Dnmt2 mutant mice and flies (Goll et al., 2006). The authors made a strong effort to state that Dnmt2 activity is limited to $tRNA^{Asp}$.
The aim of this work was to characterize the enzymatic function of Dnmt2 with special focus on the identification of further target molecules, their characterization with respect to the degree of m^5C modification, and the detailed investigation of the catalytic mechanism of the Dnmt2 m^5C methyltransferase.

2 Results

In vivo studies of Dnmt2 function and its substrates have proven to be very challenging. Especially the analysis of its DNA methylating activity requires a careful choice of model organism, as it is crucial to distinguish obtained 5-methyl-cytosine measurements from the activities of other DNA methyltransferases present in the animal model. Since the fruitfly *Drosophila melanogaster* carries the *Dnmt2* gene as the only member of the DNA methyltransferase family, it is ideally suited for the investigation of Dnmt2 function. Therefore, this work started with the characterization of an important tool for many experiments: a Dnmt2 null mutant.

2.1 The Genomic Locus of the Putative Null Mutant Dnmt2^{149}

The putative Dnmt2-null mutant Dnmt2^{149} was obtained and created by our collaborators Sameer Phalke and Günther Reuter (University of Halle) through an imprecise excision screen out of the founder line GE15695 (also called “EP”), which contains a P-element situated upstream of the *Dnmt2* gene. Upon mobilization of the P-element, it inserted into the *Dnmt2* gene and was cut out again incompletely, leaving 55 bp of transposon sequence (plus 13 bp duplicated endogenous sequence) within the *Dnmt2* gene behind (Fig. 2.1 A and B). The inserted bases cause a frameshift during codon-reading in the translation process. *In silico* translation of the *Dnmt2^{149}* gene shows a complete change in amino acid sequence after the first 18 amino acids (Fig 2.1 C).

A

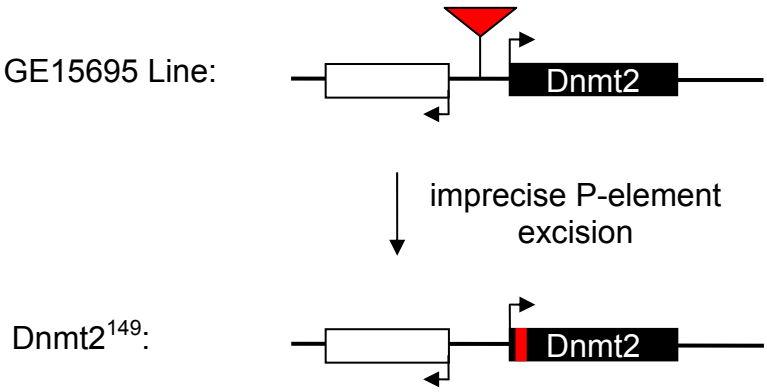

B

Sequencing of the genomic *Dnmt2*^{149} locus

Dnmt2 (Flybase):

ATGGTATTTCGGGTCTTAGAACTATTTAGTGGCATTGGCGG*CATGCATTATGCCT*TTAATTGTG
AGTTCGTCGATCATGATACATGCGAAACTAATATATACTTTTGAAGATGCCCAATTGGATGGAC
AAATAGTTGCCGCCTTGGATGTCAACACCGTGGCCAATGCGGTTTATGCGCACAATTACGGC
AGTAATTTGG

Dnmt2^{149}:

ATGGTATTTCGGGTCTTAGAACTATTTAGTGGCATTGGCGG*CATGCATTATGCC*ATGATGAAA
TAACATATGTTATGTTATGTATATGTATATATATATGTTATTTCAT*CATGCATTATGCC*TTTAATT
GTGAGTTCGTCGATCATGGTACATGCGAAACTAATATATACTTTTGAAGATGCCCAATTGGAT
GGACAAATAGTTGCCGCCTTGGATGTCAACACCGTGGCCAATGCGGTTTATGCGCACAATTA
CGGCAGTAATTTGG

C *In silico* translation

Dnmt2 protein sequence (wt):

MVFRVLELFSGIGGMHYAFNYAQLDGQIVAALDVNTVANAVYAHNYGSNLVKTRNIQSL
SVKEVTKLQANMLLMSPPCQPHTRQGLQRDTEDKRSDALTHLCGLIPECQELEYILMEN
VKGFESSQARNQFIESLERSGFHWREFILTPTQFNVPNTRYRYYCIARKGSDFPFAGGKI
WEEMPGAIAQNQALSQIAEIVEENVSPDFLVPDDVLTKRVLVMDIIHPAQSRSMCFTKGY
THYTEGTGSAYTPLSEDESHRIFELVKEIDTSNQDASKSEKILQQRLDLLHQVRLRYFTP
REVARLMSFPENFEFPPETTNRQKYRLLGNSINVKVVGELIKLLTKK

Dnmt2^{149} protein containing the 55 + 13 bp insertion:

MVFRVLELFSGIGGMHYAMMKZHMYVMYMYIY…

(See Figure legend on the following page.)

Fig 2.1: Characterization of the Dnmt2^{149} mutation
A) Establishment of Dnmt2^{149}. The founder line GE15695 contains a P-element right upstream of the *Dnmt2* gene. Mobilization of this P-element, followed by re-insertion into the ORF of Dnmt2 and subsequent, imprecise re-excision resulted in 55 bp of transposon sequence insertion within the 5´region of the Dnmt2 gene.
B) The insertion site in *Dnmt2^{149}*. Sequencing of genomic DNA of *Dnmt2^{149}* and comparison to the genomic *Dnmt2* sequence available on Flybase reveals a 55 bp insertion of transposon sequence (marked in red), followed by 13 bp dupliation (grey) of endogenous sequence (italics). The site of insertion is marked in red letters.
C) *in silico* translation of *Dnmt2^{149}*. After the first 18 residues, the frameshift leads to a change in amino acid sequence (depicted in red) compared to the wildtype protein sequence.

2.2 Characterization of Dnmt2^{149}

The first goal was to characterize the mutant on a molecular level. The 68 base pair insertion is apparent in the mRNA, as is shown by a non-quantitative RT-PCR (Fig. 2.2): The cDNA of Dnmt2 originating from Dnmt2^{149} mutants runs higher than the wt cDNA (Fig. 2.2). Even though a transcript is made, there is no translation into protein. The Western Blot in Fig 2.3 shows Dnmt2 protein in the wildtype background at the correct size of 40 kDa, whereas no Dnmt2 protein is observable in the mutant. The antibody used had been raised against a peptide near the catalytic region (Schaefer et al., 2008), and the specificity of the signal was demonstrated by including a peptide block. Equal loading was confirmed by immuno-detection of α-tubulin in the same blot. The complete absence of Dnmt2-protein confirms that Dnmt2^{149} is indeed a null mutant.

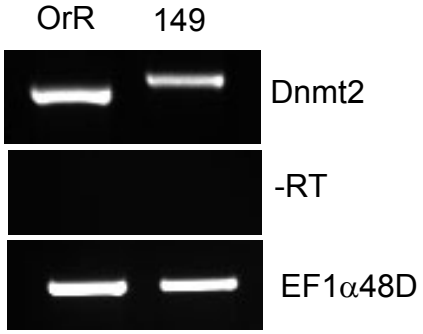

Fig. 2.2: RT-PCR of Dnmt2 cDNA.
Upper panel: The PCR-band of mutant-derived cDNA (149) runs higher than wildtype (OrR) due to the 68 bp insertion; middle panel: -RT control;
lower panel: RT-PCR of EF1α48D was used as a loading control.

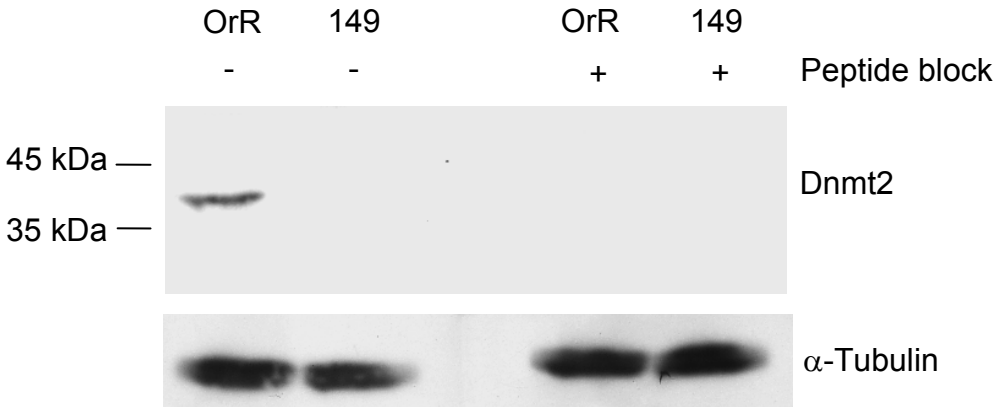

Fig. 2.3: Dnmt2-Western Blot
Upper panel: Western blot using a peptide antibody against Dnmt2. Wildtype protein runs at 40 kDa. No Dnmt2 protein is observed in mutant protein extracts. Addition of the peptide against which the antibody was designed abolishes the Dnmt2 signal, thereby underlining the specificity of the antibody reaction. Lower panel: α-Tubulin staining was used as a loading control.

Dnmt^{149} flies are viable, fertile, and exhibit no obvious phenotype. Egg laying behaviour, hatch and growth rates are comparable to wildtype flies. Cuticle stainings of embryos display normal patterning. Similarly, DAPI-staining of nuclei of young embryos shows no disturbance of the developmental programme. This is consistent with the Dnmt2 knockout mouse, of which also no aberrant phenotype has been reported (Goll et al., 2006).

2.3 Identification of the Dnmt2^{215} Revertant Fly Line

There are several fly strains that are used to generate mutants. However, their genetic backgrounds can differ, and it is of great importance to either include a wildtype control of the same genetic founder background as the mutant, or to ensure that the wildtype control is comparable to the strain of which the mutant was derived. Since the original fly strain out of which the “EP”-line was generated could not be obtained, several fly lines of the P-element excision screen (a kind gift of S. Phalke)

were screened for a precise excision of the P-element. Non-viable strains were excluded, and the precise excision was monitored by PCR (Fig. 2.4 A). Complete removal of the P-element from the Dnmt2 locus should restore Dnmt2 expression. PCR of the Dnmt2 locus and subsequent sequencing led to the identification of the fly line Dnmt2^{215}, which will thereafter also be referred to as “the revertant”, and which carries a wildtype *Dnmt2* locus (Fig. 2.4).

A

Fly lines	207	211	212	215	217
Viable without balancer	no	yes	yes	yes	yes
Precise excision	yes	no	no	yes	no

B

Fig. 2.4: Screening for a „revertant“ of identical genetic background to Dnmt2^{149}
A) The table lists the viability of several putative revertant fly lines without a balancer and the PCR experiment concerning a precise excision. **B)** PCR experiment using primers HD39 and HD57. Comparison with the wildtype amplicon reveals that only the fly line 215 has the correct amplicon size.

Northern Blotting of wildtype, revertant, mutant, and founder fly line (EP) revealed an abundance of Dnmt2-transcript in the Dnmt2^{149} mutant fly embryos compared to equal levels of Dnmt2-transcript in wildtype and revertant. Interestingly, Dnmt2-mRNA is not expressed in the EP-line, where the P-element insertion upstream of the Dnmt2 gene probably blocks the initiation of transcription (Fig. 2.5).

The corresponding Western blot shows comparable levels of Dnmt2 protein expression in the OrR (wildtype) and 215 (“revertant”) strains, whereas no Dnmt2 protein is expressed in Dnmt2^{149} fly embryos (Fig. 2.5). Therefore, the P-element has indeed been excised completely in the revertant Dnmt2^{215}, permitting Dnmt2 re-

expression. Similar mRNA and protein levels of OrR and Dnmt2^{215} fly embryos allow both fly strains to be used as suitabe wildtype control for the analysis of Dnmt2^{149} embryos.

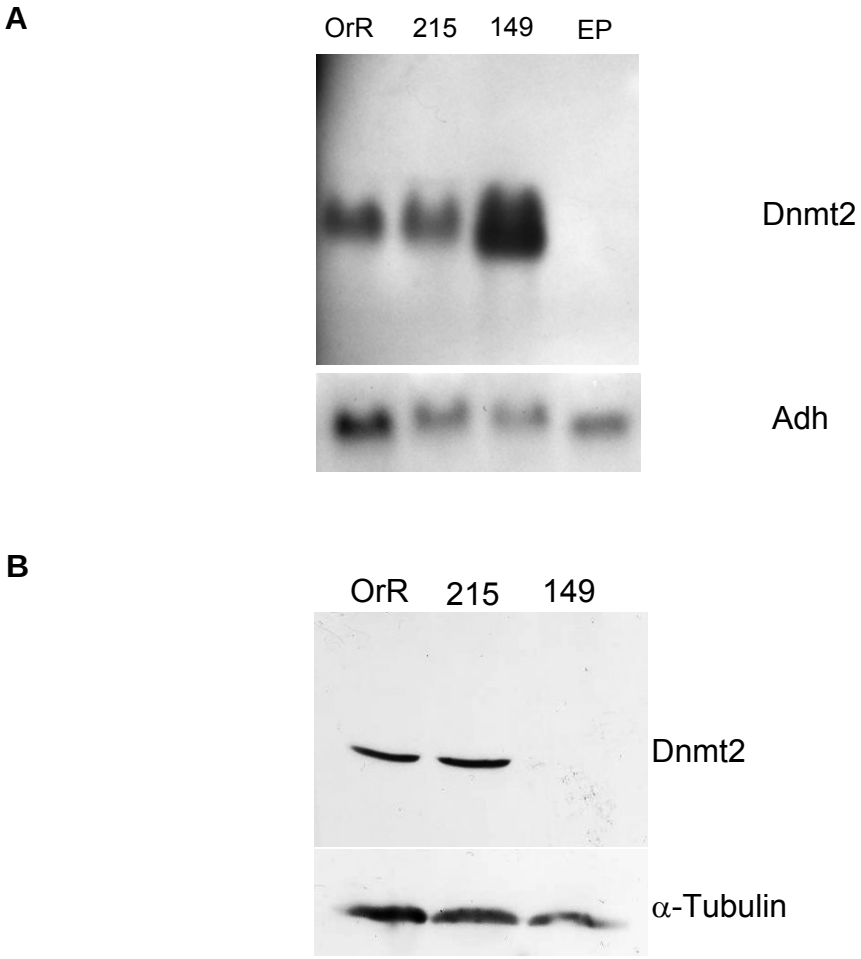

Fig. 2.5: Comparison of Dnmt2 mRNA and protein levels in wildtype, revertant and mutant
A) Northern Blot of wildtype (OrR), revertant Dnmt2^{215} (215), Dnmt2 null mutant Dnmt2^{149} (149) and founder fly strain (EP). Upper panel: probed against Dnmt2; lower panel: loading control probed with Adh mRNA. **B)** Corresponding Western Blot. Wildtype (OrR) and revertant (215) express equal levels of Dnmt2 protein. Dnmt2 is absent in Dnmt2^{149} and the EP-line. α-Tubulin was used as a loading control (lower panel).

2.4 Dnmt2 and its Role in Transposon Regulation

The silencing of repeats and retrotransposons by m^5C methylation is among the most important functions of the DNA methyltransferase Dnmt1 (Bird, 2002; Gaudet et al., 2004). To a lesser extent, Dnmt3b also contributes to the silencing of LINE-1 elements specifically on the to-be-inactivated X chromosome in humans (Hansen, 2003) and during male germ cell development in mice (Kato et al., 2007). Since *Drosophila melanogaster* lacks any other DNA methyltransferase besides Dnmt2, it is reasonable to investigate whether Dnmt2 also plays a role in this mechanism. Semi-quantitative RT-PCR was used to investigate transposon expression in wildtype and mutant fly embryos. A moderate effect of increased transposon expression could be observed in the $Dnmt2^{149}$ mutant flies. In all three examined cases – the retrotransposons invader 4, micropia, and invader 2 – the amplified cDNA band is stronger in the mutant background compared to the wildtype (Fig 2.6, upper panel). A PCR on non-reversely-transcribed RNA (-RT, middle panel) was included as a negative control. The absence of bands in the negative control confirms that the RNA preparation was free of genomic DNA contamination. EF1α48D (short: EF1α) served as the control housekeeping gene which was used as a loading control (Fig. 2.6, lower panel).

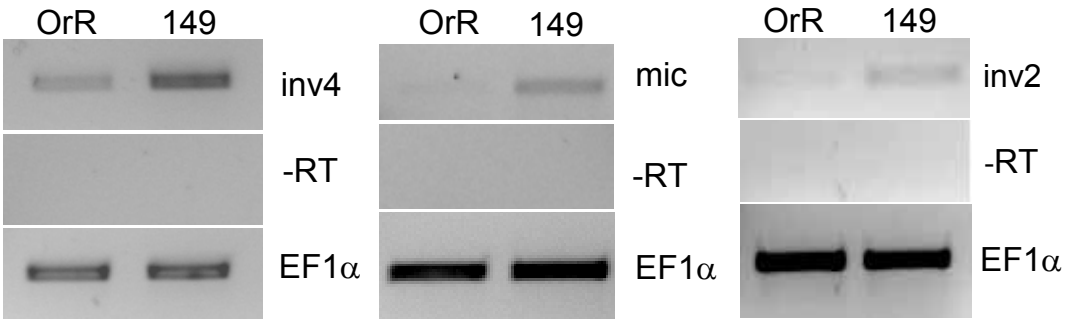

Fig. 2.6: Transposon expression differences in wt and Dnmt2 mutant embryos
RT-PCR of mRNA prepared from 0 – 3 h old embryos was performed. Expression of the transposons invader 4 (inv4), micropia (mic) and invader 2 (inv2) is increased in the mutant $Dnmt2^{149}$. –RT: negative control, without reverse transcription; EF1α (EF1α48D): loading control.

Since the small increase in transposon expression might be due to methylation changes based on the loss of Dnmt2 protein in the mutant Dnmt2^{149}, different regions of two retrotransposons were analyzed for DNA methylation. The random bisulfite sequencing approach showed dense methylation in one region of invader 2, but none in invader 4 (Fig. 2.7).

A

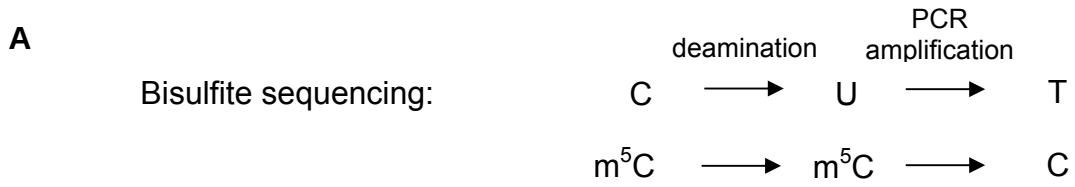

B

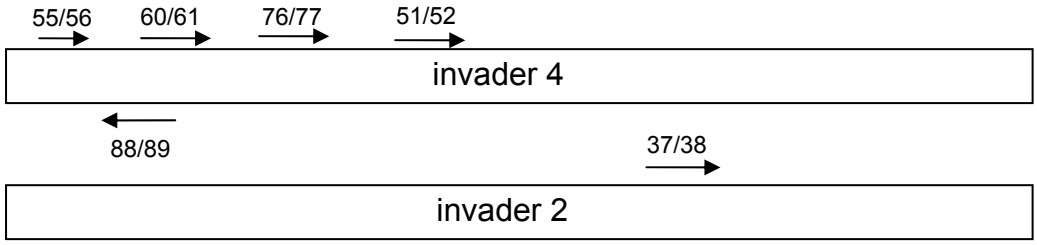

C

Transposon / primer pairs	Fly strain	meth. Clones	CpT	CpA	CpG	CpC	strand	% m^{5}C
Inv4_76/77	OrR	4 (10)	2	2	0	0	c	0.60%
Inv4_88/89	OrR	0 (10)	0	0	0	0	n.c.	0
Inv4_60/61	OrR	0 (5)	0	0	0	0	c	0
Inv4_ 51/52	OrR	0 (5)	0	0	0	0	c	0
Inv4_51/52	149	0 (2)	0	0	0	0	c	0
Inv4_51/52	OrR	0 (2)	0	0	0	0	c	0
Inv4_55/56	149	0 (2)	0	0	0	0	c	0
Inv4_55/56	OrR	1 (2)	1	0	0	0	c	1.70%
Inv4_60/61	149	0 (2)	0	0	0	0	c	0
Inv4_60/61	OrR	0 (2)	0	0	0	0	c	0
Inv2_37/38	149	0 (2)	0	0	0	0	c	0
Inv2_37/38	OrR	2 (4)	12	34	18	6	c	33%

Fig. 2.7: Random bisulfite sequencing approach of two retrotransposons
A) Overview of the bisulfite sequencing method. **B)** Scheme of the sequenced regions in invader 4 and invader 2 **C)** Summary of bisulfite sequencing analysis of different regions of invader 4 and one region of invader 2. Numbers in the first column refer to primer pairs. C: coding strand; n.c.: non-coding strand. OrR: wildtype strain; 149: Dnmt2^{149} strain.

2.5 A Defined Genomic Locus to Search for DNA Methylation

An approach to enrich for methylated sequences via immunoprecipitation of methylated sequences was unsuccessful due to the general low level of DNA methylation. The strategy was changed and the search for genomic DNA methylation was focused on a defined genomic locus. Our collaborator S. Phalke (University of Halle, Germany) had generated a fly strain (5Ha1925) which carried a mobile element insertion within a transposon sequence. The RS5 element, carrying the *white* gene (coding for red eye colour) as a marker, had inserted into an invader 4 element in the Y chromosome (Fig. 2.8). As the parental fly line is deficient for *white* gene expression, the expression of red eye colour is due to expression of the transposon sequence and is – due to the location on the Y chromosome - restricted to male flies.

It was reported by S. Phalke that crossing Dnmt2^{149} into 5Ha1925 led to an increase in red eye colour compared to 5Ha1925 only. This could be confirmed (Fig. 2.9). Furthermore, when Dnmt^{215} – the wildtype control with identical genetic background as the mutant Dnmt^{149} – was crossed into a 5Ha1925 background, the eye pigmentation was comparable to “wildtype” 5Ha1925 flies (Fig. 2.9).

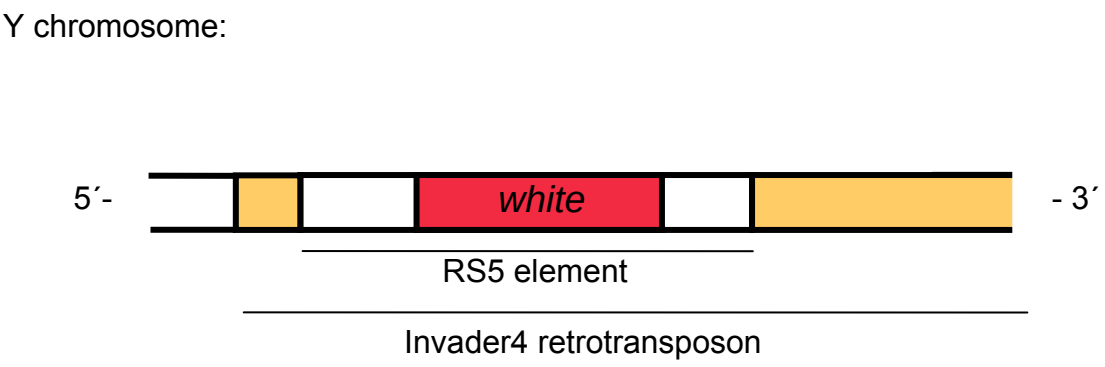

Fig. 2.8 :
The fly line 5Ha1925 carries the insertion of an RS5 element into the 5´ LTR of the retrotransposon invader 4 on the Y chromosome. Due to the marker gene “*white*” in the RS5 element, male adult flies show red eye colour whereas female flies which do not carry a Y chromosome have white eyes.

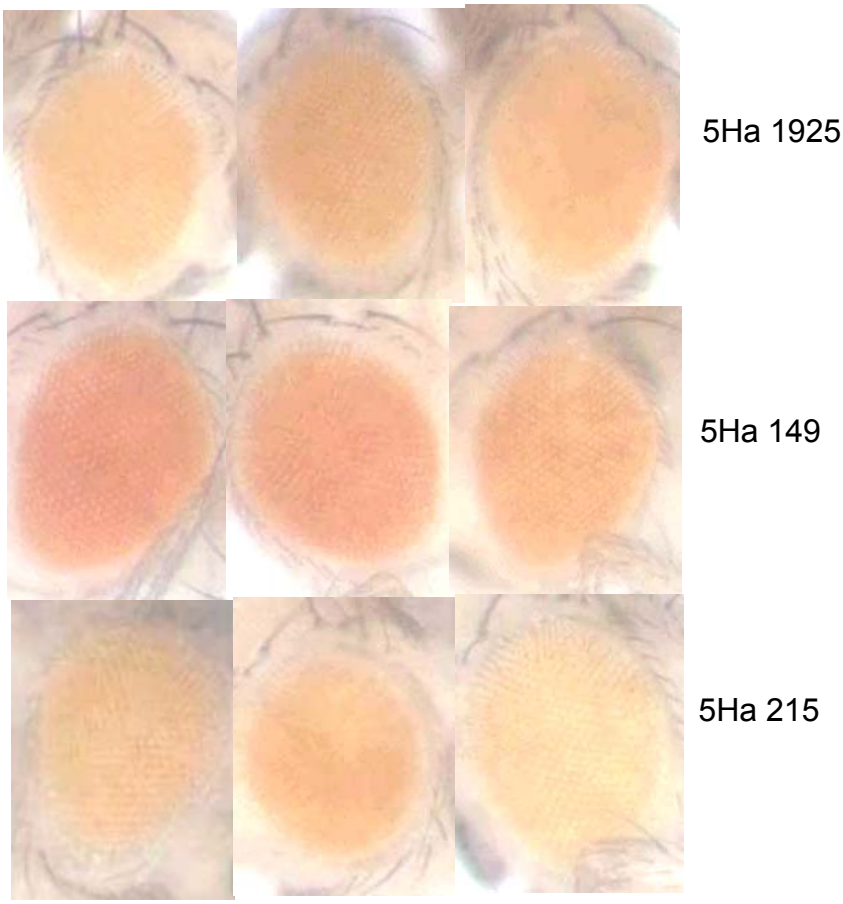

Fig 2.9: Increased eye pigment variation in the Dnmt2^{149} background
Eye pigment comparison of freshly hatched adult male flies carrying the *mini-white* gene in the RS5 element on the Y chromosome. In wt and revertant background (upper and lower panel), the eye colour is a light orange. In the Dnmt2^{149} background (middle panel), the eyes are darker, which can be attributed to increased expression of the *mini-white* gene.

Several primer pairs were designed to cover the 5´ and 3´ region of the *mini-white* marker gene as well as the transposon boundaries, where the RS5 element has inserted into the LTR of invader 4 (an overview is given in Fig 2.10).

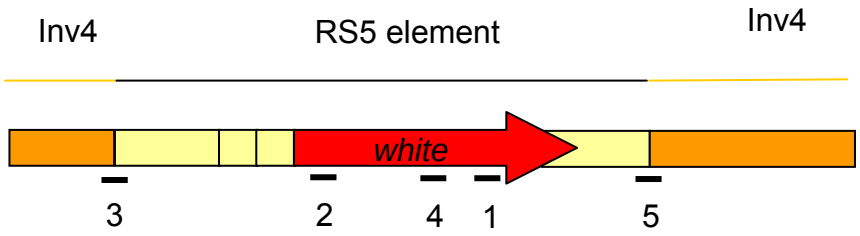

Fig. 2.10: Overview of regions within the RS5 element analyzed for m^{5}C methylation by bisulfite sequencing
The numbers one to five describe the five amplicons that were subjected to bisulfite sequencing. 1, 2, and 4 are located within the *mini-white* gene in the RS5 element, and 3 and 5 mark the boundaries of the two mobile elements.

In order to investigate the methylation status of the RS5 element, bisulfite sequencing was performed on deaminated DNA isolated from 0 - 3 h old embryos. Out of the five regions examined, only one region (No. 1), in the 3´ end of the *mini-white* marker gene, reproducibly showed dense methylation in a fraction of examined clones whereas no methylation could be observed in the Dnmt2^{149} background (see Fig. 2.11b). Of note, the methylation was not distributed evenly among sequenced clones. Rather, a few clones appeared almost fully methylated in a non-CpG context, while other clones completely lacked methylation in the wildtype background. An example of a typical electropherogram of the bisulfite treated and subsequently sequenced clones is displayed in Fig. 2.11. All cytosines in the sequencing reaction can be attributed to m^{5}C in the original sequence before bisulfite treatment and PCR reaction. Since the wildtype and mutant DNA samples were purified and deaminated in parallel under the same conditions, and there was never dense methylation found in the mutant background, deamination artefacts appear highly unlikely. Unexpectedly, no methylation could be found in other regions examined.
These data provide preliminary evidence for Dnmt2-mediated DNA methylation in a Y-chromosomal invader 4 element. Future experiments and large scale methylation analysis are needed to further investigate its function.

A

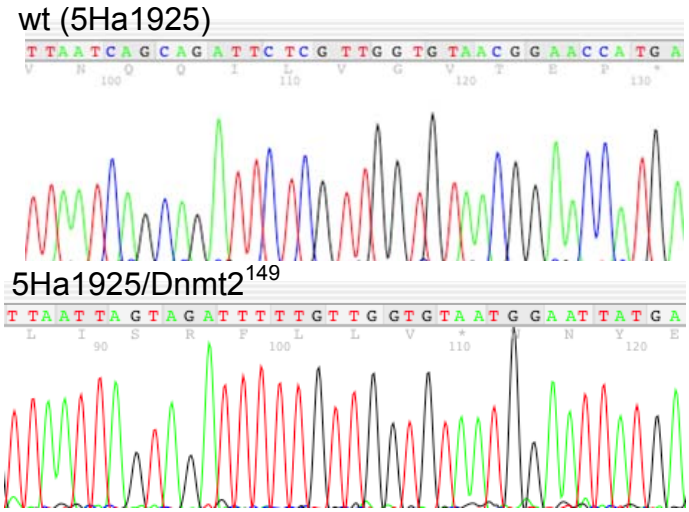

B

	Region 1	Region 2	Region 3	Region 4	Region 5
Methylation found	yes	no	no	no	no
# of sequenced clones	37/32	15/15	15/15	13/19	26/21
# of methylated clones	6/(1)	0/0	0/0	0/0	0/0
# m^5C	666/1	0/0	0/0	17/13	12/21
% m^5C	16/0	0/0	0/0	0.9/0.5	0.5/0.6

Fig. 2.11: The 3´ region of the *white* gene is methylated within the RS5 element in wildtype, but not in Dnmt2^{149} embryos
A) Example of two electropherograms of the 3´-region of the *white* gene, showing m^5C methylation in the wildtype background (upper panel). m^5C is completely absent in the Dnmt2^{149} background, where all cytidines have been converted into thymines (lower panel). **B)** Summary of the bisulfite sequencing data. Only in region 1 could substantial amounts of m^5C methylation be identified. Numbers in black correspond to m^5C in wt embryos, numbers in red correspond to 5Ha/Dnmt2^{149} embryos.

2.6 The tRNA methyltransferase Dnmt2

After the publication that Dnmt2 is a tRNA methyltransferase in 2006, the focus of this work was shifted towards the analysis of tRNA molecules as possible targets of this enzyme. Several findings of the publication (Goll et al., 2006) warranted further analysis, including the suggestion that *in vitro* transcribed tRNAs are not a target of Dnmt2, and that $tRNA^{Asp}$ is the sole target of this enzyme. The first experimental tool to address these issues was an *in vitro* methylation assay, where the target tRNA was incubated with Dnmt2 enzyme in the presence of the tritiated cofactor S-adenosyl-methionine. Upon catalysis, the radioactive methyl group is transferred onto the tRNA, which is then precipitated and subjected to liquid scintillation counting.

As a central component of the *in vitro* methylation assays, Flag-tagged Drosophila-Dnmt2 (a kind gift of Dr. Matthias Schaefer) was isolated out of stably overexpressing $S2R^+$ cells. Additionally, recombinantly expressed, His-tagged human Dnmt2 (a kind gift of Tomek Jurkowski, University of Bremen) was used. Recombinant hDnmt2 has the advantage that it can be produced in large amounts. On the other hand, typical post-translational modifications of this enzyme might be lacking. Immunoprecipitation of dDnmt2 out of Drosophila cells leads to a much lower yield, however, the environment under which the enzyme is produced is comparable to endogenous Dnmt2. Fig. 2.12 shows the quantification of a Flag-Dnmt2-immunoprecipitation with BSA as a standard. Western blotting of input, supernatant, and eluate of the IP protocol reveals a quantitative isolation of cytosolic, soluble Flag-Dnmt2 out of the cell extract.

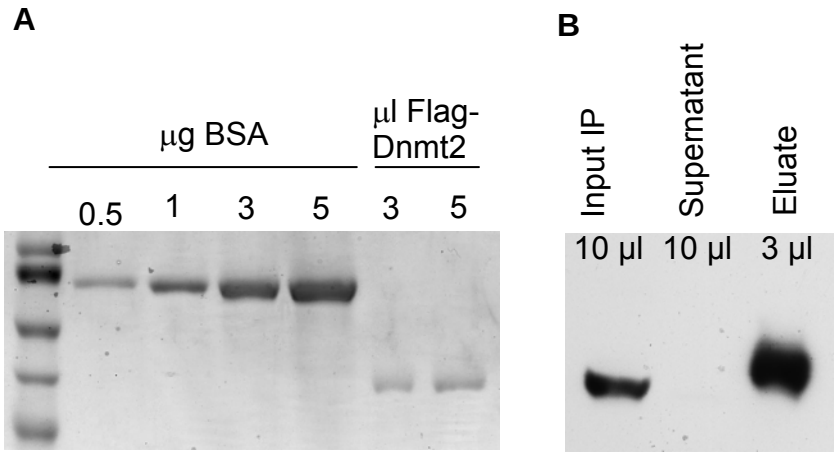

Fig. 2.12: Purification of Flag-Dnmt2 out of *Drosophila* S2R+ cells
A) Coomassie-stained gel for the quantification of Flag-Dnmt2, using BSA as a standard. **B)** Western blot against the Dnmt2 protein. No protein is detected in the supernatant fraction.

2.7 Optimization of the tRNA *In Vitro* Methylation Assay

The enzymatic activity of human and Drosophila Dnmt2 was tested with an *in vitro* assay, in which the respective enzyme was incubated with its putative targets in the presence of [^{3}H]-S-adenosyl-methionine as methyl-group-donor. Dnmt2 catalyzes the transfer of the tritiated methyl-group to its target tRNA, which is precipitated on filter paper. The amount of radioactivity is measured by liquid scintillation counting. Prior to the testing of several different *in vitro* transcribed tRNAs, the reaction conditions were optimized regarding Mg^{2+} and DTT concentration. Total tRNA of *E. coli* was used as a target substrate, as bacterial tRNA does not contain m^5C and therefore harbours several potential acceptor sites.

As shown in Fig. 2.13, the enzymatic activity of hDnmt2 clearly increases with the addition of 10 mM Mg^{2+}, whereas the addition of 30 mM Mg^{2+} leads to a reduction in activity, which is even lower than without Mg^{2+}. Therefore, 10 mM Mg^{2+} was added to all further experiments. The presence of Mg^{2+} ions has a stabilizing effect on the tertiary structure of tRNA molecules. The activity increase of hDnmt2 with the

addition of 10 mM Mg^{2+} suggests that this stabilized three-dimensional structure of tRNA is necessary in order to be recognized as a target for the Dnmt2 enzyme.

Drosophila Dnmt2, which was isolated out of overexpressing $S2R^{+}$ cells, was stored in a glycerol-containing buffer at -20 or -80 °C. However, a dramatic decrease in enzymatic activity could be observed after a few weeks of storage (first bar of Fig. 2.14). The addition of fresh DTT could reverse this effect and recover the enzymes´ original activity. As represented in Fig 2.14., a titration of several DTT concentrations ranging from 1 mM to 25 mM DTT shows that the addition of 10 mM DTT directly to the methylation reaction supports the highest raise in activity of dDnmt2. Accordingly, further *in vitro* methylation experiments were carried out in the presence of 10 mM DTT.

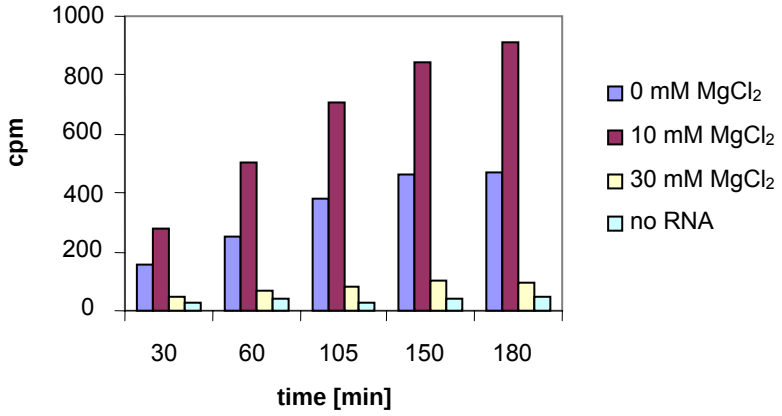

Fig. 2.13: Influence of Mg^{2+} ions on Dnmt2 activity
In vitro methylation assay with total tRNA of *E.coli* and hDnmt2 enzyme under varying Mg^{2+} concentrations.

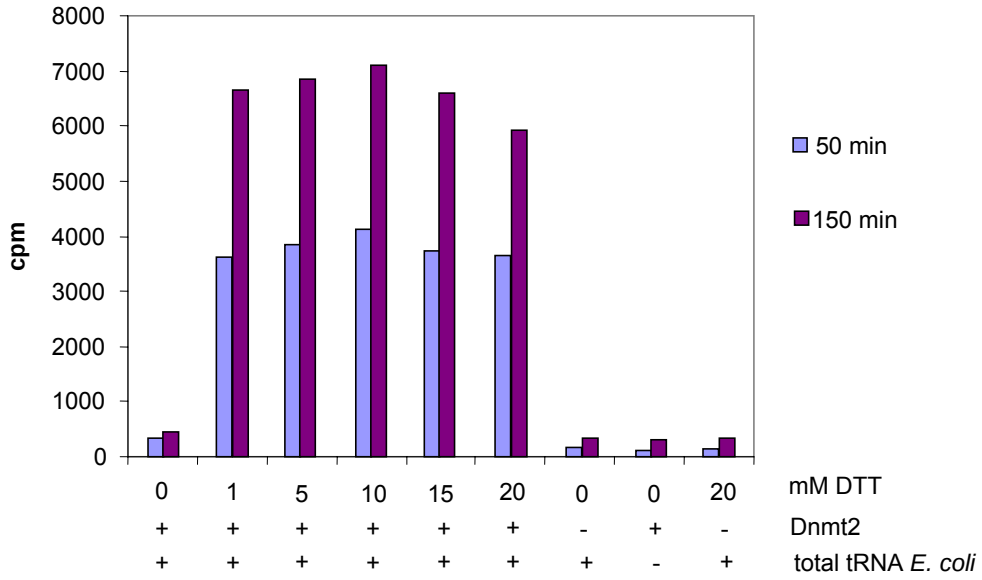

Fig. 2.14: Influence of DTT on the reactivation of dDnmt2
An *in vitro* methylation assay was performed with dDnmt2, total tRNA of *E. coli* and increasing concentrations of freshly added DTT. dDnmt2 activity peaks at 10 mM DTT added.

2.8 Dnmt2 Methylates *In Vitro* Transcribed, Unmodified tRNA^{Asp}

Goll et al. published the observation that *in vitro* transcribed, unmodified tRNA^{Asp} is not a substrate for Dnmt2 (Goll et al., 2006), however, it is possible that the observed lack of modification was a result of the chosen assay or of the *in vitro* transcription conditions. To further analyze the possibility that *in vitro* transcribed, unmodified tRNAs are a substrate for the Dnmt2 enzyme after all, mouse tRNA^{Asp} was transcribed using the hammerhead ribozyme method which facilitates transcription of tRNAs that do not start with a guanine (Fechter et al., 1998). *Drosophila* tRNA^{Asp} was transcribed without the hammerhead ribozyme. Both tRNAs differ in only four bases unrelated to the anticodon loop. After isolation, both *in vitro* transcribed tRNA^{Asp} preparations were subjected to the methylation assay using *Drosophila* or human Dnmt2 (Fig. 2.15 A - C). Although the methylation efficiency differs between dDnmt2 (Fig. 2.15 A) and hDnmt2 (Fig. 2.15 B), a modification signal clearly above background signals can be observed. Quantification of several experiments resulted in a modification efficiency of 0.15 - 0.2 mol m^5C/ mol tRNA for *Drosophila* Dnmt2, and 0.8 - 1 mol m^5C/ mol tRNA for human Dnmt2 (Fig. 2.15 C). Additionally, mouse

tRNA^{Asp} was radioactively transcribed using [α-P^{32}]-CTP. After isolation, tRNA^{Asp} was incubated with (cold) SAM, Mg^{2+}-containing buffer and Dnmt2, precipitated and digested with ribonuclease P1. The single nucleotides were then separated by 2-dimensional thin layer chromatography. An m^5C spot could clearly be detected (Fig. 2.15 D). The *in vitro* methyltransferase assay as well as the TLC approach clearly shows that *in vitro* transcribed, unmodified tRNA^{Asp} is recognized and methylated by Dnmt2. Therefore, pre-modification of tRNA^{Asp} at other sites is not a necessary requirement for the catalytic action of the Dnmt2 enzyme.

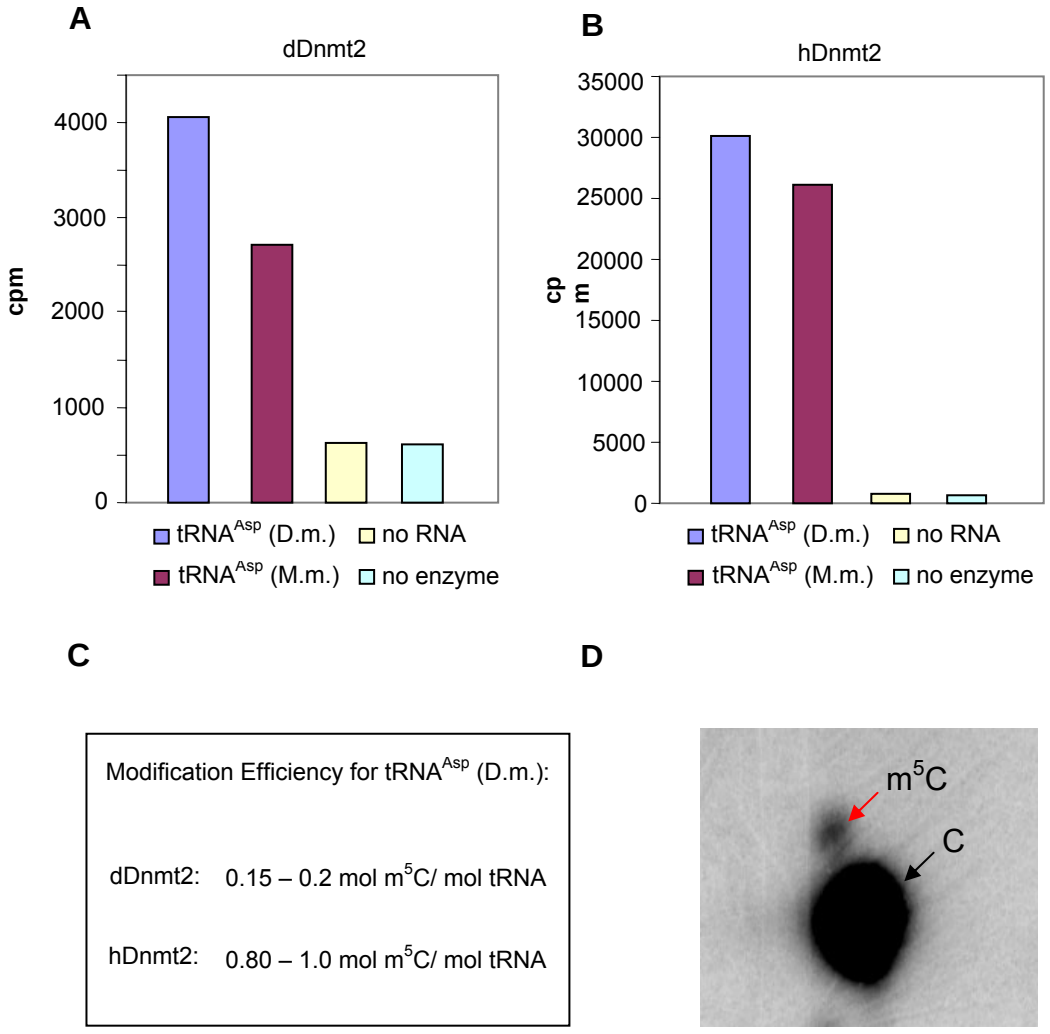

Fig. 2.15 : *In vitro* transcribed, unmodified tRNA^{Asp} is a target of Dnmt2
A) Methylation assay using hDnmt2 and *in vitro* transcribed tRNA^{Asp} of *Drosophila melanogaster* and *Mus musculus*. **B)** Methylation assay using hDnmt2 and *in vitro* transcribed tRNA^{Asp} of *Drosophila melanogaster* and *Mus musculus*. **C)** Quantification of the modification efficiency of Dnmt2-mediated methylation of tRNA^{Asp} (D.m.). **D)** Two-dimensional thin layer chromatography of radioactively transcribed ([α-P^{32}]-CTP), Dnmt2-methylated tRNA^{Asp} (M.m.). Red arrow: m^5C spot; black arrow: cytosine spot.

2.9 Structural Requirements for Target Recognition by Dnmt2

Previously, it was assumed that pre-modifications of tRNA are necessary for Dnmt2 activity. This is not the case, as could be shown in the previous chapter. So far, it has been unclear which elements of the target $tRNA^{Asp}$ are absolutely required for it to be recognized as a substrate by the Dnmt2 enzyme. Among the possibilities are the recognition of sequence elements independent of structure, short structured units (for example single loops) or the whole tRNA molecule. To analyze the structural requirements, three *in vitro* transcripts of mouse $tRNA^{Asp}$ were designed: One consisting only of the anticodon stem loop, one where the anticodon loop size was decreased by the exchange of C32 to a G32, thereby allowing Watson-Crick-base pairing, and the third construct harboured a similar change in anticodon architecture as in construct two, but this time the C38 was exchanged for a U38. This should serve as a negative control, as C38 is the site of Dnmt2 action. The constructs are depicted in Fig. 2.16 A. These constructs (including a wild type $tRNA^{Asp}$ construct) were *in vitro* transcribed, purified and precipitated, and then subjected to the *in vitro* methylation assay together with purified *Drosophila* Dnmt2.

Clearly, only the complete tRNA molecule forming a clover-leaf structure and therefore the typical L-shape in the third dimension is suited to be recognized as a target by the Dnmt2 enzyme. The anticodon stem loop alone is not sufficient. Similarly, the additional base-pairing of G32 and C38 or C32 and U38 is disadvantageous and abolishes the methylation signal almost completely. This finding contrasts with the yeast m^5C methyltransferase Trm4, which does not depend on the whole tRNA molecule for efficient methylation of position 34 in the anticodon loop. For this site, a minisubstrate encompassing the anticodon stem loop as well as an intron, is sufficient (Walbott et al., 2007a).

A

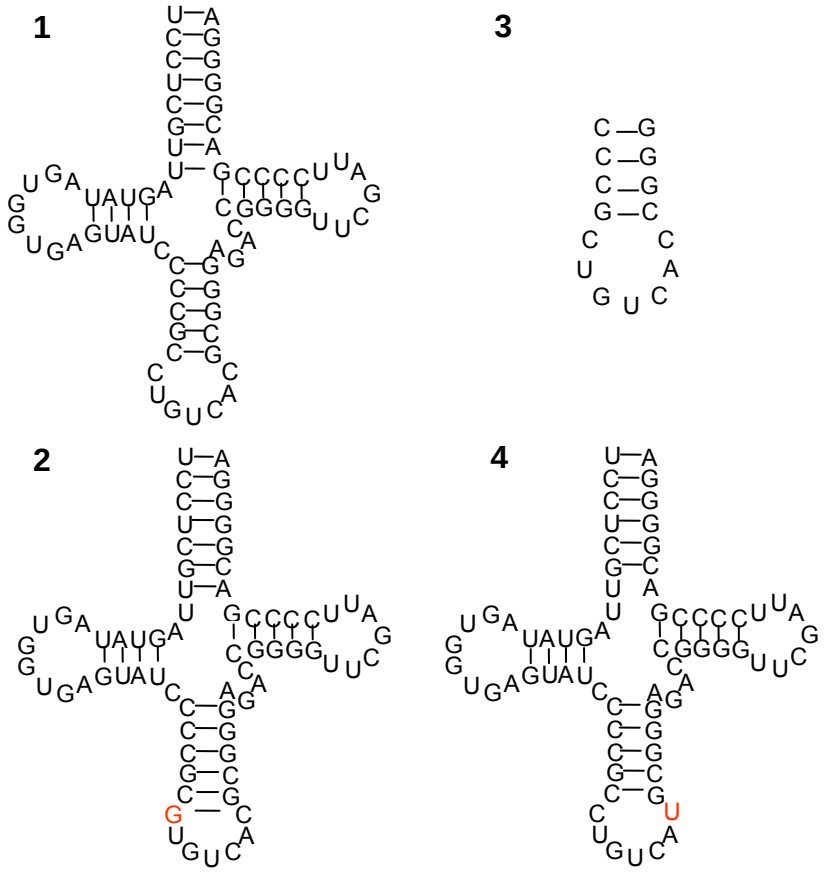

B

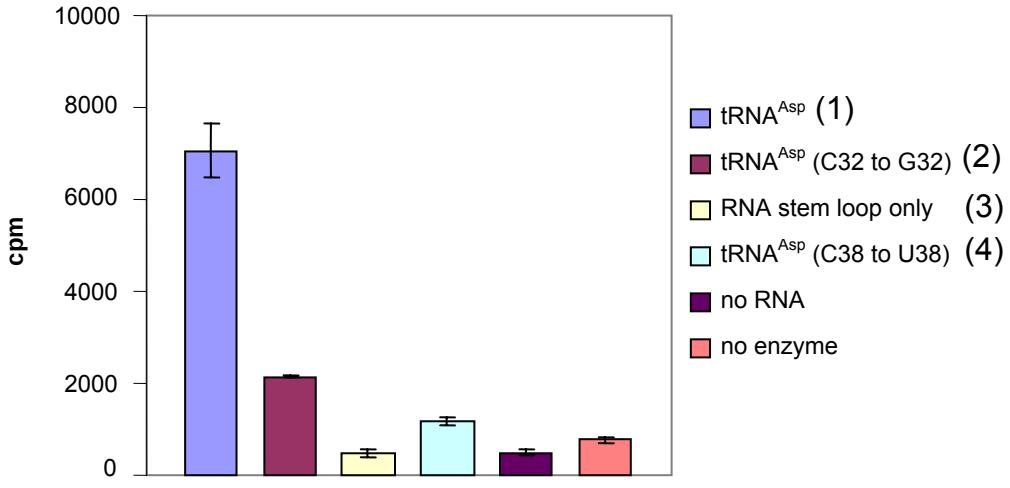

Fig. 2.16: Structural requirements for target recognition by Dnmt2
A) Overview of designed and tested constructs; 1) wildtype construct (lacking the last 4 bases for technical reasons), 2) anticodon stem loop only, 3) C32 exchanged for G32 to tighten the anticodon loop, 4) C38 exchanged for U38. **B)** Methylation assay of the *in vitro* transcribed constructs. Only the wildtype construct is methylated efficiently by dDnmt2. Triplicate measurements of one experiment are shown.

2.10 The Application of DNAzymes Facilitates the Analysis of tRNA Modification Sites

The use of 10 - 23 DNAzymes – short single-stranded DNA oligonucleotides with the ability to cleave RNA at purine-pyrimidine junctions – is a very elegant technique to analyze defined modification sites within tRNA. The DNAzyme consists of two arms which are complementary to the RNA sequence and a defined sequence forming a loop, which is necessary for the catalytic function. Due to the hybridization properties of the DNAzyme arms, the site of cutting can be directed exactly to the nucleotide of interest e.g. within tRNA, as long as a purine is followed by a pyrimidine, for example A-C, A-U, G-C, G-U (Cairns et al., 2003). This technique thereby conserves sequence context and is preferred over the detection of nucleotides via HPLC or capillary electrophoresis by which the existence of modification can be proven but not its location within the tRNA. Mass-spectrometry would also be suited to analyse tRNA fragments for their modification content, but the DNAzyme method is much more cost-efficient. However, not all purine-pyrimidine pairs are cleaved equally well, e.g. A-U is cleaved with much higher efficiency than A-C. It was reported that the cleavage efficiency of problematic combinations can be greatly improved by the introduction of inosine opposite the target pyrimidine (Cairns et al., 2003).

To determine the level of methylation of $tRNA^{Asp}$ by Dnmt2 at C38 in wildtype flies, the DNAzyme technique was chosen to cleave at the site of interest – C38 in the anticodon loop - and to quantify the methylated fraction after radioactive labelling and subsequent 2-dimensional TLC (see chapter 2.14). Prior to the analysis of material derived from *Drosophila* embryos, however, experiments were carried out with unmodified, *in vitro* transcribed $tRNA^{Asp}$ to optimize the method. Temperature cycling enables re-annealing of the DNAzyme to tRNA and increases the yield of cleaved tRNA. The improvement of $tRNA^{Asp}$ cleavage both by the introduction of inosine and repeated temperature cycling is shown in Fig. 2.17.

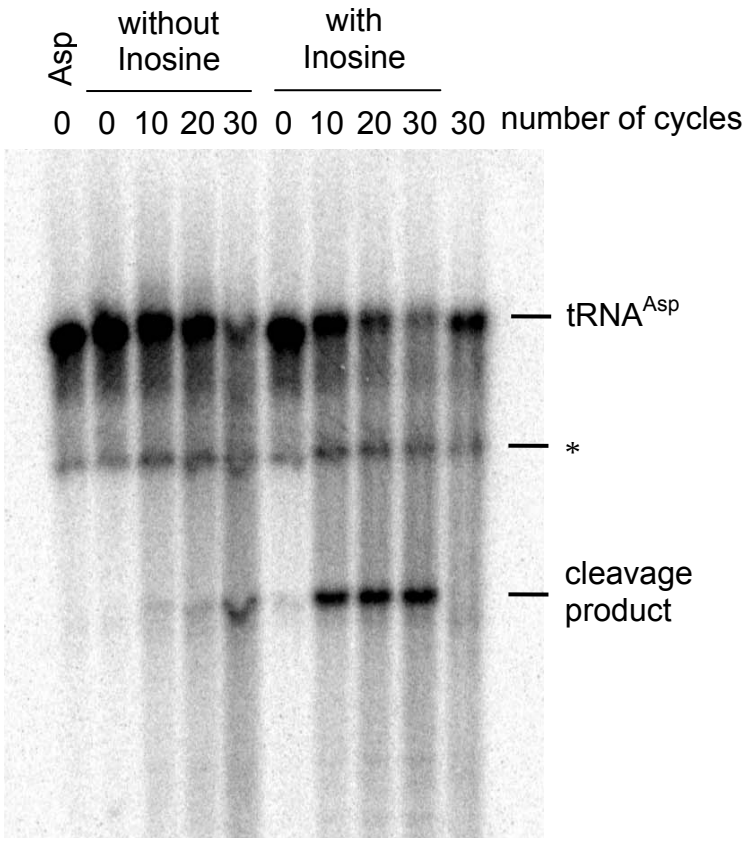

Fig. 2.17: Optimization of the DNAzyme approach
Two DNAzymes cleaving $tRNA^{Asp}$ at C38 were compared in their activity under temperature cycling conditions. Left: DNAzyme without inosine; right: DNAzyme with inosine. Clearly, the introduction of inosine greatly improves the cleavage efficiency of the DNAzyme. Asterisk: unspecific cleavage band

When the DNAzyme approach is applied to quantify modifications present at the cleavage site, it is important to consider whether the presence of the modification impairs cleavage efficiency. Additionally, not only the cleavage but also the labeling efficiency of the subsequent PNK reaction can be impaired by the presence of m^5C. To investigate this, a titration experiment was carried out. Known concentrations of oligonucleotides containing either a C or m^5C at the 5´-end were mixed and radioactively labelled using [γ-^{32}P]-ATP and PNK. After gel-purification the fragments were digested and separated by two-dimensional TLC and the C and m^5C signals were quantified. Indeed, the PNK enzyme had a slight preference for C versus m^5C.

While C was labeled with 100 % efficiency, m^5C was labeled only with about 80 – 90 % efficiency (Fig. 2.18). This has to be taken into account when quantifying the m^5C content directly via DNAzyme cutting at the modification site.

A

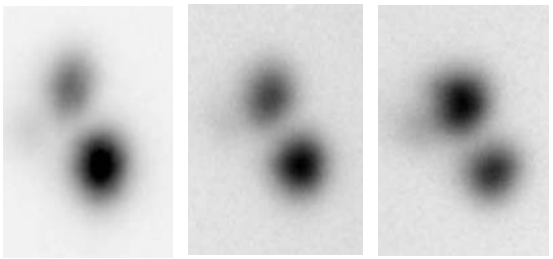

25 % m^5C 50 % m^5C 75 % m^5C

B

	25% m^5C	**50% m^5C**	**75% m^5C**
10 mM ATP	23.4 %	37.1 %	63 %
100 mM ATP	26.9 %	45.3 %	63 %
average	25 %	41.2 %	63 %

Fig. 2.18: Titration of 5´-Labeling of m^5C- or C-containing RNA oligos using PNK
A) Two-dimensional TLC of different mixtures of 5´OH-C- or 5´OH-m^5C-containing RNA oligos after PNK-labeling and P1 digest.
B) Quantification of TLC signals using ImageQuant-software.

To analyse the DNAzyme cutting efficiency in the presence of m^5C at the site of cleavage, $tRNA^{Asp}$ molecules were ligated from three RNA fragments, which carry either a C or m^5C at position C38. After radioactive labeling of the 5´-end, equal amounts of $tRNA^{Asp}$ were subjected to DNAzyme cycling, run over a polyacrylamide gel, and the cleaved fraction was compared to the uncleaved by quantification of the bands using ImageQuant software. As it turned out, the DNAzyme is indeed impaired by the presence of m^5C and cuts 4.75 times less efficiently than unmodified tRNA (see Fig. 2.19). This has to be taken into account when the DNAzyme approach is used to quantify modifications within tRNA.

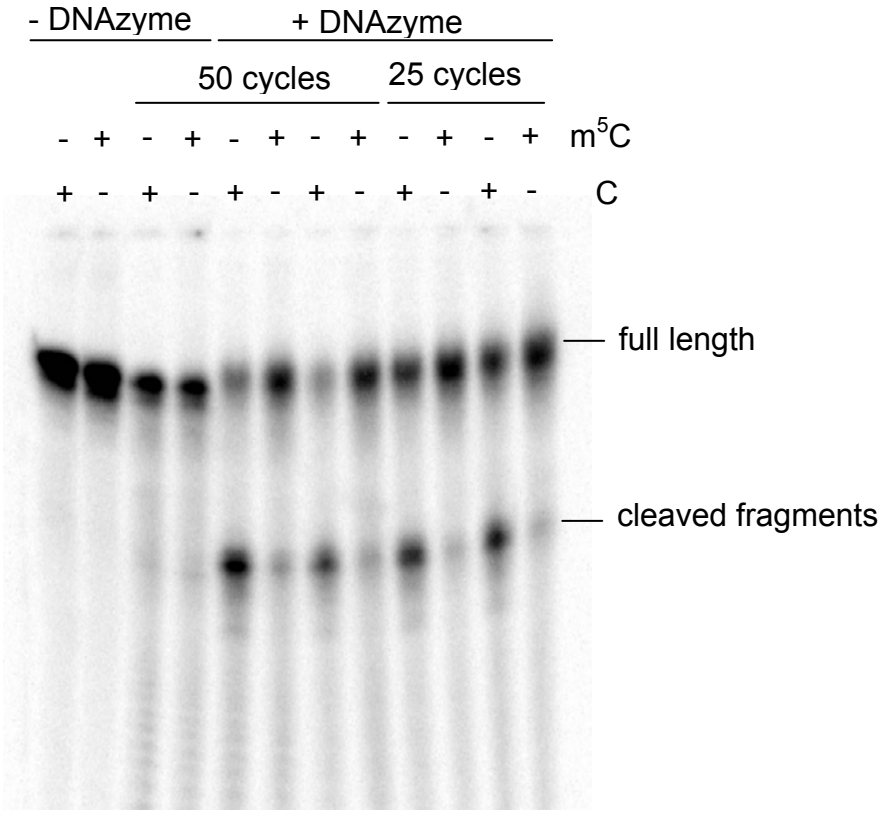

Fig 2.19: Influence of m^5C on the cutting efficiency of the DNAzyme
Radioactively labeled, ligated $tRNA^{Asp}$ containing either m^5C or C at position 38 was incubated with 10 or 100x molar excess of DNAzyme and subjected to 25 or 50 temperature cycles. The presence of m^5C at C38 severly impaired the cleavage efficiency of the DNAzyme.

2.11 A Tandem DNAzyme

Previously, only DNAzymes with one catalytic loop have been described in the literature. To cut a small oligonucleotide out of a tRNA molecule, the subsequent application of several DNAzymes is necessary. If the target regions of the DNAzymes lie too close together, there can be mutual inhibition and a decrease in cleavage efficiency. In this case a consecutive approach becomes necessary, where the cleaved fragments have to be gel-purified before being incubated with the next DNAzyme. The purification steps lead to a considerable amount of material loss. To overcome this problem, and to test whether a multiple-loop-DNAzyme is functional, a tandem DNAzyme comprising two catalytic loops was designed.

Fig. 2.20 compares the action of two DNAzymes with a single-molecule tandem DNAzyme recognizing the same cutting sites. As depicted in the two lanes on the right, the tandem DNAzyme “34” cleaves with similar efficiency as the combination of the two DNAzymes “3” and “4” (Fig. 2.20 C). This is a new method to isolate the anticodon loop of a desired target tRNA. Due to the enrichment of the desired region – e.g. the anticodon loop in this case – the analysis of the unknown modification content is facilitated and the signal-to-noise ratio can be increased. Identification of the modifications e.g. by mass spec should yield cleaner signals when analyzing only the loop region and not the entire tRNA.

2.12 Comparison of Two tRNA Methyltransferases Both Acting on $tRNA^{Asp}$

The DNAzyme technique allows the analysis and comparison of modification enzymes acting on the same target tRNA at different target sites. This approach can be used to identify and separate different modification types or to compare the same modification introduced at different positions by two modification enzymes. To demonstrate this possibility, $tRNA^{Asp}$ was methylated by the m^5C tRNA methyltransferase Trm4 from *Saccharomyces cerevisiae* on position 48 plus 49, and by *Drosophila* Dnmt2 on C38 in two separate reactions. After purification, the methylated $tRNA^{Asp}$ was subjected to DNAzyme cycling with the tandem DNAzyme 34 and the DNAzyme III which cuts after the position 58 (Fig. 2.21 A). The fragments carrying the introduced modification were gel-purified, precipitated and digested to single nucleotides (Fig. 2.21 B). Two-dimensional thin layer chromatography permitted the detection and quantification of 5-methyl-cytosine on a cellulose plate (Fig. 2.21 C). Modification by Trm4 could only be detected in the 18-mer that includes the predicted target sites 48 and 49. No Trm4-mediated methylation could be observed in the 9-mer derived from the anticodon loop (Fig. 2.21 C, upper and lower panel on the left). Dnmt2, on the other hand, was found to methylate in the 9-mer only, but not in the 18-mer (Fig. 2.21 C, upper and lower panel on the right). The methylation signal for Trm4 is higher than for Dnmt2, and was quantified to 0.8 mol m^5C per mol tRNA (the methylation signal of Dnmt2 was quantified to 0.05 mol m^5C per mol tRNA). The low Dnmt2-mediated methylation signal can be either attributed to poor performance of the enzyme prep out of Drosophila cells (in this experiment no

fresh DTT was added), or to the quantification procedure, since the intensity of the cytosine spot is out of the linear range, which could impede the exact determination of the low m^5C signal. With human recombinant Dnmt2, the modification yield is similar to the one obtained by Trm4 (compare with Fig. 2.15 A and C).

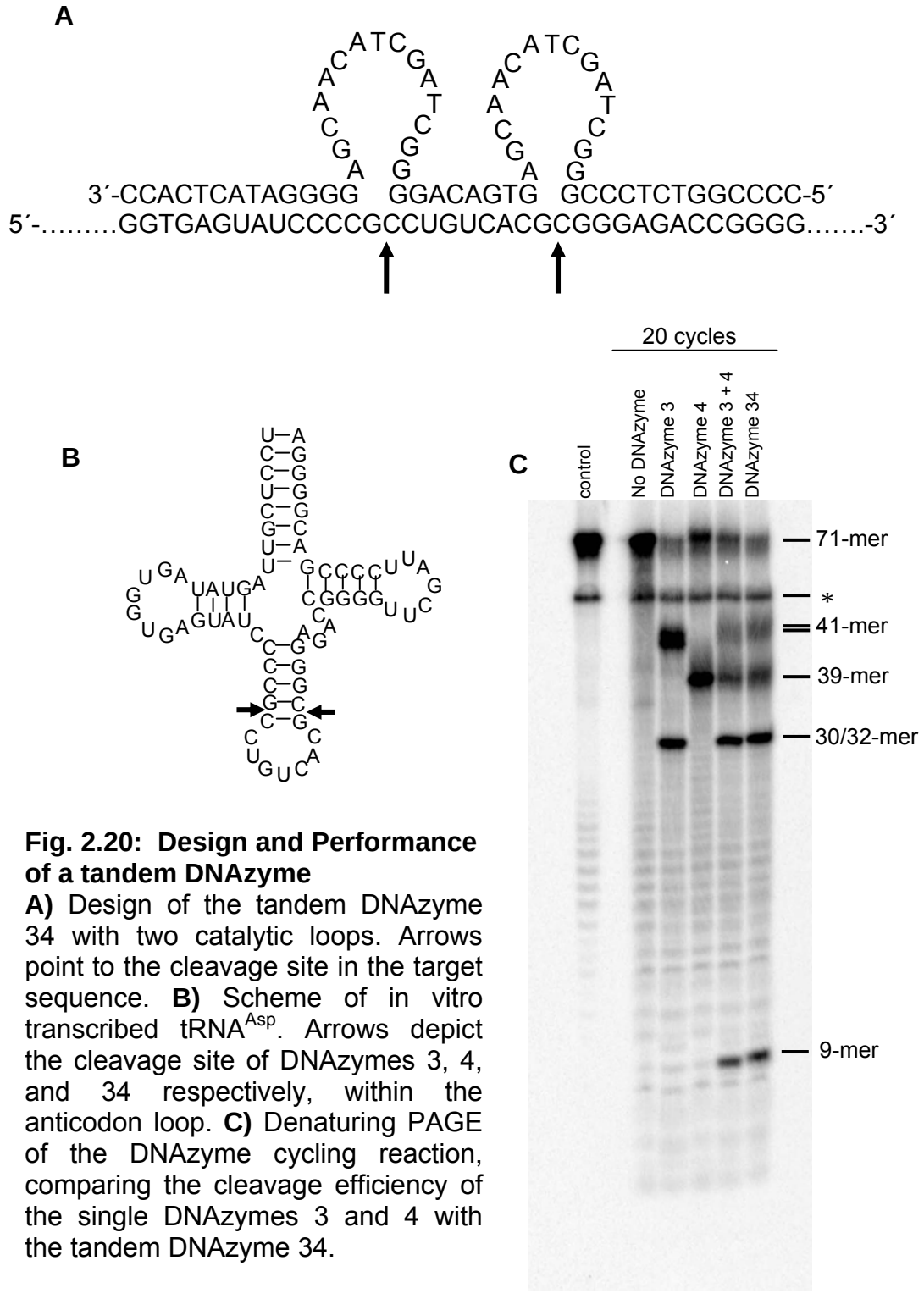

Fig. 2.20: Design and Performance of a tandem DNAzyme
A) Design of the tandem DNAzyme 34 with two catalytic loops. Arrows point to the cleavage site in the target sequence. **B)** Scheme of in vitro transcribed $tRNA^{Asp}$. Arrows depict the cleavage site of DNAzymes 3, 4, and 34 respectively, within the anticodon loop. **C)** Denaturing PAGE of the DNAzyme cycling reaction, comparing the cleavage efficiency of the single DNAzymes 3 and 4 with the tandem DNAzyme 34.

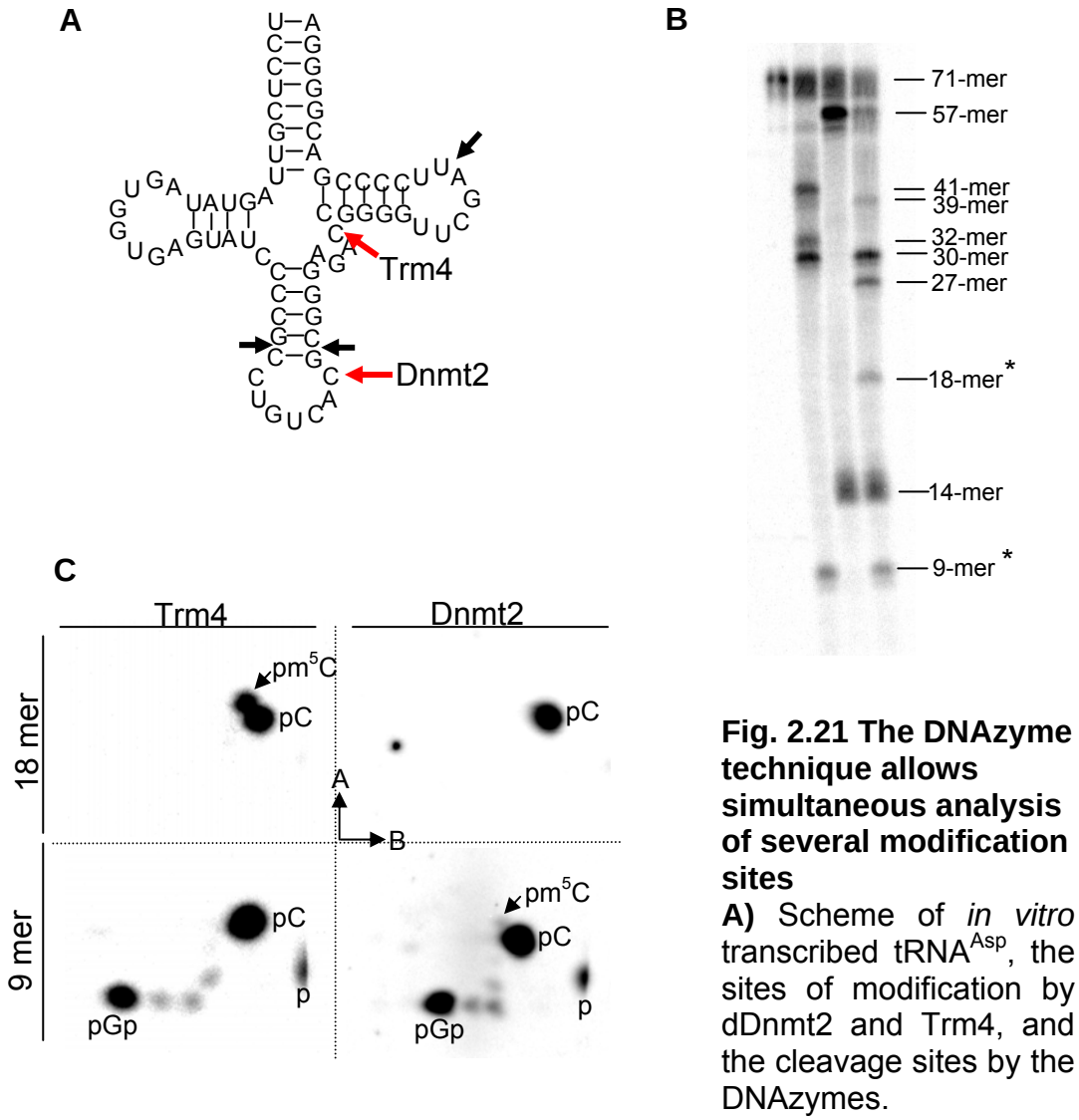

Fig. 2.21 The DNAzyme technique allows simultaneous analysis of several modification sites

A) Scheme of *in vitro* transcribed $tRNA^{Asp}$, the sites of modification by dDnmt2 and Trm4, and the cleavage sites by the DNAzymes.

B) Polyacrylamide gel electrophoresis of pre-modified, DNAzyme-cleaved $tRNA^{Asp}$. Asterisks mark bands which contain the modified cytidines. **C)** Two-dimensional TLC of the 18-mer (containing the Trm4 modification site) and of the 9-mer (containing the Dnmt2 modification site). Trm4-mediated m^5C formation is limited to the 18-mer, and Dnmt2-mediated m^5C formation is limited to the 9-mer. Purified recombinant Trm4 from *S. cerevisiae* shows a higher activity than the Flag-tagged *Drosophila* Dnmt2 which was purified out of cells.

2.13 *In Vivo* Substrates of Dnmt2

Native, fully modified tRNAs can also be a substrate for Dnmt2, as long as existing modifications do not block the methylation target site. Total tRNA preparations of *E. coli*, *S. cerevisiae*, and *D. melanogaster* were tested with *Drosophila* Dnmt2 in the *in vitro* methylation assay. Since m^5C is not present in the tRNA of bacteria, it is not surprising that the *E. coli* tRNA is a good substrate for Dnmt2 (Fig. 2.22). *S. cerevisiae* is besides *C. elegans* the only eukaryotic model organism which does not possess a Dnmt2 enzyme. Despite the absence of an endogenous competitor, however, the total tRNA preparations of brewers´ yeast are not a substrate for Dnmt2 in the *in vitro* assay. Possible explanations for this finding are that the Dnmt2 target sites are modified otherwise, that modifications located nearby interfere with the substrate recognition by Dnmt2, or that a different m^5C tRNA methyltransferase has adopted the function of Dnmt2 in yeast. Native tRNA isolated from OrR or $Dnmt2^{215}$ wildtype flies cannot be modified by Dnmt2 any further in the *in vitro* assay, indicating that all possible target sites are either fully methylated or inaccessible for further methylation, for example due to modifications in the vicinity of the target region. Total tRNA derived from a Dnmt2 null background, such as $Dnmt2^{149}$ or the founder line EP, however, can be methylated by Dnmt2 (Fig. 2.22).

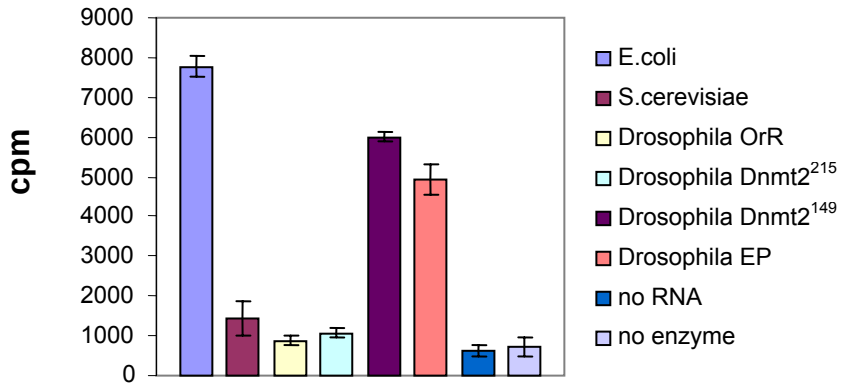

Fig. 2.22: Dnmt2 methylates total tRNA of *E. coli*, $Dnmt2^{149}$, and the founder line EP
In vitro methylation assay using *Drosophila* Dnmt2 enzyme and total tRNA of *E. coli, S. cerevisiae*, and *D. melanogaster* (OrR, $Dnmt2^{215}$, $Dnmt2^{149}$, EP). Wildtype-derived tRNA is already modified and leaves no site for additional methylation by Dnmt2. tRNA of *E. coli* contains no m^5C and is therefore readily accepted as a substrate. Even though *S. cerevisiae* contains no endogenous Dnmt2 enzyme, its tRNA is not a substrate for dDnmt2. Triplicate measurements of one experiment are shown.

2.14 Quantification of *In Vivo* tRNA^{Asp} Methylation at C38

After the establishment of the DNAzyme technique, the approach was applied to tRNA molecules which were isolated out of *Drosophila melanogaster* wildtype and mutant embryos. tRNA^{Asp} was specifically isolated out of a pool of total RNA from *Drosophila* embryos (over night collections) using a biotinylated oligo complementary to 37 bases of the tRNA^{Asp} sequence. The enrichment of tRNA^{Asp} was confirmed via a T1-ladder after end-labelling (Nuclease T1 cuts after every G and therefore leads to a sequence-specific pattern, or ladder). After gel purification, the tRNA was subjected to DNAzyme cycling. The DNAzyme cleavage leaves the C38 (the site of interest) with a free 5´OH-group, which allows radioactive labeling with T4 PNK. After another gel-purification step, the labeled fragments were digested to single nucleotides and separated by two-dimensional TLC. As expected, there was an m^{5}C spot in the TLC depicting tRNA from Dnmt2-expressing wildtype flies (either OrR or Dnmt2^{215}; Fig. 2.23 A, left and middle panel). No m^{5}C spot could be detected in tRNA isolated from Dnmt2^{149} embryos (right panel). In summary, the published observations – the methylation of tRNA^{Asp} of Drosophila melanogaster at position C38 – could be confirmed. The application of the DNAzyme technique to verify the published data was advantageous over the mass spectrometry used previously (Goll et al., 2006), as the TLC signal was clean and a smaller amount of tRNA material was needed.

The TLC signals were quantified using Imagequant software. In wildtype *Drosophila* embryos, C38 is methylated between 31 % (OrR) and 37 % (Dnmt2^{215}) of all tRNA^{Asp} molecules, whereas no m^{5}C can be detected at C38 in the Dnmt2^{149} background (Fig. 2.23 B). Compared to the data in Figure 2.22, a higher degree of methylation would have been expected. The question remains, why total tRNA isolated from wildtype is not methylated further by Dnmt2 in an *in vitro* methylation assay (Fig. 2.22), if not all C38 are converted to m^{5}C. However, it could be possible that a subgroup of tRNA^{Asp} contains modifications in close proximity to C38 which hinder the methylation at C38.

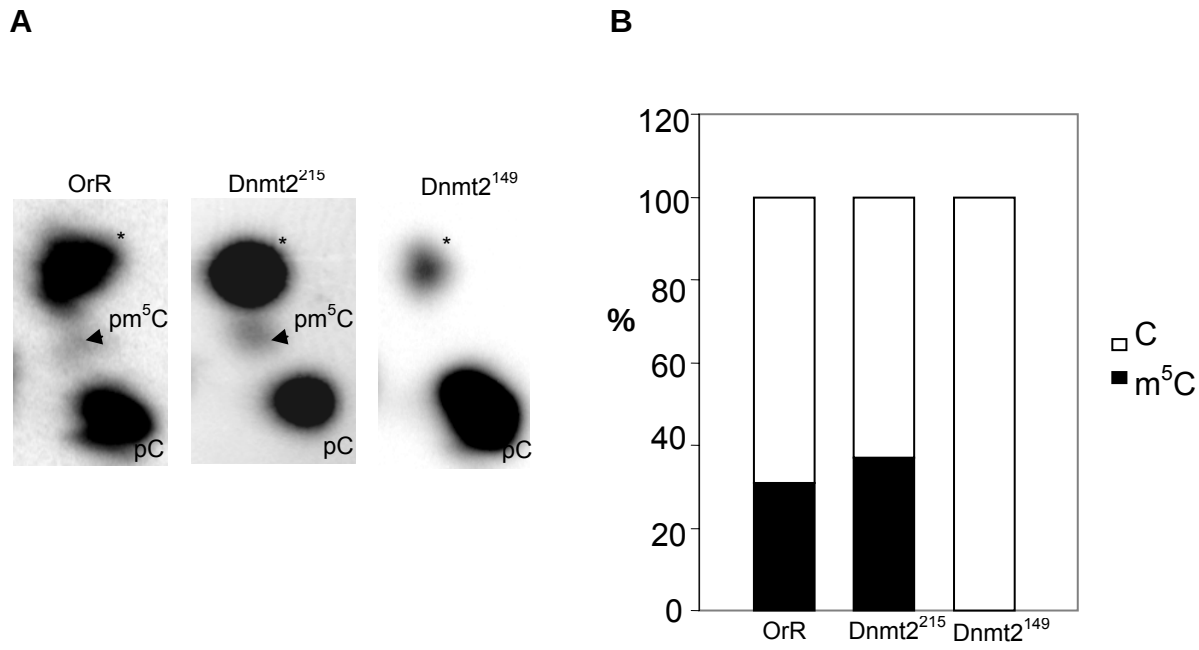

Fig. 2.23 tRNA^{Asp} is methylated *in vivo* by Dnmt2
A) Two-dimensional TLC of position 38 of isolated and DNAzyme-cut tRNA^{Asp} from *Drosophila melanogaster*. In the wildtype (OrR and Dnmt2^{215}, left and middle panel), a m^{5}C spot (pm^{5}C) is clearly visible. In the Dnmt2^{149} mutants, no m^{5}C spot is observed (right panel). Asterisk: unrelated labelling of residual DNAzyme.
B) Quantification of the TLC signal in (A) after background correction. Black: C at position 38, white: m^{5}C at position 38.

2.15 *In Vitro* Transcribed tRNA^{Val} Is Also a Target of Dnmt2

After the thorough investigation of *in vitro* transcribed and *ex vivo* isolated tRNA^{Asp} of *Drosophila melanogaster*, the analysis was extended to the search for further targets. Among obvious candidates are those tRNAs which also contain a C38. This includes tRNA^{Asp} molecules from other species (Fig. 2.24 A), for example from *Saccharomyces cerevisiae* and *Pyrococcus abyssi*. In *Drosophila melanogaster,* tRNA^{Glu}, tRNA^{Gly}, tRNA^{His}, and tRNA^{Val} also possess a C38. tRNA^{Val} of *Drosophila melanogaster* was chosen as the most promising candidate, since it had been reported to carry a m^{5}C at position 38 (Addison et al., 1982).
dDnmt2 methylates *in vitro* transcribed, unmodified tRNA^{Val} with similar efficiency as *in vitro* transcribed tRNA^{Asp} from *Drosophila melanogaster* (see Fig. 2.24 A). However, not all tRNAs carrying a C38 are automatically targets of Dnmt2.

Mitochondrial tRNA$^{Leu(CUN)}$ has a stable cloverleaf structure and could therefore be considered a target for the structure-sensitive Dnmt2 enzyme. Still, it is not recognized as a substrate (Fig. 2.24 A). This could be explained by the absence of conserved nucleotides within the substrate tRNA, which are necessary for recognition and methylation by Dnmt2, and remain to be identified.

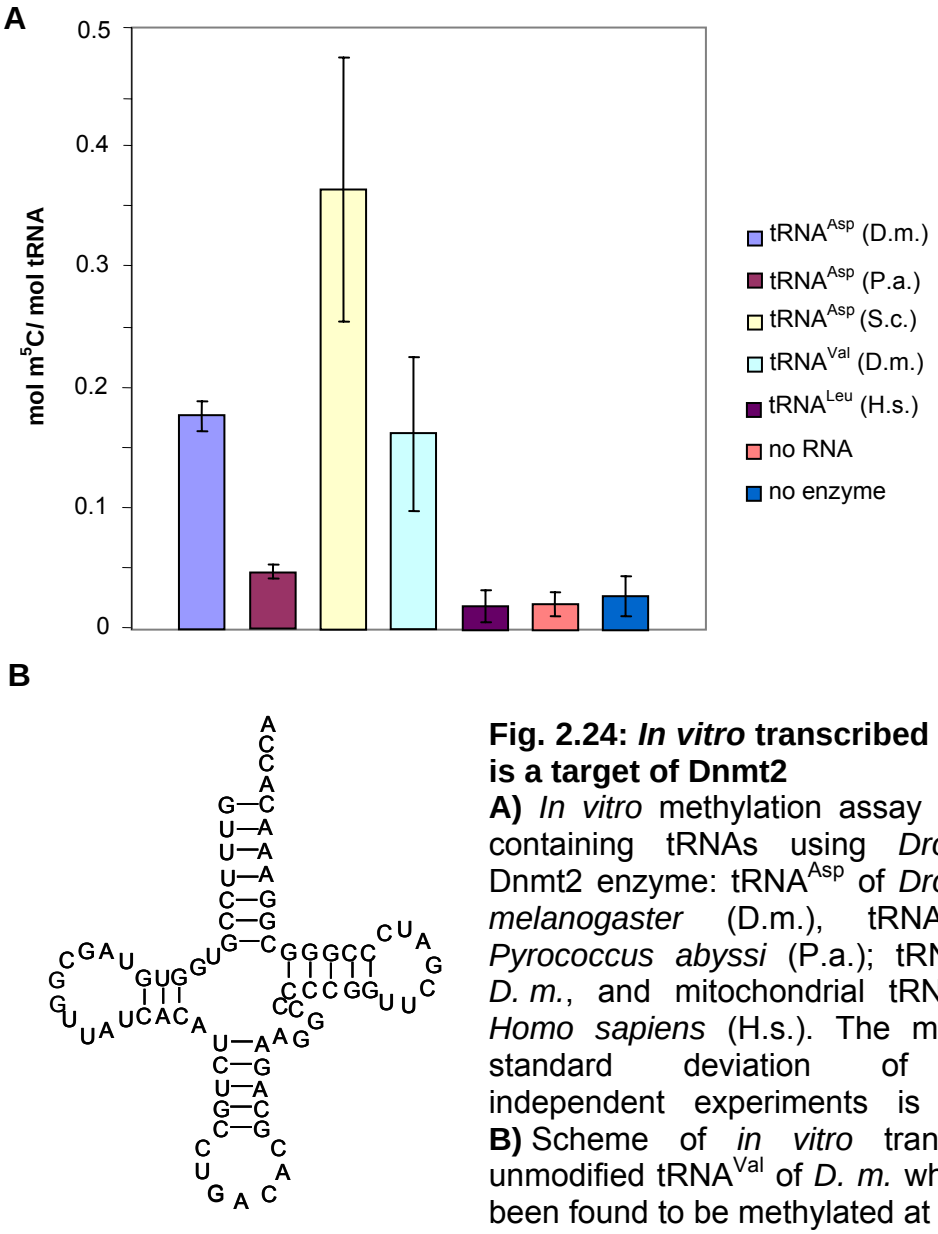

Fig. 2.24: *In vitro* transcribed tRNA^{Val} is a target of Dnmt2
A) *In vitro* methylation assay of C38-containing tRNAs using *Drosophila* Dnmt2 enzyme: tRNA^{Asp} of *Drosophila melanogaster* (D.m.), tRNA^{Asp} of *Pyrococcus abyssi* (P.a.); tRNA^{Val} of *D. m.*, and mitochondrial tRNA^{Leu} of *Homo sapiens* (H.s.). The mean +/- standard deviation of three independent experiments is shown. **B)** Scheme of *in vitro* transcribed, unmodified tRNA^{Val} of *D. m.* which had been found to be methylated at C40.

2.16 $tRNA^{Val}$ Is Methylated by Dnmt2 *In Vivo*

C38 methylation in $tRNA^{Val}$ had been reported in *Drosophila melanogaster* (Addison et al., 1982), but it remained to be determined whether the Dnmt2 enzyme was responsible for this modification. If $tRNA^{Val}$ is methylated in a Dnmt2-dependent manner, then the m^5C signal should be absent in $tRNA^{Val}$ from $Dnmt2^{149}$ mutant flies. Similar to $tRNA^{Asp}$, $tRNA^{Val}$ was isolated out of a preparation of total embryonic RNA of wildtype and mutant using an oligo complementary to $tRNA^{Val}$. Again, the specific isolation of $tRNA^{Val}$ was monitored via a T1-ladder which provides a sequence specific banding pattern. A mix of several tRNA species would result in a smear or an aberrant banding pattern. Since there was a clear banding pattern, and therefore clean enrichment of $tRNA^{Val}$, the tRNA was subjected to DNAzyme cycling, gel purification and P1 digestion similar to $tRNA^{Asp}$ (see chapter 2.14). The two-dimensional TLC showed an m^5C spot in wildtype (the revertant $Dnmt2^{215}$) embryos but not in $Dnmt2^{149}$ mutant embryos (Fig. 2.25). Therefore, the C38 methylation of $tRNA^{Val}$ is mediated by Dnmt2. The TLC spots corresponding to m^5C and C were quantified using the ImageQuant 5.2 software. However, it is crucial to take the correction factors into account since otherwise the m^5C signal will not be quantified adequately. This has two reasons: First, the DNAzyme cleaves m^5C containing RNA about 4.75 times less efficient than the same RNA containing an unmodified cytosine instead. Second, the enzyme Polynucleotide kinase (PNK) which is used for 5´-radioactive labeling also has a slight preference for C as opposed to m^5C (factor 1:0.8 – 0.9), as described in chapter 2.10. With the introduction of the correction factors, the quantification experiments show an average methylation level of C38 in $tRNA^{Val}$ of 89 % in OrR and 97 % in $Dnmt2^{215}$ wildtype embryos, whereas in $Dnmt2^{149}$ mutants, the large majority of C38 (96 %) is unmethylated. The remaining 4 % can be attributed either to background signals (m^5C signal coming from a different position, due to degradation in the DNAzyme cycling process, which was cut out with the correct-sized band) or to methylation of this site by an additional hypothetical enzyme. The methylation level of *Drosophila*-isolated $tRNA^{Val}$ is higher than Dnmt2-mediated methylation of $tRNA^{Asp}$, indicating that Dnmt2-mediated tRNA methylation can be regulated.

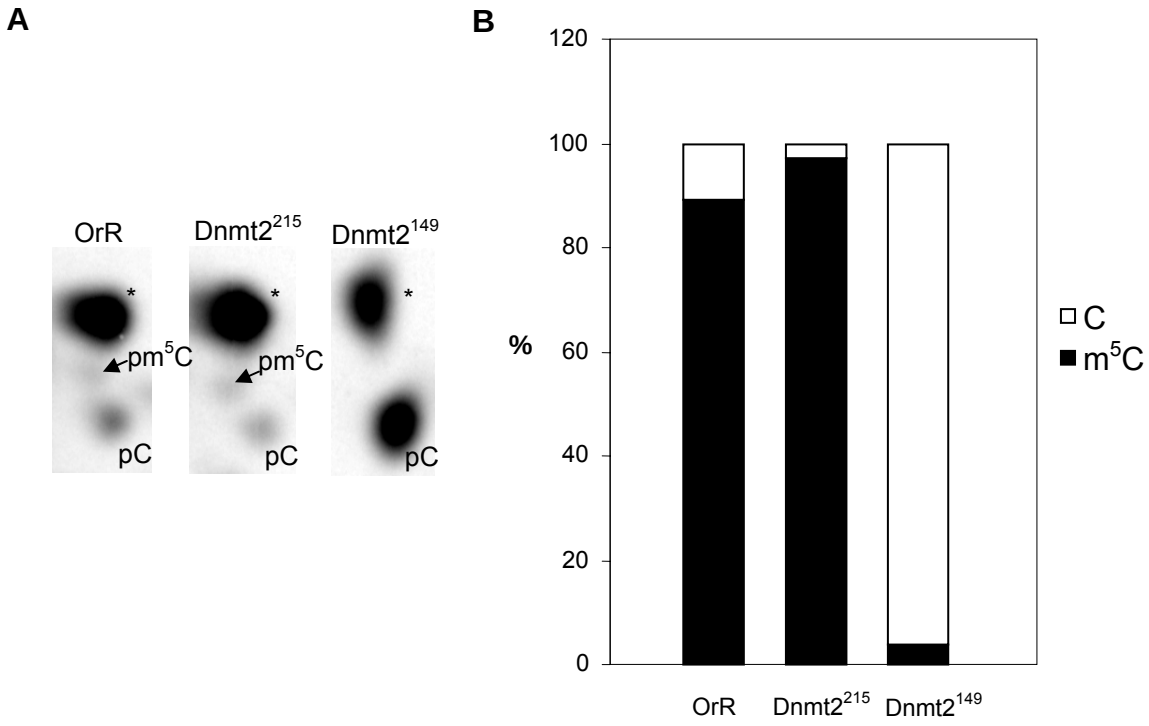

C

	tRNA^{Val} OrR	tRNA^{Val} 215	tRNA^{Val} 149
% m^{5}C at Position 38	**89 %**	**97 %**	**4 %**
% C at Position 38	**11 %**	**3 %**	**96 %**

Fig 2.25: tRNA^{Val} is methylated at C38 by Dnmt2 *in vivo*
A) Two-dimensional TLC of the C38 locus of tRNA^{Val} (isolated from *Drosophila* embryos). Left panel and middle panel: tRNA isolated from wildtype embryos (OrR and Dnmt2^{215}). An m^{5}C spot is detectable. Right panel: tRNA isolated from mutant embryos (Dnmt2^{149}). No m^{5}C signal can be detected, and the cytosine (pC) spot is stronger, arguing for complete absence of m^{5}C methylation at C38 in the Dnmt2 null background. The asterisk marks a DNAzyme derived spot which is unrelated to the C38 signal. **B)** and **C)** Quantification of the TLC signals using ImageQuant 5.2 software.

2.17 Dnmt2 Activity Is Not Limited to C38

Originally, a transcript of tRNA^{Phe} from *S. cerevisiae* was intended to be included as a negative control in the *in vitro* methylation assays, as this tRNA has no C38, but an adenine at this position instead (see Fig. 2.26). Surprisingly, when incubated with Dnmt2, tRNA^{Phe} appeared to be a substrate for the enzyme, since methylation of the

in vitro transcribed tRNA^{Phe} could be distinctly detected. Native (fully modified) tRNA^{Phe} (purified out of yeast) showed no further methylation by Dnmt2 in the assay (see Fig. 2.26 B). This implied that the methylation of tRNA^{Phe} by Dnmt2 could take place at a site which is usually modified (and thereby inaccessible for further methylation by Dnmt2). The strongest candidate was C40. Firstly, this site is methylated by an intron-dependent mechanism by Trm4. Secondly, the site of modification lies very close to the C38 site which is recognized by Dnmt2 in tRNA^{Asp} and tRNA^{Val}.

A template for *in vitro* transcription was designed, where C40 was exchanged for G40, and the corresponding, Watson-crick-pairing G30 to a C30, to keep the overall stem-loop architecture intact. This construct, where the putative modification site has been abolished, was tested together with wildtype, *in vitro* transcribed tRNA^{Phe} in the methylation assay using hDnmt2. The lack of C40 led to a complete absence of Dnmt2 activity on tRNA^{Phe} (Fig. 2.26 C), which confirms the hypothesis that tRNA^{Phe} is methylated at C40 by Dnmt2.

A

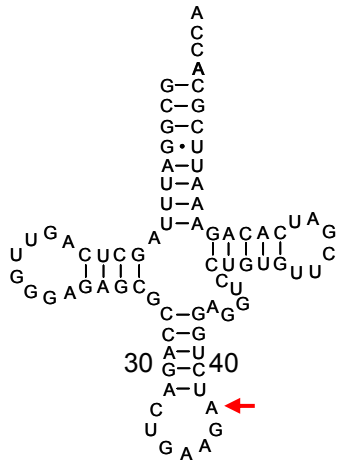

Fig. 2.26:
A) tRNA^{Phe} of *S. cerevisiae*
Schematic representation of *in vitro* transcribed tRNA^{Phe} from *S. cerevisiae*. The arrow points to position 38 which is occupied by adenine, not cytosine.

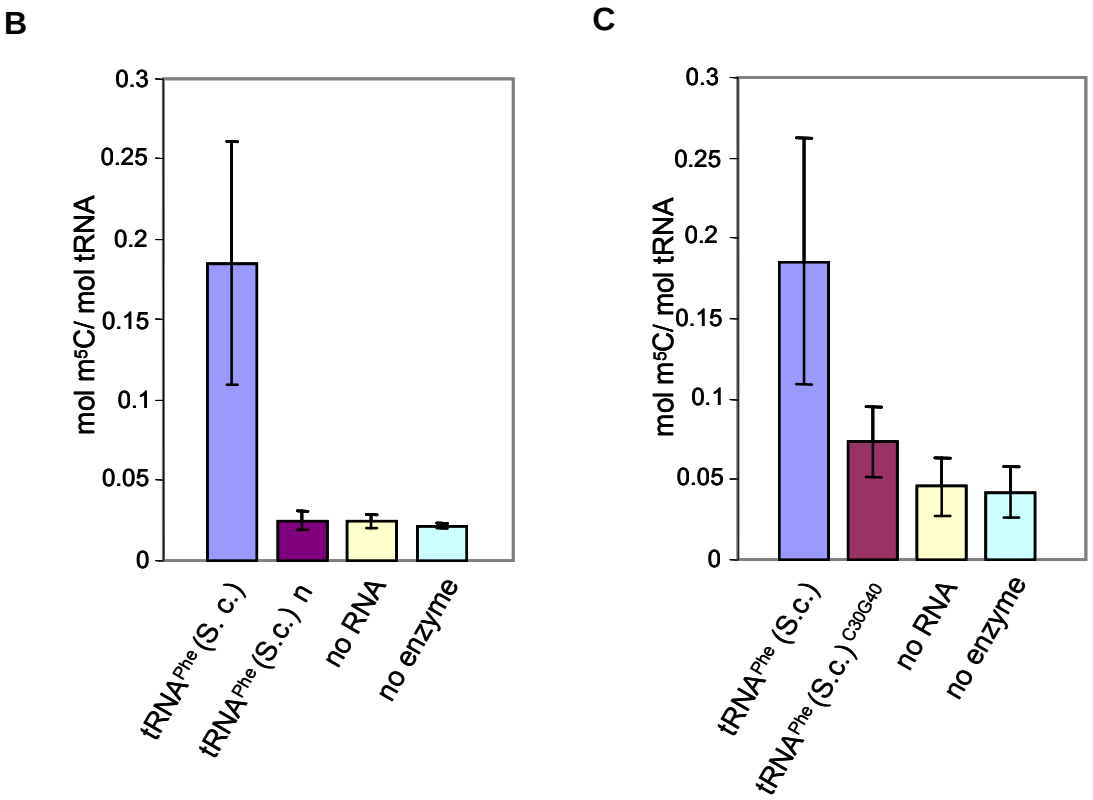

Fig. 2.26 continued

B) Dnmt2 activity is not limited to C38

Methylation assay of *in vitro* transcribed $tRNA^{Phe}$ (blue bar), native $tRNA^{Phe}$ isolated out of yeast (purple bar) and the negative controls (yellow and green bars). hDnmt2 can only methylate unmodified, *in vitro* transcribed $tRNA^{Phe}$. The mean +/- standard deviation of at least three independent experiments is shown.

C) hDnmt2 methylates $tRNA^{Phe}$ from *S. cerevisiae* at C40

The exchange of C40 to G40 and of the Watson-Crick pairing G30 to C30 abolishes the catalytic activity of hDnmt2 (violet bar) compared to wildtype (blue bar). Therefore, hDnmt2 methylates C40 in $tRNA^{Phe}$. Yellow and green bar: negative controls measuring background signals. The mean +/- the standard deviation of at least three independent experiments is shown.

2.18 Additional *In Vitro* Targets of Dnmt2

It is plausible that *in vitro* transcribed $tRNA^{Phe}$ from *S. cerevisiae* is not the only target which is lacking C38 and is still being recognized and methylated by the Dnmt2 enzyme. Since the characterization of $tRNA^{Phe}$-methylation led to the identification of C40 as second possible modification site, a panel of several non-C38 containing tRNAs was screened for their target qualities regarding Dnmt2 (Fig. 2.27). $tRNA^{Lys}$ from *H. sapiens* and from *D. melanogaster* was found to be an even better substrate than $tRNA^{Phe}$ from *S. cerevisiae*. Modification levels were calculated to 65 % for *Drosophila* $tRNA^{Lys}$, and 90 % for human $tRNA^{Lys}$. Mitochondrial human $tRNA^{Thr}$ was not a substrate for hDnmt2. Since the substrate recognition of Dnmt2 depends on the correct structure (chapter 2.9; Fig. 2.16), and the structure of mitochondrial tRNAs can deviate from the canonical cloverleaf structure, this structural divergence most likely prevents the methylation by Dnmt2.

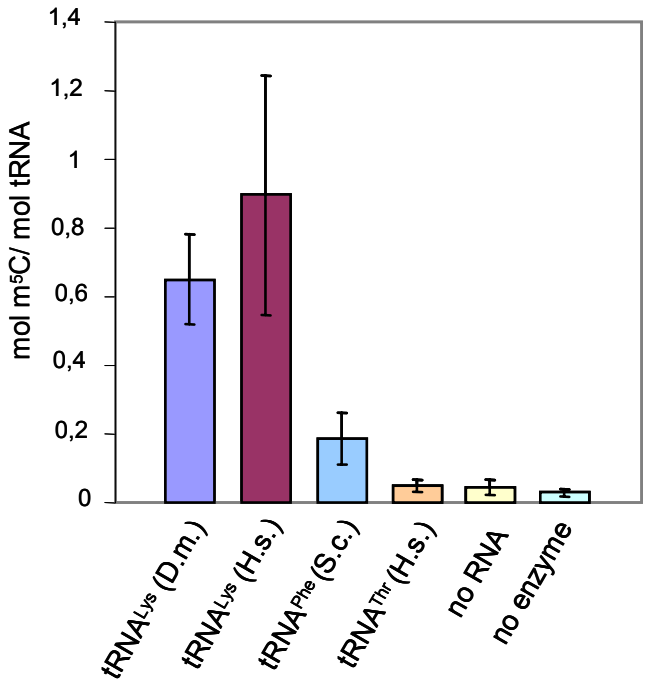

Fig 2.27: Dnmt2 methylation is not limited to C38
In vitro methylation assay of a panel of tRNAs which do not contain C38. $tRNA^{Lys(AAG)}$ from *D. melanogaster* and $tRNA^{Lys(AAA)}$ from *H. sapiens*, as well as $tRNA^{Phe}$ from *S. cerevisiae* were methylated by human Dnmt2 with varying efficiencies. Mitochondrial $tRNA^{Thr}$ of *H. sapiens* was included as a non-C38-containing tRNA that is not a target of hDnmt2. Negative controls were conducted either without enzyme or without RNA substrate. The mean +/- the standard deviation of at least three independent experiments is shown.

2.19 tRNA^{Lys} Is Modified at C40 and C42 by hDnmt2 *In Vitro*

The characterization of the modification site of *in vitro* methylated tRNA^{Lys} of *D. melanogaster* started with the rough determination of the target region. For this purpose, two DNAzymes were designed to divide the tRNA^{Lys} into three parts (Fig. 2.28 A). The efficient cutting is demonstrated in Fig. 2.28 B. Then, *in vitro* transcribed tRNA^{Lys} was subjected to *in vitro* methylation by hDnmt2 using tritiated SAM. After purification and precipitation, the tRNA carrying the radioactive methyl group was cleaved using both DNAzymes, and then resolved by denaturing polyacrylamide gel electrophoresis. [α-^{32}P]-CTP transcribed, DNAzyme-incubated tRNA^{Lys} was used as a marker to cut out the resulting bands. After elution from the gel, the remaining radioactivity was measured using liquid scintillation counting.

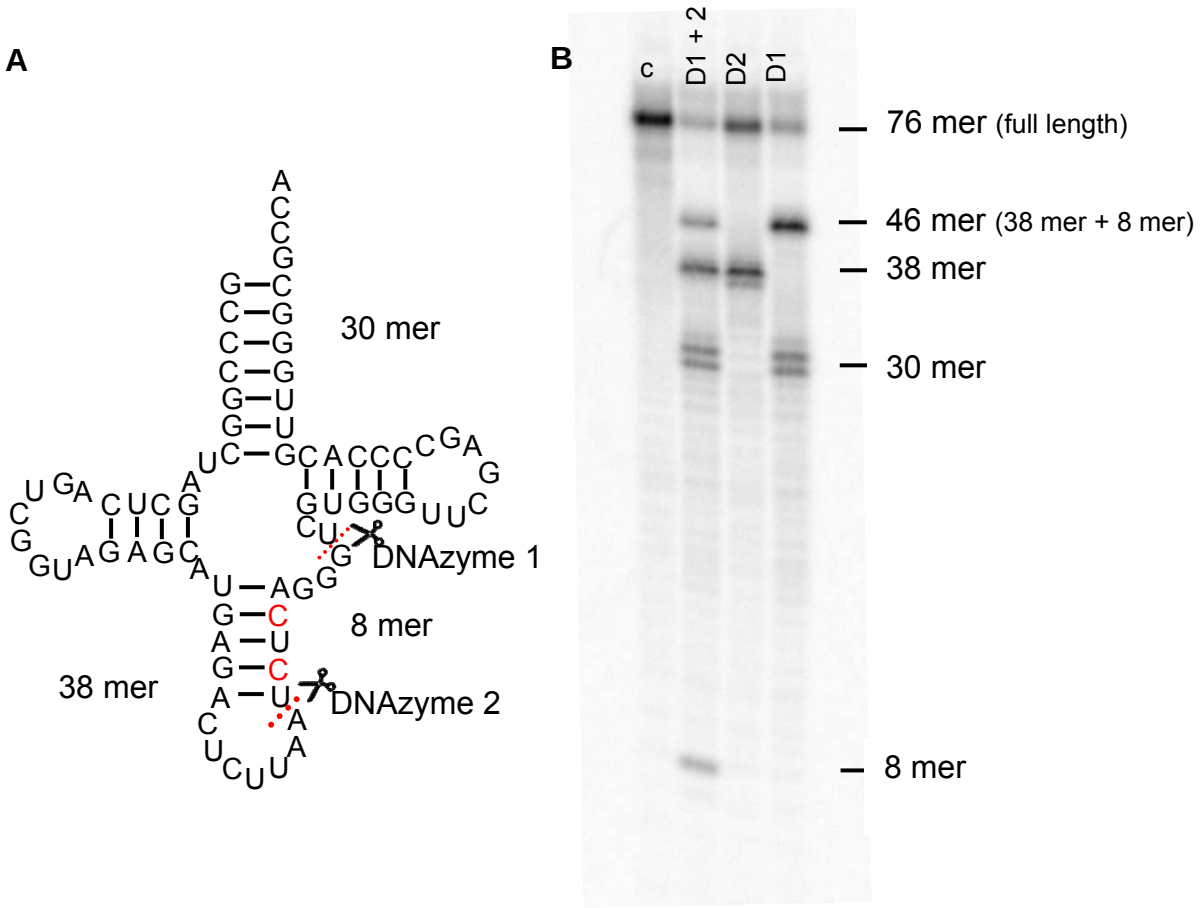

Fig. 2.28: DNAzyme design of tRNA^{Lys} of *D. melanogaster*
A) Schematic overview of *in vitro* transcribed, unmodified tRNA^{Lys} and the cutting sites of DNAzyme 1 and DNAzyme 2. **B)** Denaturing PAGE of the DNAzyme cycling reaction. Lane 1: tRNA^{Lys} only; lane 2: cycling with DNAzyme 1 and 2, lane 3: cycling with DNAzyme 2, lane 4: cycling with DNAzyme 1.

Since the $tRNA^{Lys}$ was not cut completely, there are four possible fragments which can carry the methylation signal: The cutting of DNAzyme 1 will only give rise to the fragments 46 and 30; the action of DNAzyme 2 yields two 38-mers, and the cleavage of both enzymes leads to the generation of an 8-mer. Methylation was readily detectable in the uncut fragment, the 46-mer and the 8-mer, but not in the 38-mer and the 30-mer (Fig. 2.29). Methylation in the T-Loop can therefore be completely excluded. Residual methylation signal in the 38-mer was observed in one out of two experiments and resulted from the incomplete cutting of DNAzyme1. This suggests that the methylation signal lies in the second half of the tRNA. Since this second half is comprised of the 8-mer and 30-mer, the methylation can be narrowed down to the 8-mer.

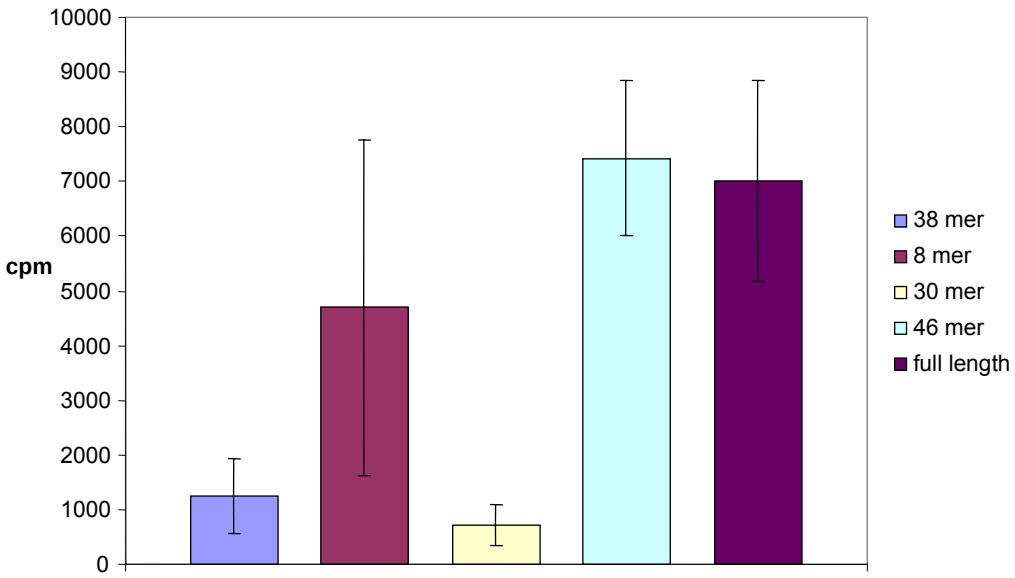

Fig 2.29: Methylation of $tRNA^{Lys}$ by hDnmt2 can be narrowed down to C40 and C42
Methylated $tRNA^{Lys}$ was subjected to DNAzyme cycling reactions. The fragments were resolved by denaturing PAGE, and subjected to scintillation counting. The 38-mer (blue bar) and 30-mer (yellow bar) did not show any methylation signal. A clear methylation signal is seen in the 8-mer (purple bar), which harbours only two cytosines, C40 and C42. The 46-mer (green bar) – arising from incomplete cutting – as well as the full length $tRNA^{Lys}$ (dark purple) also shows a methylation signal, since they both contain the 8-mer fragment. Therefore, the site of Dnmt2-dependent methylation of $tRNA^{Lys}$ can be limited to the anticodon stem. Summary of two independent experiments.

There are only two cytosines in the 8-mer (C40 and C42) which can carry a tritiated methyl group. To confirm the exact target site of Dnmt2-mediated $tRNA^{Lys}$ methylation *in vitro*, several constructs were designed for *in vitro* transcription, where one or more bases were exchanged (Fig. 2.30 B). After *in vitro* transcription and purification, the mutated $tRNA^{Lys}$ constructs were tested in the standard *in vitro* methylation assay using ^{3}H-SAM as a methyl group donor (Fig. 2.30 C). Surprisingly, only two of the six constructs showed a severe reduction (up to complete inactivation) in enzymatic activity: Construct “e” harbours two Gs lying opposite to each other, which interrupts the anticodon stem loop structure. Previous experiments showed that the correct three-dimensional architecture of tRNA is important for target recognition (Fig. 2.16). The destruction of the anticodon stem could therefore be the reason for the enzymatic inactivity. In construct “d”, all cytosines were completely eliminated from the anticodon stem and replaced by U. Due to lack of cytosine as a substrate for methyl-group transfer, the enzymatic activity is reduced. However, the elimination of only one of the two cytosines at positions 40 and 42 and their replacement by G did not have any impact on methyl group transfer by Dnmt2. In other words, *in vitro* transcribed $tRNA^{Lys}$ can be methylated at C40 and/ or C42. It is unclear, however, whether the enzyme preferentially methylates one of the two cytosines. In summary, Dnmt2 is able to methylate C40 and 42 *in vitro*, pointing to an unexpected flexibility in the target recognition process.

Due to the unfavourable sequence context of $tRNA^{Lys}$ – the absence of a purine-pyrimidine junction at position 39-40 and 41-42 – it was not possible to analyze purified $tRNA^{Lys}$ from *Drosophila melanogaster* by the DNAzyme approach. The experiment to methylate $tRNA^{Lys}$ isolated from $Dnmt2^{149}$ and wildtype embryos in the *in vitro* methylation assay was not successful. Neither wildtype- nor mutant-derived $tRNA^{Lys}$ was a target of hDnmt2. A database search comparing modified $tRNA^{Lys}$ from several animals ranging from insects to mammals revealed no methylation at the positions 40 or 42. Therefore, the methylation status of $tRNA^{Lys}$ of *Drosophila melanogaster* remains to be determined.

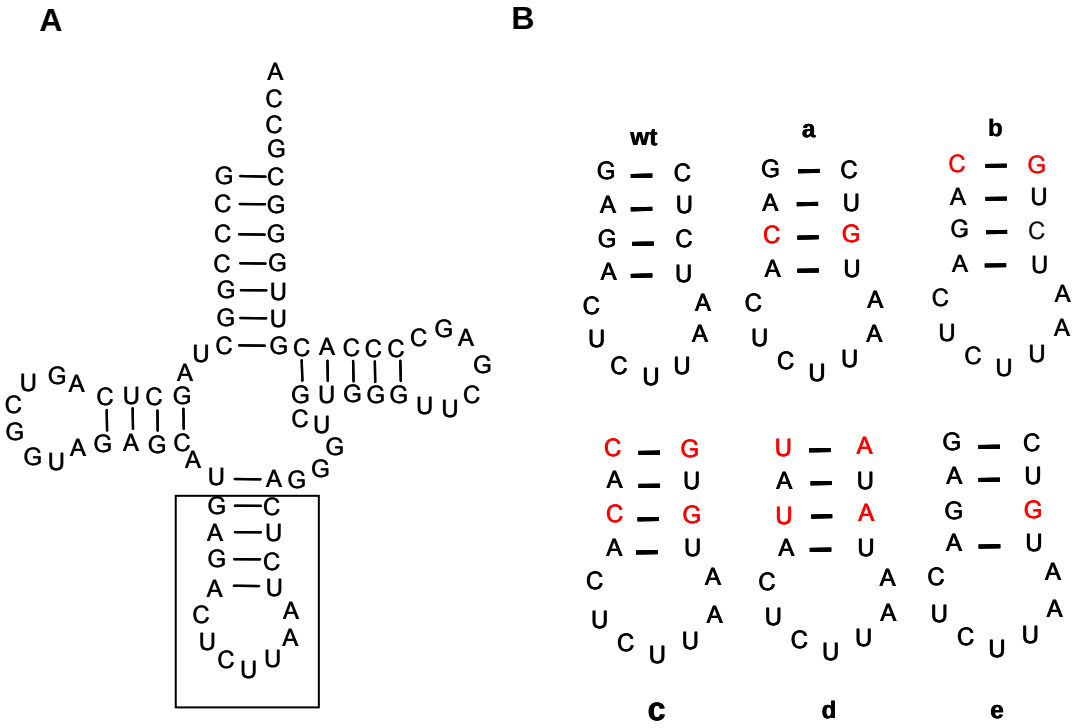

Fig. 2.30: Detailed investigation of the target methylation site of tRNA^{Lys} *in vitro*
A) Drosophila tRNA^{Lys}. **B)** Scheme of the exchanged bases within the anticodon loop. **C)** *In vitro* methylation assay comparing wildtype tRNA^{Lys} with the constructs bearing cytosine exchanges within the anticodon stem. Absence of C40 and C42 (construct d) as well as disruption of the stem architecture (construct e) led to a clear reduction of methylation activity by Dnmt2. The mean +/- the standard deviation of three independent experiments is shown.

2.20 Two Distinct Catalytic Mechanisms of Dnmt2

Dnmt2 was shown to be a tRNA methyltransferase but does not contain the cysteine in motif VI which has been postulated to be the catalytic cysteine in the tRNA methyltransferase Trm4 (Walbott et al., 2007b). Until recently, it was unclear which mechanism is used for the methylation of $tRNA^{Asp}$ by Dnmt2. In collaboration with T. Jurkowski and others, it could be shown that Dnmt2 methylates $tRNA^{Asp}$ via a DNA methyltransferase-like mechanism (Jurkowski et al., 2008). To identify the catalytic residues of importance, all cysteines and two arginine residues (previously identified to play an important role in the DNA methyltransferase MHhaI; O'Gara et al., 1998) of human Dnmt2 enzyme were exchanged for alanine. These Dnmt2 mutants were tested in their ability to methylate $tRNA^{Asp}$. It could be shown that the abrogation of the catalytic cysteine 79 abolished all enzymatic activity. Similarly, the glutamic acid residue E119 of the ENV motif, and the two arginines R160 and R162 were essential for Dnmt2-mediated methylation of $tRNA^{Asp}$ (Jurkowski et al., 2008). The ENV motif is said to be involved in the catalysis due to interaction of the glutamic acid residue with N3 of the cytidine base. A schematic overview of the C79 and E119 residues in catalysis is given in Fig. 2.31. This mechanism is reminiscent of the bacterial DNA methyltransferases.

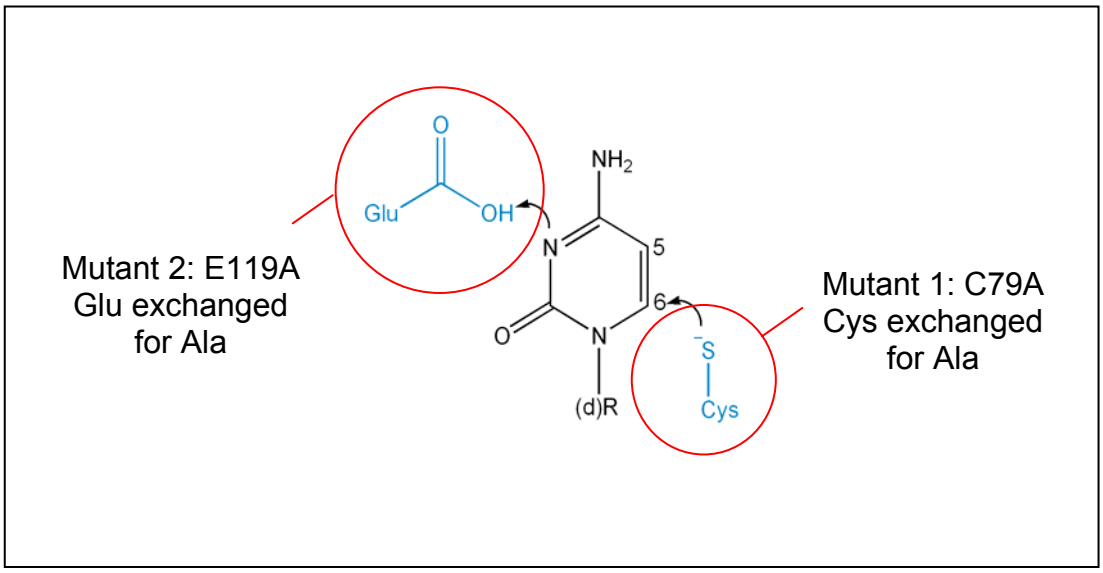

Fig. 2.31: Schematic representation of two catalytic mutants of hDnmt2
In mutant 2, also called E119A (left), the glutamic acid E119 is changed to alanine. E119 facilitates the formation of the enzyme-substrate intermediate by interaction with N3. In mutant 1 (C79A, on the right), the catalytic cysteine was exchanged for alanine, thereby abolishing all catalytic activity (adapted from Jeltsch et al., 2006).

The cysteine 292 mutant within the target recognition domain led to a reduction in methylation. In the present work, three of the generated Dnmt2 mutants – C79A, E119A, and C292A – were obtained and tested in the *in vitro* methylation assay. The results for $tRNA^{Asp}$ could be confirmed, as no methylation of $tRNA^{Asp}$ could be observed in the C79A and E119A mutants (Fig. 2.32). However, the question remained, whether the targets which are methylated at C40 or C42 use the same catalytic mechanism. When *in vitro* transcribed $tRNA^{Phe}$ of *S. cerevisiae* and $tRNA^{Lys}$ of *D. melanogaster* were tested with wildtype Dnmt2 and the three mutants C79A, E119A, and C292A, a surprising difference in catalytic activity of the E119A mutant was observed. This mutant was either equally or more active than wildtype hDnmt2 enzyme when incubated with non-C38 containing tRNAs (Fig. 2.32). Furthermore, the absence of C79 did not abolish the catalytic activity completely, when $tRNA^{Phe}$ and $tRNA^{Lys}$ were used as substrates for Dnmt2. Since 20 to 50 % of the methylation capacity of wildtype Dnmt2 remained in the C79A mutant, C79 cannot be the sole catalytic cysteine in the methylation of $tRNA^{Phe}$ and $tRNA^{Lys}$.The mutant C292A also showed a reduction in catalytic activity in all three tRNAs tested. Since the mutation is located in the target recognition domain, this effect can probably be attributed to a constraint in substrate recognition and binding, and is not directly linked to the methyl group transfer itself. These results describe an unexpected difference in the catalytic mechanism of Dnmt2 between the methylation of position 38 and 40/42. Apparently, for non-C38 targets, E119 is dispensable for Dnmt2-mediated methylation, and its absence is even advantageous for the methylation of $tRNA^{Phe}$ and $tRNA^{Lys}$. Future experiments will be necessary to determine the residues which are important for catalysis of non-C38 tRNA targets.

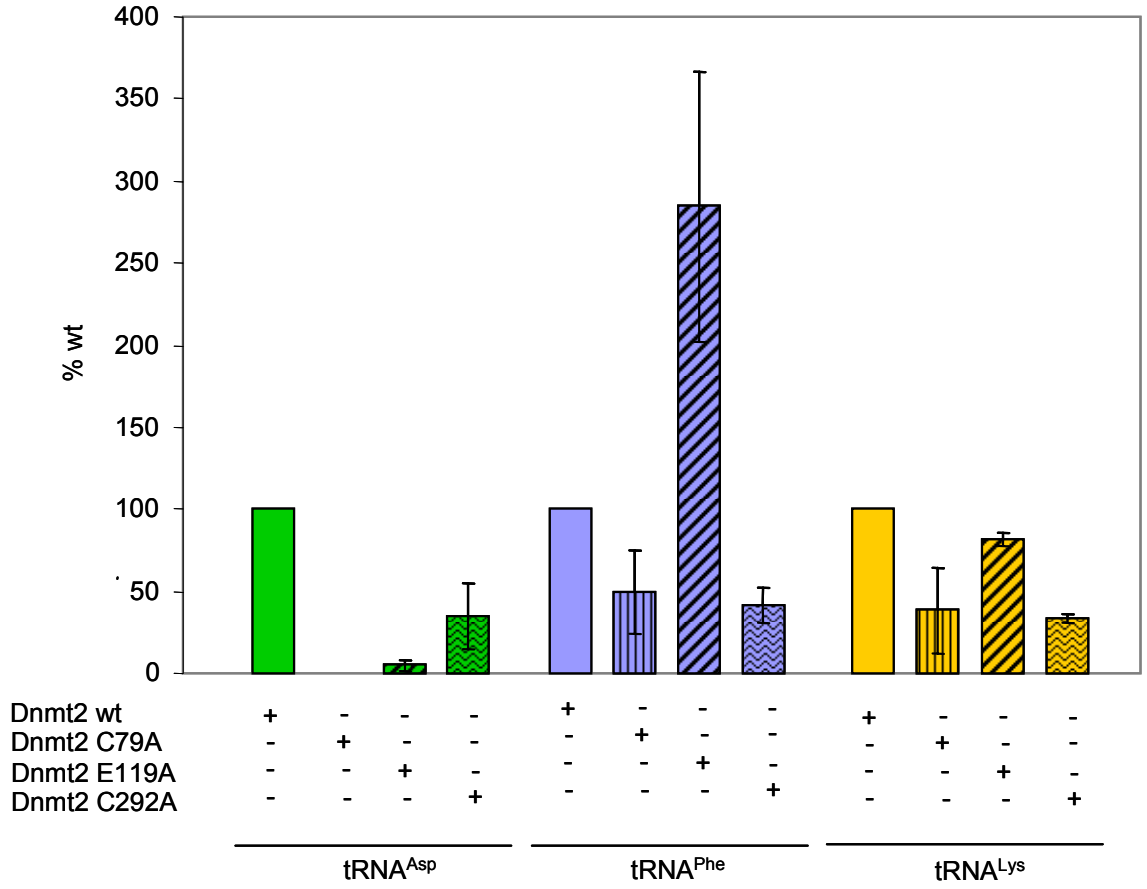

Fig. 2.32: Dnmt2 utilizes distinct enzymatic mechanisms for the methylation of different substrates.
Green bars: *In vitro* methylation assay of *in vitro* transcribed, C38 containing $tRNA^{Asp}$ of *D. melanogaster* using wildtype Dnmt2 and three catalytic mutants (see below the diagram). Mean values of three independent experiments with standard deviations are given. Blue bars: *In vitro* methylation assay of $tRNA^{Phe}$ (*S. cerevisiae*) as a substrate. Mean values of three independent experiments and the standard deviations are given. Yellow bars: *In vitro* methylation assay with non-C38 containing $tRNA^{Lys}$ of *D. melanogaster*. Mean values of two representative experiments are given.

3 Discussion

3.1 Dnmt2 and a Possible Role in Transposon Silencing

DNA methyltransferases play a crucial role in the transcriptional silencing of repeats and retrotransposons (reviewed in Goll & Bestor, 2005) which prevents mutagenesis due to transposon insertion. Absence of DNA methylation leads to increased transposon transcription, transposon transposition, and disturbed transcription of neighbouring genes. This has been shown for IAP elements in Dnmt1-deficient mouse embryos (Walsh et al., 1998). As Dnmt2 is the most conserved and most ancient member of the family of DNA methyltransferases (Goll & Bestor, 2005), it is tempting to speculate that Dnmt2 also contributes to the protection of genetic information due to the silencing of repeats and retrotransposons. In species where Dnmt2 is the only member of the DNA methyltransferase family, its function in genome defence may be of even greater importance. Previously, it had been shown that Dnmt2 does not play an essential role in the *de novo* silencing of retroviral DNA in murine embryonic stem cells (Okano et al., 1998b). However, the presence of the other Dnmt family members in murine cells may have a compensatory effect on the absence of Dnmt2. Therefore it is important to study Dnmt2 in the absence of Dnmt1 and Dnmt3a/b. *Drosophila melanogaster* is the best studied eukaryotic model organism which does not contain other members of the Dnmt family, and was therefore the model organism of choice. Semi-quantitative RT-PCR of 0 – 3 h old embryo-derived mRNA revealed a slight up-regulation of three transposons tested (Fig. 2.6). The up-regulation of other retrotransposons in the Dnmt2^{149} mutant compared to wildtype fly embryos has also been confirmed by our collaborator Sameer Phalke (personal communication). In summary, the observed effect of increased transposon expression in the absence of the Dnmt2 enzyme in *Drosophila* embryos is not as strong as the up-regulation of transposon transcription caused by the absence of Dnmt1 in mouse (Yoder et al., 1997; Walsh et al., 1998; Gaudet et al., 2004). Clearly, the global silencing of retrotransposons is not entirely mediated by Dnmt2, but a regulatory contribution of this enzyme appears likely.

Bisulfite sequencing of several regions of the transposons invader 4 and invader 2 in wildtype embryos yielded no reproducible methylation signal within the regions

examined (Fig. 2.7). However, due to the abundance of these transposons – with several full length and multiple fragment copies – the methylation of only a subgroup might remain undetected. Therefore, the insertion of a mobile element (the RS5 element carrying the *mini-white* gene as a marker) at a defined region was investigated. In the locus of interest, the mobile element RS5 had inserted into the long terminal repeat of the invader 4 retroelement on the Y-chromosome. As this work could show, methylation was absent from the Dnmt2^{149} mutant embryos. In the wildtype strain, however, the 3´-region of the *mini-white* gene was specifically found to contain dense methylation (Fig. 2.11). The methylation was not limited to CpG, but occurred in every context in the wildtype strain. It is important to note that only a fraction of the examined clones of the *mini-white*-region contained m^{5}C, but always in a very dense manner. If the presence of DNA methylation is indeed playing a role in the silencing of this locus, it becomes evident that this silencing is not pronounced, since heavy transcriptional silencing of this locus would result in white eyes. The fact that the eyes of freshly hatched male wildtype flies are orange – and therefore not fully, but rather mildly suppressed – corresponds well with the finding that not all examined clones show dense methylation.

In summary, the data of this work point to a weak role of Dnmt2-mediated DNA methylation in transposon regulation. m^{5}C within a DNA context was found within the white locus of a RS5-element which had been inserted into a transposon. In the Dnmt2^{149} mutant, no methylation was detected. The DNA samples of wildtype and mutant flies were always processed in parallel, and biological replicates were used for bisulfite treatment and cloning. It is unlikely that the methylation detected in wildtype flies is a bisulfite sequencing artefact, since these artefacts would also have been expected in the unmethylated DNA from Dnmt2^{149} – which is not the case. The finding of DNA methylation within the fly genome is in line with previous reports (Lyko et al., 2000a; Gowher et al., 2000). Still, the role of Dnmt2-mediated DNA methylation within an organism remains to be determined. Dnmt2 enzyme function seems not to be essential under laboratory conditions; however, a highly specialized function under environmental stress might not have been detected.

3.2 *In Vitro* tRNA Targets of Dnmt2

The publication which describes Dnmt2 being a tRNA methyltransferase claims that the enzyme does not recognize *in vitro* transcribed, unmodified tRNA and concludes that certain pre-modifications are necessary for Dnmt2 to be active (Goll et al., 2006). This is in conflict with the data of this work. Unmodified, *in vitro* transcribed tRNAs were reproducibly modified by Dnmt2 enzymes of *Drosophila* and human origin. The reason for these differing results probably lies in the design and performance of the *in vitro* methylation assay. In this work, the assay conditions were optimized carefully. Among the most important factors that need to be considered is the pH, as well as the Mg^{2+} and DTT concentrations. The pH varied only slightly (7.4 in Goll et al. and 8 in this work), but Goll et al did not add magnesium to the buffer. Mg^{2+} ions are crucial for tRNA structure, especially for unmodified, *in vitro* transcribed tRNA molecules (Hall et al., 1989; Maglott et al., 1998; Nobles et al., 2002). Since it had been postulated that unmodified, *in vitro* transcribed tRNAs would not be a substrate of Dnmt2, the assay optimization was conducted with total tRNA of *E. coli*. These tRNA molecules are fully modified and therefore more stable than unmodified tRNAs, but do not contain m^5C. When the influence of different magnesium concentrations on the methylation efficiency was tested, the best results could be achieved with 10 mM Mg^{2+}. There was activity measurable without Mg^{2+} due to the stability of the native tRNAs, but clearly reduced compared to 10 mM Mg^{2+}.

According to Goll et al., 2006, only the position C38 in the anticodon stem of $tRNA^{Asp}$ is methylated by Dnmt2. However, $tRNA^{Val}$ was also identified as a target. Furthermore, C40 of $tRNA^{Phe}$ (*S. cerevisiae*) and C40/C42 of $tRNA^{Lys}$ (from *D. melanogaster*) can be methylated by Dnmt2 *in vitro* (Fig. 2.26 and 2.27). This revealed an unexpected flexibility of Dnmt2 with respect to its substrate acceptance, since not only another C38-containing tRNA besides $tRNA^{Asp}$ can be methylated by Dnmt2, but also C40 and C42-containing substrates are recognized. Different modes of substrate recognition exist for tRNA modification enzymes, and examples have been described in the literature where a single tRNA modification enzyme targets several positions within tRNA, in a sequence-independent, but structural-dependent manner (Simos et al., 1996; Motorin et al., 1998; Motorin & Grosjean, 1999; Hur & Stroud, 2007). These will be compared to Dnmt2 in chapter 3.5.

3.3. *In Vivo* Targets of Dnmt2

Using alternative methods, this work could corroborate that $tRNA^{Asp}$ of *Drosophila melanogaster* is methylated at C38 by Dnmt2 (Goll et al., 2006). Furthermore, it could be clearly demonstrated that $tRNA^{Asp}$ is not the only *in vivo* target, but that $tRNA^{Val}$ is also methylated *in vivo* by Dnmt2. The use of the DNAzyme technique (see below) allowed not only the detection, but also the quantification of the m^5C signal at position 38. The mehylation status of native $tRNA^{Lys}$ derived from *Drosophila melanogaster* could not be investigated by the DNAzyme method due to the lack of purine-pyrimidine junctions at C40 and C42. However, further *in vivo* targets besides $tRNA^{Asp}$ and $tRNA^{Val}$ seem to be likely. For example, possible substrates could be the C38-containing tRNAs encoding for Glu, Gly, and His from *Drosophila melanogaster* (tRNA sequence database; Sprinzl & Vassilenko, 2005). All three of them contain a purine-pyrimidine junction at the locus 37-38, and can therefore be potentially analyzed by the DNAzyme method. Besides $tRNA^{Asp}$ and $tRNA^{Val}$, no other *Drosophila* tRNAs have been reported to contain m^5C at C38. However, the modification analysis of all Drosophila tRNAs is not complete. $tRNA^{Gly}$ has been reported to contain an m^5C at position 38 in the silkworm *Bombyx mori* (Garel & Keith, 1977), and thus represents an additional candidate target for Dnmt2-mediated methylation.

It is intriguing to speculate that Dnmt2 can methylate also other RNA species besides tRNA. It is possible that apart from tRNAs, other RNAs with loop structures – such as ribosomal RNAs, pre-microRNAs, or other small RNAs – might be targets of the Dnmt2 enzyme. The methylation of small RNAs could have an impact on the translational regulation and fine-tuning of numerous processes. A tRNA modification enzyme acting also on small nuclear RNA of the spliceosome has been reported previously. Pus1p, a pseudouridine synthase from *Saccharomyces cerevisiae*, was identified to modify uridine 44 to pseudouridine within spliceosomal U small nuclear RNAs (Massenet et al., 1999; see also chapter 3.5). So far, however, there is no evidence that Dnmt2 is able to methylate ribosomal RNA or small RNA components. A preliminary experiment analyzing ribosomal RNA as well as preparations of total small RNAs below 40 nucleotides in parallel with tRNA (all derived from wildtype as well as from $Dnmt2^{149}$ mutants) revealed tRNAs as the only RNA species to be methylated by Dnmt2. However, due to low sequence abundance of the small RNAs

compared to tRNAs, it cannot be excluded that there are rare RNAs which are also modified by Dnmt2. In this case, the *in vitro* methylation assay would not be the method of choice and should be replaced by a method which enriches for the putative targets first. This could be achieved by crosslinking the Dnmt2 targets to the enzyme via formaldehyde or 5-azacytidine treatment and subsequent immunoprecipitation of the Dnmt2-substrate complex using Dnmt2-specific antibodies. The availability of cell lines and fly strains expressing tagged Dnmt2 will further facilitate the search under *in vivo* conditions.

3.4 Advantages of the DNAzyme Method

The identification of tRNA modifications within their sequence context is challenging. The modifications *per se* can easily be detected via a two-dimensional TLC approach; however, the precise location of the modification within the tRNA sequence is not easily identified. Mass spectrometry is certainly the method of choice if large amounts of the target tRNA and the expertise to analyze the data are available. However, only a few laboratories have the requisite knowledge and experience, and therefore the mass spectrometry approach cannot be seen as a “fast core facility service” available to everybody. In addition, one to several micrograms of the tRNA of interest is needed, which is not easily obtained, especially if only one tRNA species and not total tRNA is to be analyzed. A second approach is based on the use of 2´-O-methyl- (2´-O-Me) modified oligos combined with RNase H cleavage at the site of interest. After post-cleavage radioactive labelling, the signal is resolved by 2-dimensional TLC (Yu et al., 1997; Zhao & Yu, 2004; Hou et al., 2006). The major disadvantage of this method lies in the very high cost of the 2´-O-Me oligonucleotides, and the sometimes imprecise cutting of RNase H, which requires laborious optimization of the assay conditions.

The extensive use and further development of the DNAzyme technique proved to be a highly effective and very cost-efficient method to identify m^5C in tRNA. The combination of inosine integration within the DNAzyme sequence (Cairns et al., 2003) and repeated temperature cycling (Hengesbach et al., 2008) greatly improved the cleavage yield and the detection of m^5C at position C38 in $tRNA^{Asp}$ and $tRNA^{Val}$ in wildtype fly embryos. The absence of m^5C in $tRNA^{Asp}$ and $tRNA^{Val}$ derived from $Dnmt2^{149}$ fly embryos demonstrated that Dnmt2 function is responsible for the

methylation of $tRNA^{Val}$ at C38 and that Dnmt2 is therefore not limited to $tRNA^{Asp}$ as its only target. Besides the direct proof of a suspected m^5C signal at a certain position, the DNAzyme technique has also been successfully used to narrow down the unknown modification site of $tRNA^{Lys}$ of *D. melanogaster in vitro*.

The use of DNAzymes to cleave a tRNA in defined pieces might also prove very helpful, when several modifications within one tRNA molecule are to be analyzed. In combination with mass spectrometry, for example, the analysis of smaller tRNA fragments should yield cleaner results due to less background signal. In this regard, the development of a tandem DNAzyme has been a useful tool to separate the anticodon loop from the rest of the tRNA molecule. In summary, the improved DNAzyme method is a very versatile technique which has permitted the analysis of tRNA methylation in a qualitative as well as a quantitative manner.

3.5 Comparison of Multisite-Specific tRNA-Modifying Enzymes

The multi-substrate specificity of Dnmt2 and its ability to methylate at different positions within the anticodon stem-loop is comparable to several tRNA modifying enzymes; of which three well characterized examples will be described in the following (Fig. 3.1).

TruA is a bacterial pseudouridine synthetase which modifies uridine to pseudouridine at the positions 38, 39, and 40 (Hur & Stroud, 2007). Pseudouridines within the anticodon loop contribute to the efficiency and accuracy of translation, also due to an increase in the thermal stability of the modified tRNA. Similar to m^5C methyltransferases, base flipping is used to access the substrate uridine. The anticodon stem-loop alone is not recognized as a substrate, which is another common feature between Dnmt2 and TruA. The second pseudouridine synthase which modifies several uridines in the anticodon stem-loop is Pus1p. This enzyme from yeast has been shown to catalyze pseudouridine formation *in vitro* at the positions 27, 28, 34, 35, and 36 in various cytoplasmic tRNAs (Simos et al., 1996; Motorin et al., 1998). Modifications of the anticodon appear in an intron-dependent manner (positions 34 and 36 of $tRNA^{Ile}$, and position 35 of $tRNA^{Tyr}$), while pseudouridine formation at positions 27 and 28 is intron-independent. The modification of positions 34, 35, and 36 does not require the full tRNA molecule,

since a mini-substrate consisting of the anticodon stem-loop plus the intron is modified by Pus1p (Motorin et al., 1998). Recently, position 1 has also been identified as an additional target of yeast and mouse Pus1p (Behm-Ansmant et al., 2006). Furthermore – as mentioned previously – Pus1p also modifies U2 snRNA of the spliceosome (Massenet et al., 1999; Behm-Ansmant et al., 2006).

Another multi-substrate specific enzyme from *S. cerevisiae* is the aforementioned m^5C tRNA methyltransferase Trm4 (Motorin & Grosjean, 1999), which modifies cytosines at the positions 34 and 40 in the anticodon loop, as well at positions 48 and 49 in the variable loop. Similar to Pus1p, the Trm4-mediated modifications located within the anticodon stem-loop (positions 34 and 40) are intron-dependent, while methylation within the variable loop does not require an intron.

The human Dnmt2 enzyme was found to methylate various *in vitro* transcribed tRNAs at the positions 38, 40, and 42. None of the tested tRNAs contained an intron, but it cannot be excluded that additional intron-containing tRNAs might be an *in vitro* target of Dnmt2. Out of the three cytosolic intron-containing tRNAs ($tRNA^{Leu}$, $tRNA^{Ile}$, and $tRNA^{Tyr}$), $tRNA^{Leu}$ and $tRNA^{Ile}$ could be possible targets, since $tRNA^{Leu(UUG)}$ and $tRNA^{Ile}$ carry a C40, and $tRNA^{Leu(CUG)}$ C39 and C41. For $tRNA^{Tyr}$, modifications have been described (Sprintzl database; Sprinzl & Vassilenko, 2005), but m^5C is not among the reported modifications.

The positions which are modified by the above mentioned TruA enzyme depend on the correct tRNA structure for proper target recognition, rather than a sequence context surrounding the modification site. The anticodon stem-loop plays an important role, but also the other tRNA parts are needed (Hur & Stroud, 2007). This is also the case for Dnmt2, as was shown in this work. The disruption of the anticodon stem loop of $tRNA^{Asp}$ and $tRNA^{Lys}$ abolished all activity of Dnmt2 (Fig. 2.16 and 2.30). Similarly, the tightening of the anticodon loop by Watson-Crick base pairing of positions 32 and 38 decreases the modification efficiency in Dnmt2 (Fig. 2.16) and TruA (Hur & Stroud, 2007). For the intron-dependent modification by Pus1p and Trm4, not the whole tRNA is needed, as minisubstrates are also accepted. However, it is crucial that these minisubstrates contain the intron. This also points to structural determination factors needed for Trm4 and Pus1p activity (Motorin et al., 1998; Motorin & Grosjean, 1999). Still, it cannot be excluded that for example the base composition within the anticodon loop can play a favourable role.

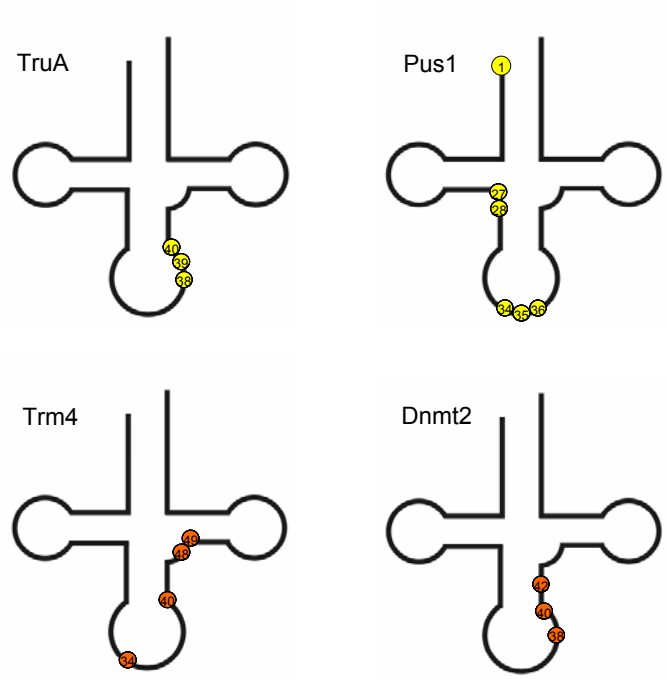

Fig. 3.1: Multisite-specific tRNA Modification Enzymes
Schematic representation of tRNA modification enzymes and their target sites. TruA ans Pus1 are pseudouridine synthases which modify different tRNAs within the anticodon stem-loop (positions marked in yellow). Trm4 and Dnmt2 are m^5C tRNA methyltransferases. The target positions are marked in orange (see text for details).

According to Hur & Stroud, 2007, the key to the regional specificity of TruA lies in the plasticity of the anticodon stem loop. Further experiments will be needed to confirm or exclude the existence of sequence elements within the substrate tRNAs of Dnmt2 that contribute to target recognition and efficient catalysis.

3.6 The Catalytic Mechanism of Dnmt2-Mediated tRNA Methylation

Dnmt2 is a tRNA methyltransferase but does not possess a catalytic cysteine in motif VI, which is the main catalytic residue in other tRNA m^5C methyltransferases (King & Redman, 2002; Walbott et al., 2007b). Dnmt2 was shown to methylate tRNA with a DNA methyltransferase-like mechanism (Jurkowski et al., 2008). This was achieved by exchanging all cysteines of human Dnmt2 as well as other potentially important sites for catalysis, such as E119, R160, and R162. The arginine residues have been proposed to also play an important role during catalysis (O'Gara et al., 1998; Gowher et al., 2006). Dnmt2 uses the cysteine of motif IV for catalysis, and is assisted by the glutamic acid of the ENV motif (Fig. 1.6). This is in accordance with DNA m^5C methyltransferases. The ability to methylate $tRNA^{Asp}$ was lost when the cysteine 79 and the glutamic acid 119 were exchanged for alanine, and it was reduced in the cysteine 292 mutant (Jurkowski et al., 2008). These data could be confirmed in this work using the *in vitro* methylation assay. Surprisingly, residual activity of the C79A mutant of 20 – 50 % wildtype activity was still measurable when the non-C38 containing tRNAs (Phe and Lys) were analyzed (Fig. 2.32). The E119A mutant showed even higher activity, yielding methylation levels comparable either to wildtype levels ($tRNA^{Lys}$) or even above ($tRNA^{Phe}$). This suggests that the non-C38 containing tRNAs are methylated by a catalytic mechanism which differs from the “canonical” DNA-methyltransferase-like mechanism. So far, it is unclear, which residues perform the methylation reaction in the catalytic mutants, as the exchange of the other cysteines did not show an effect (Jurkowski et al., 2008). It is possible that the “main” catalytic cysteine and the glutamic acid can be partially replaced by other residues. In this respect, it would be interesting to generate and analyze double mutants, where two cysteines have been simultaneously exchanged for alanines.

An *in vitro* evolution experiment of the DNA m^5C methyltransferase SinI which methylates the internal cytosine of GGACC or GGTCC sequences led towards a relaxation of its substrate specificity to GGGCC and GGCCC (Timar et al., 2004). The substitution of only two amino acids between the motifs VI and VII led to a 20 fold increase of enzymatic activity towards the new substrates, whereas the original activity was lowered only 5 fold (Timar et al., 2004). Similarly, directed evolution of the DNA m^5C methyltransfease MHaeIII led also to the acceptance of alternative

substrates, and increased even the methylation efficiency of the canonical sequence GGCC (Cohen et al., 2004). In this mutant, only four amino acids in the target recognition domain were exchanged. These protein engineering experiments using the two DNA m^5C methyltransferases SinI and MHaeIII have shown that changes of only a few residues are sufficient to enlarge the substrate specificity of an enzyme, with only a minor negative impact on the methylation of the original target sequence. The methylation of cytosine at different positions requires a flexible enzyme and therefore conformational changes. Especially loop regions of proteins have been described to have the ability to adapt different conformations, also depending on the bound substrate. In other words, the protein structure can differ depending on the substrate which was present at the time of crystallization. Structural data of Dnmt2 have been generated so far only with a deletion mutant of human Dnmt2 (lacking residues 191-237) in the presence of S-adenosyl-homocysteine (Dong et al., 2001). A substantial information gain could probably be achieved by structural analysis of Dnmt2 crystals, which were generated in the presence of $tRNA^{Asp}$ (as a C38 target) or $tRNA^{Lys}$ (as a C40 target), as well as the co-factor S-adenosyl-methionine. Differences in conformation might then identify the residues that are involved in non-C38 target methylation.

3.7 Dnmt2 – a Promiscuous Enzyme?

Broad substrate specificity and the ability to perform several catalytic reactions was a feature of ancestral enzymes and a prerequisite for the evolution of multiple, highly specialized enzyme families. Over time, randomly occurring mutations led to increased metabolic efficiency of one catalytic activity compared to the others. Selective pressure such as environmental stress signals together with duplication events caused the specialization of enzymes for one catalytic activity, often accompanied by loss of broad substrate acceptance and loss of alternative catalytic reactions (Aharoni et al., 2005; Khersonsky et al., 2006). Despite the high specialization of many enzymes throughout evolution, there still exist many cases of enzyme promiscuity. Usually, these enzymes exert one main catalytic reaction, and are also able to perform others, albeit with lower efficiency. Alternatively, there are many cases where there is a single catalytic reaction type, but several substrates. The main substrate is usually turned over at a much higher rate than the secondary

substrates (reviewed in Khersonsky et al., 2006). Could Dnmt2 be a promiscuous enzyme?

The Dnmt2 enzyme was found to be the oldest and most widely distributed member of the Dnmt family among eukaryotes. It has been characterized to be a tRNA methyltransferase methylating C38 of $tRNA^{Asp}$ (Goll et al., 2006). The work at hand has identified a new *in vivo* substrate – $tRNA^{Val}$ – and several new *in vitro* targets which are methylated by Dnmt2 in a flexible manner at different target sites. Although the *in vivo* relevance of these alternative methylation sites still remains to be determined, it has become clear that the Dnmt2 enzyme is not as specialized as it was previously thought (namely, the methylation of exclusively one premodified tRNA – $tRNA^{Asp}$ – at one position: C38). When the structure of human Dnmt2 was solved, it was shown to be nearly super-imposable onto the structure of the bacterial DNA methyltransferase MHhaI (Dong et al., 2001). Structure and sequence analysis of bacterial and eukaryotic DNA m^5C methyltransferases has revealed a high degree of conservation (Goll & Bestor, 2005). This can lead to the general assumption that eukaryotic m^5C methyltransferases evolved from bacterial methyltransferases via horizontal transfer (Bestor, 1988). However, the molecular phylogenetic analysis of 88 DNA m^5C methyltransferases supports a different view: that the m^5C methyltransferases were already present in the last common ancestor of bacteria, archaea, and eukaryotes (Bujnicki & Radlinska, 1999). The investigation of sequence-structure-function relationship of the yeast Trm4 m^5C tRNA methyltransferase in comparison to m^5U tRNA methyltransferases and m^5C DNA methyltransferases revealed that tRNA m^5C methyltransferases evolved from m^5U tRNA methyltransferases, and that the DNA m^5C methyltransferases then evolved from tRNA m^5C methyltransferases (Bujnicki et al., 2004). This makes sense in the light of the fact that the “RNA world” is older than the “DNA world”, and that tRNA modification molecules must have occurred at a rather early stage of evolution, since they can be found in every organism in all three kingdoms. A tRNA modification enzyme – the tRNA (m(1)G37) methyltransferase – was even found in the smallest genome of an organism sequenced to date: *Mycoplasma genitalium*. This parasite is a unicellular bacterium which has reduced its genome to a size of 480 kb (Bjork et al., 2001; de Crecy-Lagard et al., 2007). The fact that this organism has retained a gene for tRNA modification despite its limited coding capacity underlines the importance of tRNA modification and its role in translation fidelity regulation. It is very probable that

already before the separation of the three kingdoms into bacteria, archaea, and eukaryotes, a common ancestor possessed tRNA modifying enzymes. Since bacteria do not harbour m^5C as a tRNA modification, it was most likely lost during or shortly after the separation from archaea and eukaryotes.

The data of this thesis and other works (Goll et al., 2006) point towards the new hypothesis that the eukaryotic DNA methyltransferases did not evolve out of bacterial DNA methyltransferases, but out of an ancestor of Dnmt2. This new model is supported by several findings: tRNA m^5C methyltransferases are older than m^5C DNA methyltransferases, and m^5C is not found among the tRNA modifications of bacteria, but is common to eukaryotes and archaea. The Dnmt2 enzyme represents a conserved eukaryotic m^5C tRNA methyltransferase, which already possesses the catalytic motifs and the structural requirements needed for DNA methylating activity. Dnmt2 might therefore be seen as a conserved promiscuous enzyme, which represents the transit state from m^5C tRNA to m^5C DNA methylation. According to the model (see Fig. 3.2), the common ancestor of archaea and eukaryotes would have carried *a bona fide* tRNA m^5C methyltransferase. This ancestral tRNA methyltransferase probably contained a cysteine in motif VI for catalysis, similar to most tRNA m^5C methyltransferases (Bujnicki et al., 2004; Walbott et al., 2007b). The ENV motif, which is conserved in DNA methyltransferases, was not yet present (this is in line with its absence for example in Trm4, Motorin & Grosjean, 1999). Several mutations would then have led to the loss of the cysteine in motif VI, and acquirement of the ENV motif in Dnmt2. The presence of the cysteine and the glutamic acid in the catalytic pocket enabled the Dnmt2 enzyme then to retain its activity as a tRNA m^5C methyltransferase. As a promiscuous enzyme, Dnmt2 not only had broader substrate specificity on tRNA, but would also have had the ability to recognize and methylate DNA to a small extent. During evolution, further mutations, duplication events, and gene fusion led then to the development of the DNA methyltransferases of the Dnmt1 and 3 families. The N-terminal domain, which is missing in Dnmt2, but is present in Dnmt1 and 3a and b, probably facilitates their nuclear localization and the tethering of the Dnmts to DNA. Dnmt2, on the other hand, is mainly cytoplasmic (Goll et al., 2006; Schaefer et al., 2008). Additional mutations which still remain to be determined led to the abolishment of tRNA methylating activity and an increase in DNA methylating activity in the Dnmt1 and Dnmt3a and b enzymes.

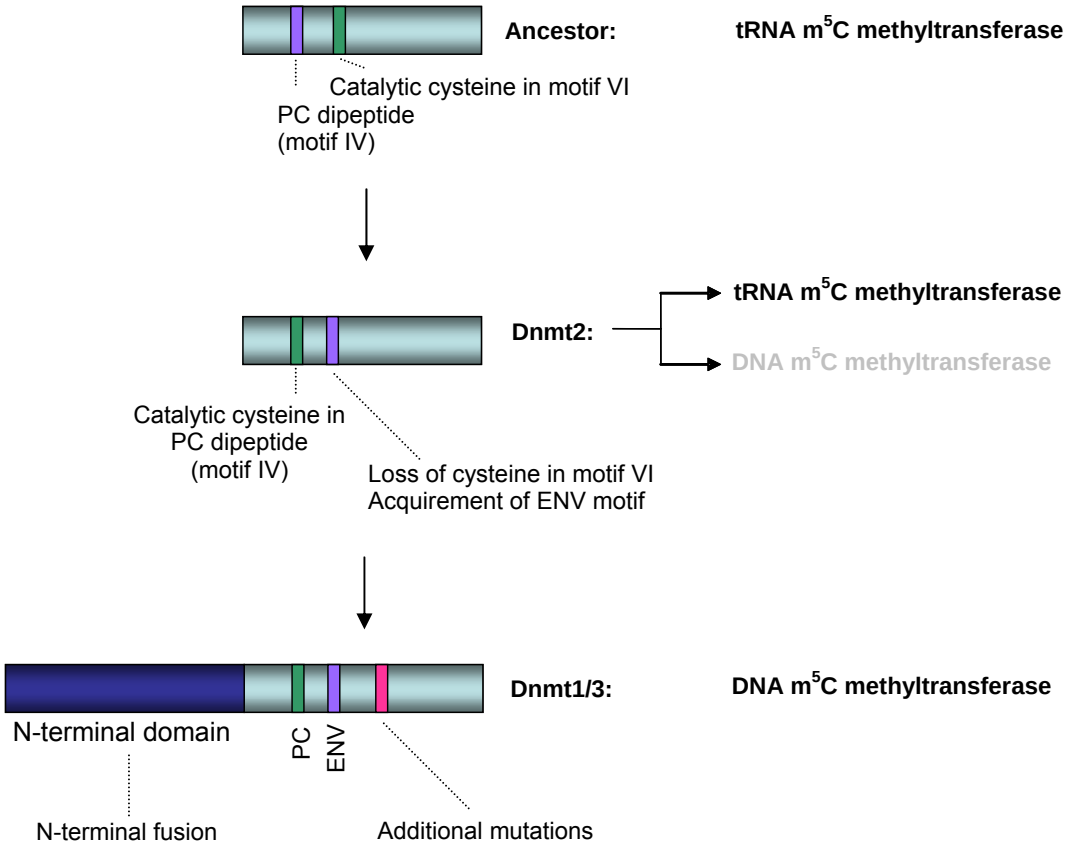

Figure 3.2: Dnmt2 as the evolutionary link between tRNA m^5C and eukaryotic DNA m^5C methyltransferases
This model describes the emergence of eukaryotic m^5C DNA methyltransferases out of tRNA m^5C methyltransferases. The Dnmt2 enzyme probably evolved out of an ancestral tRNA m^5C methyltransferase. The original catalytic cysteine in motif VI was lost, and the cysteine in motif IV became the catalytic residue. A glutamic acid was acquired within the ENV motif which is also needed for C38 methylation. The Dnmt2 enzyme displays good tRNA methyltransferase activity and a minor DNA methyltransferase activity. Mutation of further, currently still uncharacterized residues and the fusion with other proteins – generating the N-terminal domain – led then to the evolution of the *bona fide* eukaryotic DNA m^5C methyltransferases.

In this respect, it would be interesting to investigate, whether the catalytic domains of the eukaryotic DNA m^5C methyltransferases 1 and 3a/b display residual tRNA methylating activity. Full length Dnmt1 and 3b were tested in preliminary experiments and did not show any activity on tRNA as a substrate. Even if the catalytic domain of Dnmt1 and 3a/b is not accepting tRNA as a substrate, it is possible that the exchange of one or more bases can introduce the tRNA methylating activity of Dnmt1 and

Dnmt3a/b. This should be tested via protein engineering experiments. Complimentary to this approach, engineering experiments using Dnmt2 enzyme in combination with fusions of the N-terminal domain of Dnmt1 and/ or Dnmt3a/b may increase its ability to methylate DNA.

In summary, this work has contributed to the identification of novel *in vitro* and *in vivo* substrates of Dnmt2 using an optimized DNAzyme technique. The investigation of catalytic mutants revealed an alternative catalytic mechanism for non-canonical (non-C38) targets. This surprising promiscuity of the Dnmt2 enzyme led to the hypothesis that Dnmt2 could provide the link between tRNA m^5C and DNA m^5C methyltransferases. Future experiments will be necessary to support this idea. The extensive search for further targets in combination with the analysis of additional Dnmt2 mutants should contribute to a profound understanding of Dnmt2 function and the evolution of the eukaryotic DNA methyltransferases.

4 Material and Methods

4.1 Materials

4.1.1 Chemicals, Enzymes, and Reagents

Acetic Acid	Merck, Darmstadt
Acetone	Sigma-Aldrich, Seelze
Acrylamide/Bis solution (19:1)	Serva, Heidelberg
Acrylamide/Bis solution (29:1)	Roth, Karlsruhe
Agar-Agar	Roth, Karlsruhe
Agarose	Sigma-Aldrich, Seelze
Ammonium persulfate	Sigma-Aldrich, Seelze
Ammonium acetate	Sigma-Aldrich, Seelze
Ammonium solution (25 %)	Sigma-Aldrich, Seelze
Ammonium sulphate	Merck, Darmstadt
Ampicillin	Sigma-Aldrich, Seelze
[γ-^{32}P]-ATP	Hartmann, Braunschweig
β-Mercaptoethanol	Sigma-Aldrich, Seelze
Bakers´ Yeast	Lesaffre, FR
BAP enzyme	Fermentas, St. Leon-Rot
Blasticidin	AppliChem, Darmstadt
Boric acid	Sigma-Aldrich, Seelze
Bovine serum albumine	New England Biolabs, Frankfurt
Bradford Reagent	Biorad, München
Bromphenol blue	Merck, Darmstadt
BSA	Fermentas, St. Leon-Rot
CDP star	Roche, Mannheim
Chloramphenicol	Sigma-Aldrich, Seelze
Chloroform	Sigma-Aldrich, Seelze
Complete-mini-protease inhibitor	Roche, Mannheim
Copper sulfate	Sigma-Aldrich, Seelze

[α-^{32}P]-CTP	Hartmann, Braunschweig
Deoxynucleotide triphosphates	Rapidozym, Berlin
Diethylpyrocarbonate (DEPC)	Sigma-Aldrich, Seelze
Disodium hydrogen phosphate	AppliChem, Darmstadt
Dithiothreitol	Sigma-Aldrich, Seelze
DNase I	Fermentas, St. Leon-Rot
DNAzol	Invitrogen, Karlsruhe
ECL solution (Western Lightening)	Perkin Elmer, Überlingen
Ethanol (absolute)	Sigma-Aldrich, Seelze
Ethidium bromide	Roth, Karlsruhe
Ethylenediaminetetraacetic acid (EDTA)	Gerbu, Gaiberg
Fetal Calf Serum (FCS)	Invitrogen, Karlsruhe
Flag peptide (3x)	Sigma-Aldrich, Seelze
Formaldehyde	JT Baker, Deventer, NL
Formamide	Merck, Darmstadt
Glycerol	JT Baker, Deventer, NL
Glycine	Gerbu Biotechnik, Gaiberg
4-(2-hydroxyethyl)-1-piperazineethanesulfonic acid (HEPES)	Roth, Karlsruhe
Hydrochloric acid	VWR, Darmstadt
Hydroquinone	Sigma-Aldrich, Seelze
Isopropyl β-D-1-thiogalactopyranoside (IPTG)	Roche, Mannheim
Isobutyric acid	Sigma-Aldrich, Seelze
Kanamycin	Sigma-Aldrich, Seelze
Lithium perchlorate	Sigma-Aldrich, Seelze
Magnesium chloride	Merck, Darmstadt
Maleic acid	Sigma-Aldrich, Seelze
Methanol	Sigma-Aldrich, Seelze
Milk Powder	Roth, Karlsruhe
Mineral Oil	Sigma-Aldrich, Seelze
MOPS	Sigma-Aldrich, Seelze
N,N,N´,N´-Tetramethylenediamine (TEMED)	Roth, Karlsruhe
Nucleotide triphosphates	Sigma-Aldrich, Seelze
NP-40 (Igepal)	Sigma-Aldrich, Seelze

Penicillin/ Streptomycin	Gibco, Karlsruhe
Phenol	Roth, Karlsruhe
Ponceau staining solution	Sigma-Aldrich, Seelze
Polynucleotide kinase	Fermentas, St. Leon-Rot
Potassium chloride	Sigma-Aldrich, Seelze
1-Propanol	AppliChem, Darmstadt
2-Propanol	Sigma-Aldrich, Seelze
Proteinase K	Qiagen, Hilden
Rotiphorese Sequencing Gel buffer (10x)	Roth, Karlsruhe
Rotiphorese Sequencing Gel Concentrate	Roth, Karlsruhe
Rotiphorese Sequencing Gel Diluter	Roth, Karlsruhe
S-adenosyl-methionine	New England Biolabs, Frankfurt
[^{3}H]-S-adenosyl-methionine	Hartmann, Braunschweig
Sucrose	Sigma-Aldrich, Seelze
Sodium chloride	Sigma-Aldrich, Seelze
Sodium citrate	Sigma-Aldrich, Seelze
Sodium hydrogencarbonate	AppliChem, Darmstadt
Sodium dihydrogen phosphate	AppliChem, Darmstadt
Sodium hydroxide	Sigma-Aldrich, Seelze
Sodium pyrosulfite	Sigma-Aldrich, Seelze
Sodiumhypochlorite solution	Neolab, Heidelberg
Spermidine	Sigma-Aldrich, Seelze
Streptavidin MagneSphereR Paramagnetic Particles	Promega, Mannheim
Trichloroacetic acid	Roth, Karlsruhe
Trizma base	Sigma-Aldrich, Seelze
Trizol	Invitrogen, Karlsruhe
Triton X-100	AppliChem, Darmstadt
tRNA *E. coli* (total)	Roche, Mannheim
Trypton	Roth, Karlsruhe
Tween 20	Sigma-Aldrich, Seelze
Yeast extract	Gerbu Biotechnik, Gaiberg
Xylene cyanol	Sigma-Aldrich, Seelze
Zinc chloride	Sigma-Aldrich, Seelze

All other chemicals not listed above were obtained either from the “Zentralbereich Neuenheimer Feld” of the University of Heidelberg or from the central storage department of the German Cancer Research Center (Heidelberg).

4.1.2 Equipment

Centrifuge	Neolab, Heidelberg
Cerenkov Counter LS 6500	Beckman Coulter, Krefeld
Electrophoresis chamber	Biorad, München
Incubator (37 °C): Innova 4200	New Brunswick Scientific, Nürtingen
Microscope (Zeiss Axiovert 40)	Zeiss, Göttingen
Nanodrop 1000	Thermo Scientific, Dreieich
PTC-200 Peltier Thermal Cycler	Biozym, Hess. Oldendorf
Photometer	Neolab, Heidelberg
Shaker	Neolab, Heidelberg
Speedvac	Thermo Scientific, Schwerte
Thermomixer	Neolab, Heidelberg
Typhoon 9400	GE Healthcare, München
UV-Stratalinker-1800	Stratagene, Heidelberg
X-ray films (Fuji Medical SuperRX)	Fujifilm, Düsseldorf

4.1.3 Kits

DIG Northern Starter Kit	Roche Diagnostics, Mannheim
DNeasy Blood and Tissue Kit	Qiagen, Hilden
Epitect Bisulfite Kit	Qiagen, Hilden
GeneClean DNA Purification Kit	Oncor Appligene, Heidelberg
Ni-NTA Fast Start Kit	Qiagen, Hilden
Plasmid Mini Prep Kit	Qiagen, Hilden
Plasmid Midi Kit	Qiagen, Hilden
Qiaquick Gel Extraction Kit	Qiagen, Hilden
Qiaquick PCR Purification Kit	Qiagen, Hilden
QuickPrep Micro mRNA Purification Kit	GE Healthcare, München

T7 Megascrip Kit (Ambion)	Applied Biosystems, Darmstadt
Thermoscript RT-PCR System	Invitrogen, Karlsruhe
TOPO TA Cloning Kit for Sequencing	Invitrogen, Karlsruhe

4.1.4 Primer, DNA templates, DNAzymes, Antibodies, Enzymes, and Fly Strains

All sequences are depicted from 5´ to 3´ and were obtained either by IBA (Göttingen) or MWG Biotech (München).

Primer:

RT-PCR Primer for the *Dnmt2* gene:

HD11: GGGGCCCGGGTATGGTATTTCGGGTCTTAGAACTATTTAGTGGC

HD12: CGAATTCTTTTATCGTCAGCAATTTAATAAGTTCACCG

HD39: CACCAAATTACTGCCGTAATTGTGC

HD57: ATCCTCACTGGCTTCCCC

RT-PCR Primer for *Micropia*:

MM_25: TGCCGAAAGCTGTGTTAATG

MM_26: CTCATTCGGGATTTCTGCAT

RT-PCR Primer for *Invader 4*:

MM_47: TGAGAGAAGACACGCCAATG

MM_48: GATCGACGTCAGCAGTCAAA

RT-PCR Primer for *Invader 2*:

MM_34: GCAGGAAAGCATATGCAACA

MM_35: ATCTCAAACGGCACATTTCC

RT-PCR Primer for *EF1α48D*:

EF1α48D_For : AGCAGCTGATCGTTGGTG

EF1α48D_Rev: TCACGGACACGTTCTTGAC

Primer Northern Probe *Dnmt2*:

For: GGGGCCCGGGTATGGTATTTCGGGTCTTAGAACTATTTAGTGGC

Rev: TAATACGACTCACTATAGGGAGACCACATTTAATAAGTTCACCG

Primer Northern Probe *Adh*:

Adh for: GCGATCTGAAGAACCTGGTG

Adh rev: AATTAACCCTCACTAAAGGGAGAGGTTCAGCTCGATAGCCTTG

Bisulfite Sequencing Primer for *Invader 2*:

MM_37: ATAAAATTTTTGAAATGAGAAATGG

MM_38: TCTTCAAATATAAAACAAATCCCCC

Bisulfite Sequencing Primer for *Invader 4*:

MM_51: GGAGGAGATTGTGGTTTTGG

MM_52: CCACATATCCCATTTCATCACA

MM_60: TGGTTGTGTTGGAGGTATAAAA

MM_61: AACAACCAACATCTCCATTCC

MM_55: TGAGTGAGGTTTGATTGAGTGG

MM_56: 5´-TCAACAAAACAAAAATCTACC-3´

MM_88: TGGTATTTGGTGAATTTGTGG

MM_89: CATTTTAAACAAACATCCAACACC

MM_76: TGTTTTGTTGGTATTATGTGGTTGTAG

MM_77: CCAACTTTCCCACAAAAATAAC

Bisulfite Sequencing Primer within the RS5 Element:

Region 1

For TTGGGGTATGTGGTGTTTGA

Rev CCATCTTCCTCTTCCTAACCAA

Region 2

For TATTGATGTTATTGATTTATTTAGAGTT

Rev CTTACATACCCCATTATTCTCTATTC

Region 3

For GTTGAAGAAGGGAAATGTAAGAAG

Rev TTTTACTCCAATCACAACTTT

Region 4

For TTATATAGTGAGTATAGTTATTAGAATAAT

Rev TAGGTCGATAGCGTCAATGTCCGCCTTCA

Region 5

For AAGTGGATGTTTTTTGTTGATGGGA

Rev CAATCAACACAACCAATCAAACTT

Primer for tRNA construct amplification:

MH53 T7 Polymerase Primer:

CGCGCGAAGCTTAATACGACTCACTATA

tRNA^{Asp} (*M. musculus*) Primer (rev):

TGGCTCCCGTCGGGGAATCGAA

tRNA^{Asp} (*D. melanogaster*) Primer (rev):

TGGCGCCCCGACGGGGAATTG

MH159 tRNA^{Asp} (*P. abyssi*) Primer :

TGGCGCCCGGGCCGGGATTT

MH60 tRNA$^{Leu(CUN)}$ (*H. sapiens*):

TGGTACTTTTATTTGGAGTT

DNA templates for *in vitro* transcription:

tRNA^{Asp} (*M. musculus*)

MH117:

TGGCTCCCCGTCGGGGAATCGAACCCCGGTCTCCCGCGTGACAGGCGGGGAT
ACTCACCACTATACTAACGAGGAGACGGTACCGGGTACCGTTTCGTCCTCACGG
ACTCATCAGTCCTCGTTATCTCCCTATAGTGAGTCGTATT

MH346 (71mer):

TCCCCGTCGGGGAATCGAACCCCGGTCTCCCGCGTGACAGGCGGGGATACTC
ACCACTATACTAACGAGGAGACGGTACCGGGTACCGTTTCGTCCTCACGGACTC
ATCAGTCCTCGTTATCTCCCTATAGTGAGTCGTATT

MH238 (anticodon stem loop only; "2"):
CCCGCGTGACAGGCGGGGACGGTACCGGGTACCGTTTCGTCCTCACGGACTC
ATCAGCCCGCCTGTTCTCCCTATAGTGAGTCGTATT

MH237 (C32 → G32):
TGGCTCCCCGTCGGGGAATCGAACCCCGGTCTCCCGCGTGACACGCGGGGAT
ACTCACCACTATACTAACGAGGAGACGGTACCGGGTACCGTTTCGTCCTCACGG
ACTCATCAGTCCTCGTTATCTCCCTATAGTGAGTCGTATT

MH239 (C38 → U38):
TGGCTCCCCGTCGGGGAATCGAACCCCGGTCTCCCGCATGACAGGCGGGGAT
ACTCACCACTATACTAACGAGGAGACGGTACCGGGTACCGTTTCGTCCTCACGG
ACTCATCAGTCCTCGTTATCTCCCTATAGTGAGTCGTATT

tRNA^{Asp} (*D. melanogaster*):

TAATACGACTCACTATAGGCCTCGATAGTATAGTGGTTAGTATCCCCGCCTGTCA
CGCGGGAGACCGGGGTTCAATTCCCCGTCGGGGCGCCA-3´

tRNA^{Val} (*D. melanogaster*)

MH202: tRNA^{Val} T7 DNA template
TGGTGTTTCCGCCCGGGATCGAACCGGGGGCCTTCTGCGTGTTAGGCAGATGT
GATAACCGCTACACCACGGAAACGACGGTACCGGGTACCGTTTCGTCCTCACG
GACTCATCAGGTTTCCGTGTCTCCCTATAGTGAGTCGTATT-3´

tRNA^{Asp} (*P. abyssi*) MH156:
TGGCGCCCGGGCCGGGATTTGAACCCGGGTCGCGGGAGTGACAGTCCCGCAT
GATAGGCCGGGCTACACCACCCGGGCTATAGTGAGTCGTATTA

tRNA^{Lys} (*D. melanogaster*):

GGTCGCCCAACGTGGGGCTCGAACCCACGACCCTGAGATTAAGAGTCTCATGC
TCTACCGACTGAGCTAGCCGGGCCCTATAGTGAGTCGTATTA

tRNA^{Lys} (*D. melanogaster*): (a) G30 → C30; C40 → G40

TGGCGCCCAACGTGGGGCTCGAACCCACGACCCTGACATTAAGAGTGTCATGC
TCTACCGACTGAGCTAGCCGGGCCCTATAGTGAGTCGTATTA

tRNA^{Lys} (*D. melanogaster*): (b) G28 → C28; C42 → G42

TGGCGCCCAACGTGGGGCTCGAACCCACGACCCTCAGATTAAGAGTCTGATGC
TCTACCGACTGAGCTAGCCGGGCCCTATAGTGAGTCGTATTA

tRNA^{Lys} (*D. melanogaster*): (c) G28 → C28; G30 → C30; C40 → G40; C42 → G42

TGGCGCCCAACGTGGGGCTCGAACCCACGACCCTCACATTAAGAGTGTGATGC
TCTACCGACTGAGCTAGCCGGGCCCTATAGTGAGTCGTATTA

tRNA^{Lys} (*D. melanogaster*): (d) G28 → U28; G30 → U30; C40 → A40; C42 → A42

TGGCGCCCAACGTGGGGCTCGAACCCACGACCCTTATATTAAGAGTATAATGCT
CTACCGACTGAGCTAGCCGGGCCCTATAGTGAGTCGTATTA

tRNA^{Lys} (*D. melanogaster*): (e) C40 → G40

GGTCGCCCAACGTGGGGCTCGAACCCACGACCCTGACATTAAGAGTCTCATGC
TCTACCGACTGAGCTAGCCGGGCCCTATAGTGAGTCGTATTA

tRNA$^{Leu(CUN)}$ (*H. sapiens*):

TGGTACTTTTATTTGGAGTTGCACCAAAATTTTTGGGGCCTAAGACCAATGGATA
GCTGTTATCCTTTAAAAGTGACGGTACCGGGTACCGTTTCGTCCTCACGGACTC
ATCAGACTTTCTCCCTATAGTGAGTCGTATT

tRNA^{Phe} (*S. cerevisiae*) : G30 → C30 ; C40 → G40

TGGTGCGAATTTCTGTGATCGAACACAGGACCTCCACATCTTCAGTGTGGCGCT
CTCCCAACTGAGCTAAATCCGCCCTATAGTGAGTCGTATTA

The plasmid encoding tRNA^{Phe} (wt) from *S. cerevisiae* was a gift from O. Uhlenbeck; native tRNA^{Phe} and the plasmid encoding human mitochondrial tRNA^{Thr} was a gift from C. Florentz; the plasmid encoding tRNA^{Asp} from *S. cerevisiae* was a gift from G. Keith (all to M. Helm); the plasmid encoding the gene for human tRNA^{Lys} was a gift from J.-L. Darlix to F. Lyko.

DNA Oligos (biotinylated):

MH119: Biotin-Sonde tRNA Asp
TGACAGGCGGGGATACTCACCACTATACTAACGAGGA

3´-Biotin

Valin_Sonde_Bio:

TGTTAGGCAGATGTGATAACCGCTACACCACGGAAAC

3´-Biotin

MM_Lys2_Oligo:

CGCCCAACGTGGGGCTCGAACCCACGACCCTGAGATTA

5´-Biotin

DNAzymes:

MH143: DNAzym_Asp (C38)
CCGGTCTCCCGCGGGCTAGCTACAACGAGACAGGCGGGGA

DNAzym_Asp_F:

ACCCCGGTCTCCCGCXGGCTAGCTACAACGAGACAGGCGGGGA

5´- fluorescein

X: inosine

DNAzym 3:

CCCGCGTGACAGGGGCTAGCTACAACGAGGGGATACTCACC

DNAzym 4:

CCCCGGTCTCCCGGGCTAGCTACAACGAGTGACAGGCGGGG

DNAzym 34B:

CCCCGGTCTCCCGGGCTAGCTACAACGAGTGACAGGGGCTAGCTACAACGAGG
G

DNAzym_Val_F:

GGGGGCCTTCTGCXGGCTAGCTACAACGAGTTAGGCAGATGTG

X: Inosine

5´: Fluorescein (FAM)

DNAzym_Lys_1:

TCGAACCCACGAGGCTAGCTACAACGACCTGAGATTA

5´: Fluorescein

DNAzym_Lys_2:

ACGACCCTGAGAGGCTAGCTACAACGATAAGAGTCTCA

5´: Fluorescein

RNA Oligos:

MH352: UCCUCGUUAGUAUAGUGGUGAGUAUCCCCGCCUGUCA

MH353: F^5CGCGGGAGACCGGGGUUCGA

MH354: m^5CGCGGGAGACCGGGGUUCGA

MH355: CGCGGGAGACCGGGGUUCGA

MH356: P-UUCCCCGACGGGGAGCCA

Antibodies :

Rabbit anti-Dnmt2 peptide 2; 1:500	(Kunert et al., 2003); (Schaefer et al., 2008)
Mouse anti-tubulin; 1:10000	Sigma-Aldrich, Seelze
goat–α-rabbit-HRP; 1:10000	Jackson Immuno Research, Suffolk, GB
goat–α-mouse-HRP; 1:10000	Jackson Immuno Research, Suffolk, GB
anti-Flag	Sigma-Aldrich, Seelze
anti-Digoxigenin	Roche, Mannheim

Enzymes:

BAP	Fermentas, St. Leon-Rot
BstNI	New England Biolabs, Frankfurt
DNase I	Fermentas, St. Leon-Rot
DNase-free RNase	Roche, Mannheim
EcoRI	New England Biolabs, Frankfurt
P1 RNase	Roche, Mannheim
PNK	Fermentas, St. Leon-Rot
Proteinase K	Qiagen, Hilden
Rapidozym Taq Polymerase	Gentherm, Rapidozym, Berlin
RNase H	Invitrogen, Karlsruhe
T1 RNase	Gibco, Invitrogen, Karlsruhe
T4 Ligase	Fermentas, St. Leon-Rot
T7-RNA-Polymerase	Fermentas, St. Leon-Rot
Thermoprime Polymerase	Abgene, Hamburg
Thermoscript Reverse Transcriptase	Invitrogen, Karlsruhe

Fly strains:

OrR	BloomingtonStock Center (Indiana University)
EP	Gift from Sameer Phalke (University of Halle)
$Dnmt2^{149}$	Gift from Sameer Phalke (University of Halle)
$Dnmt2^{215}$	Gift from Sameer Phalke (University of Halle)
5Ha1925	Gift from Sameer Phalke (University of Halle)

4.1.5 Buffers and Solutions

10x boric acid buffer
15.46 g boric acid
ad 1 l with H_2O
adjust pH to 8.8

Detection buffer (Southern and Northern Blot):
0.1 M Tris-HCl
0.1 M NaCl
pH 9.5

Dialysis buffer 1:
300 mM KPO_4 pH 7.5
300 mM KCl
1 mM EDTA
0.1 mM DTT
10 % glycerol

Dialysis buffer 2:
30 mM KPO_4 pH 7.5
200 mM KCl
1 mM EDTA
0.1 mM DTT
60 % glycerol

5x DNAzyme Buffer:
250 mM Tris-HCl pH 7.5
750 mM KCl
50 mM $MgCl_2$

Egg wash:
7 g NaCl
1 g (w/v) Triton X-100
ad 1 l with H_2O

KL-buffer:

50 mM Tris-HCl pH 7.4

10 mM $MgCl_2$

LB medium:

10 g tryptone

5 g yeast extract

10 g NaCl

H_2O ad 1 l

LB-agar:

LB medium supplemented with 1.5 % (w/v) agar

Loading buffers:

Loading buffer for DNA:

0.25 % w/v Bromphenol blue

0.25 % w/v Xylene cyanol

30 % v/v glycerol

Loading buffer (denaturing) :

90 % formamide

9.8 % 10x TBE

0.1 % Xylene cyanol

0.1 % Bromphenol blue

Loading buffer (native):

90 % TBE

9.8 % glycerol

0.1 % Xylene cyanol

0.1 % Bromphenol blue

Loading buffer (for Northern Blot):

For a volume of 500 µl:

250 µl 100 % formamide

83 µl 37 % formaldehyde

50 µl 10x MOPS

50 µl 100 % glycerol

10 µl 2.5 % Bromphenol blue

57 µl H_2O_{DEPC}

10x MOPS buffer:

200 mM MOPS

50 mM NaAc

20 mM EDTA

pH 7.0 with NaOH

Pb-Stop Solution:

1x TBE

8 M urea

10 mM EDTA

0.1 % Xylene cyanol

0.1 % Bromphenol blue

QEB-buffer:

50 mM MOPS pH 7.5

15 % EtOH

300 mM NaCl

0.1 % Triton X-100

QEL-buffer:

50 mM MOPS pH 7.5

15 % EtOH

750 mM NaCl

QLW-buffer:
50 mM MOPS pH 7.5
15 % EtOH
300 mM NaCl

5x SDS-Loading buffer:
250 mM Tris-HCl pH 6.8
10 % SDS
0.5 % Bromphenol blue
50 % glycerol
500 mM β-Mercaptoethanol

Shearing buffer:
TE pH 8
10 % glycerol

20x SSC:
3 M NaCl
0.3 M sodium citrate
pH 7.0

Strasbourg Buffer:
40 mM Tris-HCl pH 8.1
1 mM Spermidine
5 mM DTT

10x TBE:
108 g Tris-Base
55 g boric acid
200 ml 0.5 M EDTA pH 8.0
ad 1 l with H_2O

T1-Buffer:

40 mM Tris-HCl pH 7.5

40 mM NaCl

10 mM $MgCl_2$

TBST:

50 mM Tris-HCl pH 8.0

150 mM NaCl

0.1 % Triton X-100

TE:

10 mM Tris-HCl pH 7.4

1 mM EDTA pH 8.0

Wash buffer 1 (Southern and Northern Blot):

2x SSC

0.1 % SDS

Wash buffer 2 (Southern and Northern Blot):

0.5x SSC

0.1 % SDS

Wash buffer 3 (Southern and Northern Blot):

0.1 M Maleic acid

0.15 M NaCl

0.3 % Tween-20

pH 7.5

4.1.6 Marker

DNA Marker:	Hyperladder I	Bioline, Luckenwalde
Protein Marker:	PageRuler Prestained Protein Ladder	Fermentas, St. Leon-Rot

4.2 Methods

4.2.1 Standard maintenance of *Drosophila melanogaster*

Flies were raised in glass vials with foam plugs at 25 °C and ~ 70 % humidity. Fly food was prepared by the Division of Developmental Genetics of the DKFZ (standard fly food: 10 l H2O; 80 g agar; 180 g dry yeast; 100 g soy flour; 220 g beet syrup; 800 g cornmeal; 24 g Nipagin; 62.5 ml propionic acid), and directly poured into the glass vials. Every one to two weeks, freshly hatched flies were moved to a new vial.

4.2.2 Acetic acid agar plates

For 1 l, 17 g of agar were mixed with 500 ml H_2O and shortly boiled in the microwave oven. Another 500 ml H_2O and 8 ml acetic acid were added. After thorough mixing, the liquid acetic acid agar was poured into standard petri dishes. After cooling, the agar plates were stored in sealed plastic bags to avoid drying out.

4.2.3 Embryo collection

Flies were put into plexiglass collection cages. The opening was sealed with an acetic-acid-agar plate containing bakers´ yeast mixed with water as a food source in the middle of the plate. Flies were allowed to acclimate one day to the cage. One hour prior to the start of the collection, the plate was exchanged for a fresh one, so the female flies could lay their withheld eggs. With the starting of the collection time, a new plate was fixed on the cage for the desired collection time, ranging from 3 to 24 hours. Afterwards, the plate was removed and exchanged for a fresh one for further collection. The embryo containing collection plate was cleaned of dead flies, and the yeast was cut out. The chorion membrane was removed by bleaching for 3 min in 50 % sodium hypochlorite solution. The embryos were washed extensively with egg wash (7 g NaCl, 1 g (w/v) Triton X-100 in 1 l H_2O), transferred into a tube and frozen in liquid nitrogen after complete removal of residual egg wash. Frozen embryos were stored at -80 °C until further use.

4.2.4 Preparation of genomic DNA using DNAzol and the DNeasy tissue kit

Unless indicated otherwise, genomic DNA of 0 - 3h old embryos was prepared by applying two subsequent purification steps using DNAzol (Invitrogen) and the DNeasy tissue Kit (Qiagen). The protocols supplied with the kits were closely followed. Briefly, 50 – 100 µl of flash-frozen 0 - 3 h old embryos were homogenized in 1 ml DNAzol (Invitrogen) using a loose fitting glass homogenizer. Debris was removed by a 10 min centrifugation step at 10000 x g. The supernatant was transferred to a new reaction vial and the DNA was precipitated by the addition of 100 % Ethanol. After centrifugation, the DNA pellet was washed with 70 % ethanol and dissolved in 8 mM NaOH according to the manufacturer´s instructions. The pH was adjusted to 7.2 by the addition of 1 M HEPES buffer. Residual RNA was removed by an one hour digest using 10 µl DNase-free RNAse (10 u/µl; Roche) at 37 °C, followed by a 5 h to overnight incubation with proteinase K (10 mg/ml; Qiagen) at 50 °C to digest protein. In a second purification step, the DNA was bound to the column provided in the DNeasy tissue Kit and further purified using the supplied wash buffers. Finally, the genomic DNA was eluted in 10 mM TrisHCl pH 8.0.

4.2.5 Shearing of DNA

Genomic DNA was sheared to an average size of 1000 bp using the Nebulizer technique (Invitrogen) by following the instructions of the corresponding protocol. In short, 700 µl DNA were mixed with 1.3 – 2 ml shearing buffer (TE pH 8 containing 10 % glycerol), transferred to the Nebulizer and subjected to a pressure of 2 bar for 2 min. The sheared fragments were precipitated by the addition of 3 M sodium acetate and Isopropanol, washed with 70 % Ethanol and dissolved in 10 mM Tris-HCl.

4.2.6 Restriction digest

Digestion of genomic DNA was performed according to the manufacturer´s instructions. Most enzymes were purchased from New England Biolabs and were used with the supplied reaction buffers under appropriate reaction conditions.

4.2.7 Standard PCR

PCR was performed using Thermoprime Plus DNA Polymerase (5 u/µl) and 10x Reddy Mix™ PCR Buffer (Thermo Scientific/ ABgene). A standard PCR reaction contained 2 µl DNA template, 2 µl 10x Reddy Mix, 2 µl dNTPs (100 µM end concentration), 2 µl forward primer (10 µM end), 2 µl reverse primer (10 µM end), 0.3 µl Thermoprime polymerase, 9.7 µl H_2O. PCR reactions were incubated in a PTC-200 Peltier Thermal Cycler (MJ Research). The temperature steps of a typical PCR programme were: step 1: 94 °C for 2 min, step 2: 94 °C for 30 s, step 3: 50 – 60 °C for 30 s (depending on the optimal annealing temperature for the chosen primers), step 4: 72 °C for 1 min. Steps 2 – 4 were repeated for a total of 25 – 30 cycles. After a final incubation of the PCR reaction at 72 °C for 5 min, the PCR reaction was either directly loaded on an 1 % agarose gel or stored at -20 °C.

4.2.8 Standard gel electrophoresis (agarose gels)

DNA or RNA preparations, digestion fragments, and PCR reactions were resolved on 1 – 3 % agarose gels consisting of agarose melted in TAE-buffer (1 g agarose per 100 ml buffer). After heating in the microwave and a brief cooling period, 2 µl of ethidium bromide stock solution (10 mg/ml) were added per 100 ml of melted agarose. The liquid gel was poured into previously prepared gel chambers and a comb was added. After polymerization, the samples were mixed with 6x loading buffer (0.25 % w/v bromphenol blue; 0.25 % w/v xylene cyanol; 30 % v/v glycerol). Unless stated otherwise, gels were run in 1x TAE at 100 V for 20 – 30 min.

4.2.9 Bisulfite treatment of DNA

Bisulfite treatment of DNA was carried out after the following protocol: up to 1 µg of purified, protein-free DNA was dissolved in 50 µl H_2O; 5.5 µl of freshly prepared 3 M NaOH were added for denaturing. The mixture was incubated for 20 min at 37 °C. Meanwhile, 2.16 g sodium bisulfite were added to 3 ml of H_2O. The pH was adjusted to 5.0 by adding 200 µl of 10 M NaOH (also freshly prepared). 0.11 g hydroquinone were dissolved in 5 ml H_2O. 250 µl of the fresh hydroquinone solution were added to the bisulfite solution (final concentration 10 mM), and the volume of the bisulfite-hydroquinone solution was adjusted to 5 ml final with H_2O. 600 µl of the hydroquinone-bisulfite solution was added to the denatured DNA, mixed thoroughly and layered with mineral oil. The reaction was incubated for 12 – 14 h at 55 °C.

Afterwards, the deaminated DNA was purified according to the instructions of the GeneClean DNA purification kit (Oncor Appligene) using glass milk and the supplied washing buffers. After ethanol-precipitation, the DNA pellet was resuspended in 1 mM Tris-HCl pH 8 and stored at -20 °C.

4.2.10 Topo TA cloning for sequencing

To determine the sequence of PCR fragments of interest, the gel-purified PCR fragments were cloned into the pCR4-TOPO-vector in accordance with the instructions provided with the TOPO TA Cloning Kit for Sequencing (Invitrogen). Briefly, 0.5 to 4 µl of gel-purified PCR product were mixed with 1 µl salt solution, 1 µl TOPO vector and H_2O to a final volume of 6 µl. After 5 min of incubation at room temperature, 2 µl of the reaction were added to one vial of One Shot Chemically Competent *E. coli*, gently mixed and stored for 20 min on ice. Heat shock was performed for 30 s at 42 °C. Tubes were immediately put on ice and 250 µl SOC medium was added. After one hour at 37 °C and 200 rpm under constant shaking, appropriate volumes were spread on LB-agar plates containing 100 µg/ml ampicillin as antibiotic.

4.2.11 Expression of transformed *E. coli*

For liquid cultures of transformed *E. coli* – small scale for a Mini-Prep or large scale for a Midi-Prep – single colonies were picked with a sterile toothpick and incubated in an appropriate volume of LB medium (5 ml for a Mini-prep, 100 ml for a Midi-Prep) supplemented with the selection antibiotic ampicillin (100 µg/ml final concentration). The cultures were incubated at 37 °C under constant shaking at 220 rpm.

4.2.12 Mini-and Midi-Prep

Plasmid preparations on a “mini” or “midi” scale yielding from a few to up to 100 µg DNA were performed using the Qiagen Mini/Midi plasmid purification kit in accordance with the manufacturer´s instructions.

4.2.13 Sequencing

The bisulfite treated, PCR-amplified, and cloned sequences were diluted in water to a concentration of 100 ng/µl. Sequencing was performed by the company GATC

(Konstanz, Germany) using T7 or T3 standard primers. The sequences were analyzed using the 4peaks software (GATC).

4.2.14 Isolation of total RNA out of 0 – 3 h old *Drosophila* embryos

Total RNA was isolated using the reagent Trizol (Invitrogen) in accordance with the manufacturer´s instructions. The embryos were homogenized in appropriate volumes of Trizol using a plastic homogenizer, debris was removed by centrifugation, and total RNA was separated from DNA and proteins by the addition of chloroform. The aqueous, RNA containing phase was transferred to a new reaction vial and the RNA was precipitated with isopropanol, washed with 70 % Ethanol and dissolved in 200 µl H_2O_{DEPC}. The RNA yield was quantified using a photometer at 260 nm wavelength. The integrity of the RNA was confirmed on an 1 % agarose gel.

4.2.15 mRNA Preparation

mRNA was prepared using the QuickPrep micro mRNA purification kit (GE Healthcare). Either frozen embryos were disrupted according to the manufacturer´s instructions or total RNA preparations were used as starting material. In short, 500 µg total RNA was mixed with extraction buffer to a final volume of 400 µl, and 800 µl elution buffer were added. 1 ml oligo(dT) cellulose was prepared as stated in the protocol, mixed with the RNA and incubated for 3 min on a rotating wheel. Washing steps were performed as recommended, adding to a total of 5 times high salt wash and 2 times low salt wash. After the addition of oligo(dT) cellulose to the column, the column was washed two more times with low salt buffer. The mRNA was eluted by adding 200 µl prewarmed (65 °C) elution buffer to the column and subsequent centrifugation for 5 s at maximum speed.

After the elution, the mRNA was precipitated by adding 20 µl potassium acetate (provided with the kit), 5 µl glycogen and 500 µl 100 % ethanol and 1 h incubation at -20 °C. Subsequent centrifugation and washing was performed as in the preparation of total tRNAs. The precipitated mRNA was resuspended in 50 µl H_2O_{DEPC} .

4.2.16 Reverse transcription

cDNA Synthesis was performed according to the instructions provided with the ThermoScript™ RT-PCR System (Invitrogen) using oligo(dT) primers. Briefly, RNA,

primer, H_2O_{DEPC} and dNTPs were mixed and incubated at 65 °C for 5 min and then placed on ice. 5x cDNA synthesis buffer, DTT, RNaseOUT and Thermoscript reverse transcriptase were added as stated in the protocol. The reaction was incubated for one hour at 55 °C and afterwards terminated by heating for 5 min at 85 °C and by the addition of 1 µl of RNase H (2 u/µl; from *E. coli*; Invitrogen) with subsequent incubation at 37 °C for 20 min. The synthesized cDNA was stored at -20 °C or directly subjected to PCR.

4.2.17 Semi-quantitative RT-PCR

As a measure to compare expression levels of certain mRNAs, a semi-quantitative PCR was performed on cDNA which was obtained by reverse transcription of *Drosophila* mRNA (see above). The cDNA was used as a template for standard PCR (see above), but special care was taken to remain within the linear amplification range by using low cycle numbers (20 – 22) and including a housekeeping gene as a control for equal loading. For very weakly expressed mRNAs and therefore low amounts of cDNA, the cycle number was raised to 30. After the PCR, the housekeeping-gene-PCR was loaded on an 1 % agarose gel in different concentrations to adjust equal loading between PCR of wt and mutant and to be able to determine the corresponding volumes of the PCR of the cDNA of interest. Gels were photographed.

4.2.18 Northern blot

Northern Blots were performed as downward blots using 20x SSC for capillary transfer. By closely following the instruction manual of the DIG Northern Starter Kit (Roche), DIG-labeled probes were generated and the labeling efficiency determined.
Up to 5 µg total RNA was mixed with 2 - 3 volumes of freshly prepared loading buffer (250 µl 100 % formamide, 83 µl 37 % formaldehyde, 50 µl 10x MOPS, 50 µl 100 % glycerol, 10 µl 2.5 % bromphenol blue and 57 µl H_2O_{DEPC}), heated for 10 min at 65 °C, then chilled on ice for 1 min and run on a 2 % formaldehyde gel (3.6 g agarose, 282 ml 1x MOPS, 16.2 ml 37 % formaldehyde) in 1x MOPS running buffer for 2 - 5 h. Prior to blotting, the gel was rinsed in 20x SSC for 2 x 15 min. The blot was assembled from bottom to top as follows: a 3 – 4 cm stack of dry whatman paper, one whatman paper soaked in 20x SSC, the positively charged nylon membrane (Roche) soaked in 20x SSC, the gel, 3 pieces of whatman paper soaked

in 20x SSC, one large whatman paper soaked in 20x SSC (functioning as “bridge” by touching the 20x SSC surface with its edges), and on top a light weight (e.g. a plastic lid or an empty plastic box). Blotting was performed over night at room temperature. The RNA was fixed on the membrane by UV-crosslinking in a UV-stratalinker (Stratagene) with 120000 microjoules/ cm^2 for 20 – 25 seconds. After the crosslink the membrane was stored dry at 4 °C.

Prehybridization, hybridization and subsequent washes, as well as blocking and antibody incubation were performed using the reagents supplied with the DIG Northern Starter Kit (strictly following the protocol). For signal detection, the membrane was equilibrated in detection buffer (0.1 M Tris-HCl, 0.1 M NaCl pH 9.5) for 5 min. 2 ml of detection buffer was spread in several drops on a plastic surface and mixed with CDP-Star (a kit component). The membrane was placed upside down on the buffer-CDPS-mixture. Air bubbles were carefully avoided, excess liquid removed and the plastic bag was sealed. After 20 min incubation at room temperature, the membrane was exposed to an X-ray film for 5 – 10 min. Due to the signal increase during the first 24 h, multiple exposures could be taken.

4.2.19 Stripping and reprobing of Northern blots

To remove probe and antibody signal, the membrane was first thoroughly soaked in H_2O_{DEPC} and then incubated in freshly prepared stripping buffer (50 % formamide, 50 mM TrisHCl pH 7.5, 5 % SDS) for 2 x 60 min at 80 °C. Then the membrane was rinsed in 2x SSC for 2 x 5 min. The membrane was stored at 4 °C in 2x SSC in a sealed bag or directly used for prehybridization.

4.2.20 Embryonic protein extracts

Roughly 100 - 200 µl embryos were transferred from collection plates into a glass homogenizer using a soft brush and egg-wash (0.1 % Triton and 7 g NaCl/l). The embryos were rinsed two more times with egg-wash. Finally, the last wash was completely removed and replaced with 200 µl protein extraction buffer (50 mM HEPES, 0.5 mM EDTA, 100 mM NaCl, 0.05 % NP-40; pH 7.5); just before use, proteinase inhibitor cocktail was added (Complete mini EDTA free, Roche). Twenty strokes with a tight-fitting pestle were sufficient to homogenize the embryos. After 20 min incubation on ice, the homogenate was transferred into a 1.5 ml reaction tube and was centrifuged for 30 min at 4 °C and 13200 rpm in a tabletop-centrifuge.

The supernatant was carefully transferred into another reaction tube. For Western blotting, appropriate amounts of 5x SDS loading buffer were added, and the extract was incubated for 5 min at 95 °C. Quantification of total protein was determined by Bradford assay.

4.2.21 Western blot

For two 10 % polyacrylamide gels, the following ingredients were mixed: separation gel: 10 ml 30 % acrylamide, 13.6 ml H_2O, 6 ml 1.6 M Tris-HCl pH 6.8; 200 µl 10 % SDS, 150 µl 10 % APS and 15 µl TEMED. Stacking gel: 4.5 ml 30 % acrylamide, 0.6 M Tris-HCl pH 6.8; 19 ml H_2O, 300 µl 10 % SDS, 150 µl 10 % APS, 15 µl TEMED. Up to 100 µg protein extract was run per mini-gel lane in a SDS-PAGE electrophoresis chamber (“Mighty-small II for 8 x 7 cm gels”, Amersham Biosciences) with 90 V (constant) through the stacking gel and 130 V (constant) through the separation gel. The running buffer consisted of 14.4 g glycine (192 mM), 3.03 g Tris base (25 mM), and 1 % SDS per litre. The pH was adjusted to 8.3.

The wet transfer was performed in a vertical wet chamber (“Mini trans-blot cell”, Biorad) using transfer buffer (600 ml H_2O, 200 ml methanol, 100 ml 10x borate buffer, 4 ml EDTA (0.5 M), 1 ml DTT (1M)) for 5 min at 100 mA (constant), 5 min at 200 mA (constant), 5 min at 300 mA (constant) and 45 min at 400 mA (constant). After the blotting, the membrane was stained with Ponceau S for 5 min, then destained with water, and the blotting efficiency was determined by scanning the Ponceau S signal. The membrane was blocked in 5 % non-fat dried milk in 1x PBS for 1 h at room temperature or at 4 °C over night, then the first antibody (anti-peptide 2 from rabbit; dilution 1:500) was added in 5 % milk/ PBS for 1 h at room temperature. Subsequent washing of the membrane was performed for 3 x 10 min in blocking solution. The secondary antibody (goat-anti-rabbit, from Jackson Immuno Research) was added in a 1:10000 dilution for 30 min at room temperature. This was again followed by three washes in blocking solution, followed by one wash in 1x PBS/ 0.1 % Tween 20.

ECL solution was prepared according to the manufacturers instructions and applied to the membrane for 1 min at room temperature. The membrane was sealed in a plastic bag and exposed to X-ray films (Fujifilm).

4.2.22 Stripping and reprobing of Western blots

The to-be-stripped membrane was incubated twice for 1 h in 100 ml stripping buffer (4.5 g glycine, 3 ml 10 % SDS, 3 ml Tween 20; ad 300 ml with H_2O; pH 2.2) at room temperature, then rinsed for another 10 min in stripping buffer at room temperature. Subsequently, the membrane was washed four times for 5 min in TBST, and then blocked for one hour in 5 % milk/PBS prior to incubation with the new first antibody.

4.2.23 Pseudo-PCR

To fill in the second strand of the single-stranded tRNA-ribozyme-oligo, 3 µl of template oligo (3 µM final concentration) were mixed with 6 µl 50 mM $MgCl_2$, 10 µl 10x PCR buffer (Rapidozym Gentherm), 3 µl T7-Primer (3 µM final concentration), 10 µl of each dNTP (final concentration 1 mM) 36 µl H_2O and 2 µl Taq polymerase (5 u/µl; Rapidozym, Gentherm) in a total volume of 100 µl. The reaction mixture was subjected to temperature cycling, which included the following steps: 1. 94 °C for 2 min; 2. 94 °C for 30 s; 3. 54 °C for 30 s; 4. 72 °C for 30 s; 5. go to step 2 for 34 additional cycles; 6. 72 °C for 3 min. Samples were stored at -20 °C.

4.2.24 Digest of plasmids for *in vitro* transcription

Some tRNAs were not encoded by a single stranded DNA template but had been obtained from collaborators cloned into a plasmid (see above). Prior to *in vitro* transcription, the plasmid had to be linearized right behind the tRNA sequence to generate a stop for the T7 polymerase. Linearization was achieved by cutting the plasmid (0.4 µg/µl) with 0.5 u/µl of the restriction enzyme BstNI (10 u/µl; New England Biolabs) in buffer NEB2 supplemented with BSA for 3 hours at 60 °C. After linearization, the DNA was purified via phenol-diethylether extration and precipitated in 0.5 M ammonium acetate and ethanol. The pellet was washed once in 80 % ethanol and resuspended in water.

4.2.25 *In vitro* transcription

Prior to transcription, a 2x “T7-Premix” was prepared, containing 400 µl 5x Strasbourg buffer (200 mM TrisHCl, pH 8.1; 5 mM Spermidine, 25 mM DTT and 0.05 % Triton X-100), 60 µl 1M $MgCl_2$, 20 µl 1M DTT, 4 µl BSA [1 mg/ml], and H_2O ad 1 ml. Also, a 5x NTP mastermix was prepared, with 25 mM each NTP. For

radioactive *in vitro* transcription, the concentration of the cold nucleotide triphosphate which was also added in a radioactive form, e.g. [α-^{32}P]-CTP, was lowered to 5 mM - resulting in 1 mM final concentration of cold nucleotide triphosphate - while the other NTPs were kept constant at 5 mM final concentration in the transcription mixture. The transcription reaction was usually set up in a volume of 400 µl, containing 100 µl PCR reaction, 200 µl 2x T7-premix, 80 µl 5x NTP-mix, 10 µl T7-polymerase (250 u/µl, Fermentas) and 10 µl H_2O. For radioactive transcription, the reaction was supplemented with 10 – 20 µl [α-^{32}P]-CTP (10 µCi/µl). The transcription reaction was incubated for 3h at 37 °C in a waterbath. Alternatively, the T7-Megascript Kit (Ambion) was used following the manufacturer´s instructions.

4.2.26 Polyacrylamide-Gel-Electrophoresis (PAGE)

Polyacrylamide gels in various sizes and thicknesses were poured using standard glass plates and spacer sets. Unless indicated otherwise, 12 % denaturing polyacrylamide gels were used to separate tRNAs. For one 12 % polyacryamide gel, the glass plates were cleaned thoroughly and coated with 2 % dichlordimethylsilane (Fluka) in chloroform. Roughly 60 ml of 12 % stock solution (prepared from Rotiphorese sequencing gel buffer concentrate, acrylamide concentrate, and diluter (Roth)) were mixed with 500 µl 10 % APS and 100 µl TEMED and poured. After polymerization, the gel pockets were rinsed with 1x TBE buffer. After fitting the gel tightly into the gel running apparatus, the samples were loaded, and the gel was run in 1x TBE for two hours at 20 – 25 W (constant). To avoid overheating, the glass plates were cooled with a ventilator.

4.2.27 Elution and precipitation of gel-purified tRNAs

tRNA was eluted from the excised gel piece by over night incubation in 400 µl 0.5 M ammonium acetate. On the following day, the solution was cleared from residual gel fragments by centrifuging for 3 min at 2700 rpm through a Nanosep 0.45 µm centrifugal device (Pall Life Sciences). Precipitation of tRNA was performed by adding 800 µl 100 % EtOH cooled to -80 °C, incubation for 30 min at -20 °C and centrifugation at 13000 rpm for at least 40 min. Then the EtOH was carefully removed, and the pellet washed once with 80 % EtOH. After a brief drying period (under vacuum), the tRNA pellet was resuspended in H_2O and stored at -20 °C.

4.2.28 Precipitation of small tRNA fragments using lithium perchlorate

RNA fragments smaller than 15 nucleotides were precipitated using 2 % lithium perchlorate in acetone (2 g in 100 ml) to ensure quantitative recovery of the RNA out of the solution. After clearance from gel pieces by centrifugation through the column (see above), the RNA containing solution was divided into 100 µl aliquots in fresh eppendorf tubes. Per aliquot, 1 ml of lithium perchlorate/acetone solution was added, followed by centrifugation for at least 40 min at 13000 rpm at room temperature. Salt pellets were clearly visible.

4.2.29 NAP5 Column Purification

For desalting of the small precipitated radioactive RNA fragments, the pellets were dissolved in 100 µl H_2O and purified over a NAP5 column (GE Healthcare). The column was equilibrated with two times 5 ml H_2O (gravity flow). After addition of the sample, the column was washed with 400 µl H_2O once, followed by two times 500 µl H_2O. Aliquots of three drops were collected and the RNA-containing fractions determined by Cerenkov counting of the aliquots. The correct fractions were pooled and the water was evaporated using a speedvac.

4.2.30 Autoradiography

Radioactive gels and cellulose plates were exposed to luicide imaging screens (Amersham, GE Healthcare, Munich) in light-proof film cassettes. Scanning of the imaging screens was performed using the phosphoimager Typhoon 9400 (Amersham). The images were analysed using ImageQuant software (Version 5.2).

4.2.31 Liquid scintillation counting and Cerenkov counting

Tritiated samples were spotted on whatman filters and measured by scintillation counting in 3 ml UltimaGold scintillation liquid (Packard) in a LS 6500 Counter (Beckman Coulter, Krefeld). [α-^{32}P]-CTP labeled samples were measured without scintillation liquid by Cerenkov-counting.

4.2.32 Magnetic Bead Experiment

600 µl Streptavidin MagneSphereR ParaMagnetic Particles (Promega) were put into the magnetic rack and the supernatant removed. The magnetic beads were washed

twice with 600 µl solution A (100 mM NaOH, 50 mM NaCl) for 2 min at room temperature, then twice with 600 µl solution B (100 mM NaCl).

To coat the magnetic particles with the biotinylated oligo via the biotin-streptavidin interaction, 180 µl biotinylated Oligo (30 µM end) was pipetted to 420 µl B+W-solution (10 mM Tris-HCl pH 7.5; 1 mM Na_2EDTA; 2 M NaCl) and incubated for 20 min at 37 °C. The beads were again put into the magnetic rack, and the supernatant saved for reuse. The beads were washed twice for 2 min in 12x SSC (made from a dilution of 20x SSC in H_2O_{DEPC}) and stored in 600 µl 12x SSC at 4 °C. 400 - 1000 µg total RNA or 50 - 100 µg of total tRNA in 600 µl H_2O_{DEPC} were heated for 5 min at 75 °C, as well as 600 µl of prepared magnetic beads in 12x SSC . Then the beads and the RNA were pooled in one tube and heated for additional 5 min at 75 °C. After a cooling period of 40 min at room temperature, the beads were washed twice for 2 min with 6x SSC and then directly resuspended in 30 – 50 µl of loading buffer.

4.2.33 Dephosphorylation

tRNA (10 µl) isolated from *Drosophila* embryos mixed with 5 µl 10x BAP-buffer (Fermentas) and 35 µl H_2O. After 5 min of incubation at 80 °C, 0.5 µl BAP enzyme (150 u/µl, Fermentas) was added, followed by 15 min incubation at 37 °C, 15 min at 50 °C and 15 min at 65 °C.

4.2.34 Phenol-Diethylether-Extraction

After dephosphorylation, the enzyme was removed by a phenol-diethylether extraction. 50 µl reaction mix were added to 50 µl Roti-Aqua-Phenol (Roth), vortexed and centrifuged for 3 min at 3000 rpm. The aqueous phase was removed and the extraction repeated with another 50 µl phenol. After centrifugation, the aqueous phase was added to 150 µl diethylether (saturated with water). After vortexing, the mixture was centrifuged for 3 min at 3000 rpm. The diethylether-extraction-step was repeated once as well. The aqueous phase was transferred into a new reaction tube and 100 µl 100 % EtOH (-80 °C) were added. Precipitation of the tRNA was performed over night at -20 °C.

4.2.35 End-Labeling

5´-Endlabeling with [γ-^{32}P]-ATP was performed with polynucleotide kinase (Fermentas). 14 µl tRNA in H_2O were incubated with 2 µl buffer A (Fermentas), 2 µl [γ-^{32}P]-ATP (10 µCi/µl) and 2 µl PNK (10 u/µl, Fermentas) for one hour at 37 °C in a waterbath.

4.2.36 OH^--Ladder

1 µl tRNA (3000 – 20000 cpm) was incubated with 1 µl total tRNA from *E. coli* (10 µg/µl) and 8 µl $NaHCO_3$ (pH 9) for 10 min at 90 °C, then immediately put on ice for 2 min and afterwards mixed with 10 µl Pb-Stop-solution.

4.2.37 T1-Digest

1 µl tRNA (3000 – 20000 cpm) was incubated with 1 µl tRNA *E.coli* (10 µg/µl) and 8 µl T1-Puffer (40 mM Tris-HCl pH 7.5; 40 mM NaCl; 10 mM $MgCl_2$) for 10 min at 55 °C. 2 µl T1-RNase (several dilutions; 0.1 – 0.001 units, Gibco) were added, followed by 10 min incubation at 55 °C. After cooling on ice for 2 min, 10 µl Pb-Stop-solution were added.

4.2.38 DNAzyme experiment and subsequent quantitative end-labeling

Appropriate amounts of tRNA (depending on the experiment from 60 ng to several micrograms) were mixed with a 5 - 10 molar excess of DNAzyme, 5 µl 5x buffer (250 mM TrisCl pH 7.5; 750 mM KCl, and 50 mM $MgCl_2$), and H_2O to an end volume of 25 µl. The tRNA was cut by the DNAzyme during 15 – 20 cycles of incubation at 80 °C for 2 min, controlled cooling to 37 °C by 0.3 °C/sec, and 5 min at 37 °C. After that, ^{32}P-labeled tRNA was loaded directly onto a 12 % polyacrylamide gel. Unlabeled tRNA was end-labeled quantitatively by directly adding 2.5 µl buffer A (Fermentas), 1 µl [γ-^{32}P]-ATP (10 µCi), 2.5 µl non-radioactive ATP (100 µM), 18 µl H_2O and 1 µl PNK (10 u/µl, Fermentas) and incubating the reaction for 1 h at 37 °C in a waterbath. DNAzyme was afterwards removed by the addition of 1 µl Dnase I (50 u/µl, Fermentas) for 30 min at 37 °C. The end-labeling reaction was then gel-purified.

4.2.39 P1-Digest

4 µl tRNA in H_2O were mixed with 1 µl total tRNA of *E. coli* (10 µg/µl), 1 µl 5 mM ZnCl, 1 µl 0.2 M NaOAc pH 5.5 and 3 µl P1 (0.3 u/µl Roche), in a total volume of 10 µl. The reaction mixture was incubated for 2 h at 50 °C.

4.2.40 TLC (Thin-Layer-Chromatography)

Two-dimensional TLC was carried out on 20 x 10 cm cellulose F plates (Merck). 1 - 1.5 µl of a P1 digest were spotted. After drying, the first (20 cm) dimension (solvent A: isobutyric acid/ 25 % ammonium solution/ H_2O (70/ 1.1/ 28.9: v/v/v)) was run over night. After complete drying of the cellulose plate, the second dimension was run in solvent B (0.1 M sodium phosphate pH 6.8/ ammonium sulphate/ 1-propanol (100/60/2; v/p/v)) for 5 – 6 h. The cellulose plate was dried and exposed to a luicide imaging screen (Amersham).

4.2.41 *Drosophila* S2R$^+$ cell culture

Stably Flag-Dnmt2 transfected S2R$^+$ cells (a gift of Dr. Matthias Schaefer) were cultured in Schneider´s medium supplemented with penicillin (1000 u/ml), streptomycin (100 µg/ml) and 10 % FCS. To ensure the stable expression of the transfected sequences, blasticidin was added as a selection reagent at a final concentration of 2.5 µg/ml. Cells were splitted once a week in 75 cm^2 – 175 cm^2 flasks in a 1:5 to 1:10 ratio. Briefly, cells were detached from the flask bottom by gentle rinsing with a 10 ml pipette. Since the cells are only semi-adherent, the addition of trypsin was not necessary. To pellet, cells were centrifuged for 3 min at 130 g. The debris containing supernatant was removed, fresh medium was added in an appropriate volume, and cells were plated in a new flask. The cells were incubated at 25 °C in an incubator or at room temperature.

4.2.42 Preparation of *Drosophila* cell extracts and immunoprecipitation of Flag-Dnmt2

Cells were grown in Schneider´s Medium which had been supplemented with penicillin (1000U/ml), streptomycin (100 µg/ml), 10 % FCS and blasticidine as described above. Protein expression was achieved by adding $CuSO_4$ (1 mM stock) to a final concentration of 1 µM for 72 h. After the induction period, the cells were collected into a 50 ml Falcon tube using a cell scraper and centrifuged at 150 g for

10 min at 4 °C. The cells were once suspended in 10 ml ice-cold PBS, a 500 µl aliquot was taken for cell count determination, and the cells were spun a second time at 150 g for 10 min at 4 °C.

PBS was removed and the cells were resuspended in 1 ml hypotonic buffer A (10 mM HEPES pH 7.9; 10 mM KCl; 340 mM Sucrose; 1.5 mM $MgCl_2$; 1 mM DTT; 10 % glycerol; proteinase inhibitor cocktail (from Roche; 1 tablet per 15 ml); 1 mM PMSF), transferred to an eppendorf tube and incubated on ice for 10 min for swelling. The cells were broken open by drawing them 10 times through a syringe, using a hypodermic needle (25 G); next Triton X-100 was added to a final concentration of 0.1 %. For continued lysis, the cells were rotated at 4 °C for 15 min, then centrifuged at 480 g for 9 min at 4 °C to remove cell debris. The supernatant was transferred into a new tube and again spun down at 1300 g for 5 min at 4 °C (this step separated intact nuclei from cytosol). Again the supernatant was transferred and centrifuged at 16100 g for 30 min at 4 °C. 50 µl of the supernatant were taken as an input control for Western analysis as well as for Bradford protein measurement.

The anti-FLAG M2 affinity gel resin (Sigma) was thoroughly resuspended to form a uniform 50 % slurry. Per ml protein extract, 60 – 70 µl slurry was used. The aliquoted resin was centrifuged at 8200 g for 30 s and let to settle for 1 - 2 min. The supernatant was carefully removed, and the packed gel was washed twice for 5 min at RT with 0.5 ml TBS with constant rotation. Following centrifugation and supernatant removal, the resin was equilibrated by washing it once with 0.5 ml buffer A. For immunoprecipitation, the protein extract was added to the resin-containing tubes and rotated at 4 °C over night. Next, the resin was centrifuged at 8200 g to remove the supernatant, and the beads were washed five times for 5 min with 0.5 ml buffer A at 4 °C. The washing was repeated once with 0.5 ml tRNA-MT assay buffer (100 mM Tris pH 8.0; 100 mM NH_4OAc; 10 mM DTT (freshly added), 0.1 mM EDTA; 10 mM $MgCl_2$) at 4 °C. The supernatant was removed completely. To elute the FLAG-Dnmt2-protein from the resin, 3 µl of a 5 µg/µl 3x FLAG peptide stock solution were added to 100 µl tRNA-MT assay buffer. 100 µl of this elution solution were added to each tube of resin, and the samples were incubated with gentle shaking at 25 °C for 15 min. The resin was spun down for 30 s at 8200 g. The protein-containing supernatant was transferred to a new reaction tube, supplemented with 50 % glycerol, and stored at -20 °C.

4.2.43 Preparation of recombinant, His-tagged hDnmt2

The plasmid pET28a(+) containing His-tagged, human *Dnmt2* gene was a gift from Tomek Jurkowski (Jacobs University Bremen; Hermann et al., 2003; Jurkowski et al., 2008). 200 µl of *E. coli* (DE3) Rosetta 2 pLysS cells (Novagen) were transformed with 50 ng of the plasmid as follows: Cells were carefully thawed on ice, mixed with the plasmid DNA and incubated on ice for 5 min. After a 30 s heat shock at 42 °C, cells were again incubated on ice for 2 min, followed by the addition of 300 µl SOC-medium. Expression of the resistance genes was allowed for one hour by constant shaking at 37 °C. Aliquots ranging from 50 to 150 µl were spread on kanamycin/ chloramphenicol-containing LB-agar plates. The concentration for kanamycin was 50 µg/ml; for chloramphenicol 170 µg/ml. On the next day, a single colony was picked and an over night culture was prepared in 10 ml LB medium supplemented with kanamycin and chloramphenicol (same antibiotics concentration as above) under constant shaking at 220 rpm at 37 °C over night. A large-scale culture (250 – 500 ml) was inoculated with the over night culture and grown to an optical density of 0.6. Then, the culture was induced with 1 mM IPTG (final concentration) and grown for an additional three hours. The bacteria were harvested by centrifugation for 20 min at 4000 g. Purification of the recombinant protein was performed according to the protocol of the Qia*express* Ni-NTA fast start kit (Qiagen). Briefly, the cells were lysed under native conditions, cell debris was removed by centrifugation and the cleared supernatant poured over a Ni-NTA column. After washing with the supplied wash buffer, the hDnmt2 protein was eluted with the elution buffer supplied with the kit in 4 x 0.5 ml aliquots. The aliquots containing the highest protein concentration were pooled and dialyzed in a 2 l volume of dialysis buffer 1 for two hours, then in 2 l of dialysis buffer 2 over night.

4.2.44 *In vitro* methylation assay

The *in vitro* methylation assay measures the transfer of a tritiated methyl group from its donor S-adenosyl-methionine (SAM) onto the target tRNA, which is catalyzed by m^5C methyltransferases. The tRNA is precipitated on small filters and the radioactive signal counted in a scintillation counter. The standard reaction volume was 40 µl. Unless stated otherwise, 120 pmol tRNA were diluted in water and heated to 80 °C for 2 min. tRNA-MT-assay buffer and DTT were added immediately to final concentrations of 100 mM Tris-HCl pH 8.0; 100 mM NH_4OAc; 0.1 mM EDTA, 10 mM

$MgCl_2$ and 10 mM DTT. ^{3}H-SAM-Stock solution (10x; containing cold and ^{3}H-SAM) was added to a final concentration of 20 µM SAM and 1 µCi per sample. After 2 min incubation at 37 °C, the enzyme of interest was added to final concentrations of 0.5 – 1 µM and mixed well by pipetting. After 140 min, the reaction was spotted onto small whatman filters and precipitated in 5 % ice-cold TCA, followed by two washes for 10 min in 5 % TCA on ice. Then the filters were swirled in EtOH. After drying, the incorporated tritium signal was measured by liquid scintillation counting. One microliter of the 10x SAM-stock solution was also spotted in duplicate.

4.2.45 Visualisation of gel shifts on native (non-denaturing) Gels

Native gels were poured by diluting 19:1 acrylamide: bisacrylamide solution (corresponding to 40 %) in 0.5x TBE to 8 %. Polymerization was achieved by the addition of 400 µl 10 % APS and 80 µl TEMED. Gels were prerun for 1 h at 8 – 10 W in 0.5x TBE at 4 °C. Samples were mixed with native gel loading buffer prior to loading. After the samples had run into the gel at 10 W, the gel was run over night at 75 V (constant) in the cold room.

4.2.46 Splint Ligation of mouse tRNA^{Asp} containing either C, m^{5}C or F^{5}C at C38

RNA oligos can be ligated to a full length tRNA molecule with the help of a DNA splint. The ligation of mouse tRNA^{Asp} was essentially performed as described in (Kurschat et al., 2005). Prior to ligation, the oligo comprising the middle part of the tRNA was phosphorylated. 3000 pmol oligo MH353 (or MH354 or MH355) were incubated in 50 mM TrisHCl pH 7.4; 10 mM $MgCl_2$ final concentration (pipetted as 5 µl 5x KL-buffer), 5 mM ATP and 5 mM DTT, as well as 3.75 µl PNK (Fermentas, 10 u/µl) in a total volume of 40 µl for one hour at 37 °C. Next, 3000 pmol of the 5´-oligo (MH352) and of the 3´-oligo (MH356) were added, together with 10 µl 5x KL buffer, 30 µl DNA splint (oligo MH117; final concentration 10 µM), 2.5 µl 100 mM ATP and 2.5 µl 100 mM DTT to a total volume of 91 µl. The reaction mixture was incubated first for 5 min at 75 °C, then for 15 min at room temperature. 10 µl of T4 DNA Ligase (30 weiss units/µl; Fermentas) were added, and the reaction incubated over night at 16 °C. On the next day, the DNA splint was digested with 300 weiss units of Dnase I (Fermentas; 30 weiss units/µl). The ligated tRNA was then purified via denaturing PAGE.

5 References

Addison WR, Gillam IC, Tener GM. 1982. The nucleotide sequence of tRNA4Val of Drosophila melanogaster. Chloroacetaldehyde modification as an aid to RNA sequencing. *J Biol Chem 257*:674-677.

Agris PF, Malkiewicz A, Guenther R, Basti M, Sengupta R, Stuart J. 1995. Importance of modified nucleosides to the structure and function of tRNAs. *Nucleic Acids Symp Ser*:254-255.

Agris PF, Vendeix FA, Graham WD. 2007. tRNA's wobble decoding of the genome: 40 years of modification. *J Mol Biol 366*:1-13.

Aharoni A, Gaidukov L, Khersonsky O, Mc QGS, Roodveldt C, Tawfik DS. 2005. The 'evolvability' of promiscuous protein functions. *Nat Genet 37*:73-76.

Banerjee S, Fisher O, Lohia A, Ankri S. 2005. Entamoeba histolytica DNA methyltransferase (Ehmeth) is a nuclear matrix protein that binds EhMRS2, a DNA that includes a scaffold/matrix attachment region (S/MAR). *Mol Biochem Parasitol 139*:91-97.

Baranowski W, Dirheimer G, Jakowicki JA, Keith G. 1994. Deficiency of queuine, a highly modified purine base, in transfer RNAs from primary and metastatic ovarian malignant tumors in women. *Cancer Res 54*:4468-4471.

Baylin SB, Herman JG. 2000. DNA hypermethylation in tumorigenesis: epigenetics joins genetics. *Trends Genet 16*:168-174.

Behm-Ansmant I, Massenet S, Immel F, Patton JR, Motorin Y, Branlant C. 2006. A previously unidentified activity of yeast and mouse RNA:pseudouridine synthases 1 (Pus1p) on tRNAs. *Rna 12*:1583-1593.

Bestor TH. 1988. Cloning of a mammalian DNA methyltransferase. *Gene 74*:9-12.

Biniszkiewicz D, Gribnau J, Ramsahoye B, Gaudet F, Eggan K, Humpherys D, Mastrangelo MA, Jun Z, Walter J, Jaenisch R. 2002. Dnmt1 overexpression causes genomic hypermethylation, loss of imprinting, and embryonic lethality. *Mol Cell Biol 22*:2124-2135.

Bird A. 2002. DNA methylation patterns and epigenetic memory. *Genes Dev 16*:6-21.

Bjork GR, Ericson JU, Gustafsson CE, Hagervall TG, Jonsson YH, Wikstrom PM. 1987. Transfer RNA modification. *Annu Rev Biochem 56*:263-287.

Bjork GR, Jacobsson K, Nilsson K, Johansson MJ, Bystrom AS, Persson OP. 2001. A primordial tRNA modification required for the evolution of life? *Embo J 20*:231-239.

Brzezicha B, Schmidt M, Makalowska I, Jarmolowski A, Pienkowska J, Szweykowska-Kulinska Z. 2006. Identification of human tRNA:m5C methyltransferase catalysing intron-dependent m5C formation in the first position of the anticodon of the pre-tRNA Leu (CAA). *Nucleic Acids Res 34*:6034-6043.

Bujnicki JM, Feder M, Ayres CL, Redman KL. 2004. Sequence-structure-function studies of tRNA:m5C methyltransferase Trm4p and its relationship to DNA:m5C and RNA:m5U methyltransferases. *Nucleic Acids Res 32*:2453-2463.

Bujnicki JM, Radlinska M. 1999. Molecular phylogenetics of DNA 5mC-methyltransferases. *Acta Microbiol Pol 48*:19-30.

Cairns MJ, King A, Sun LQ. 2003. Optimisation of the 10-23 DNAzyme-substrate pairing interactions enhanced RNA cleavage activity at purine-cytosine target sites. *Nucleic Acids Res 31*:2883-2889.

Cheng X. 1995. DNA modification by methyltransferases. *Curr Opin Struct Biol 5*:4-10.

Cheng X, Roberts RJ. 2001. AdoMet-dependent methylation, DNA methyltransferases and base flipping. *Nucleic Acids Res 29*:3784-3795.

Chiang PK, Gordon RK, Tal J, Zeng GC, Doctor BP, Pardhasaradhi K, McCann PP. 1996. S-Adenosylmethionine and methylation. *Faseb J 10*:471-480.

Cohen HM, Tawfik DS, Griffiths AD. 2004. Altering the sequence specificity of HaeIII methyltransferase by directed evolution using in vitro compartmentalization. *Protein Eng Des Sel 17*:3-11.

Cohn WE. 1960. Pseudouridine, a carbon-carbon linked ribonucleoside in ribonucleic acids: isolation, structure, and chemical characteristics. *J Biol Chem 235*:1488-1498.

Cohn WE, Volkin E. 1951. Nucleoside-5´-phosphates from ribonucleic acid. *Nature 167*:483-484.

Davis FF, Allen FW. 1957. Ribonucleic acids from yeast which contain a fifth nucleotide. *J Biol Chem 227*:907-915.

de Crecy-Lagard V, Marck C, Brochier-Armanet C, Grosjean H. 2007. Comparative RNomics and modomics in Mollicutes: prediction of gene function and evolutionary implications. *IUBMB Life 59*:634-658.

Decatur WA, Liang XH, Piekna-Przybylska D, Fournier MJ. 2007. Identifying effects of snoRNA-guided modifications on the synthesis and function of the yeast ribosome. *Methods Enzymol 425*:283-316.

Dirheimer G, Baranowski W, Keith G. 1995. Variations in tRNA modifications, particularly of their queuine content in higher eukaryotes. Its relation to malignancy grading. *Biochimie 77*:99-103.

Dong A, Yoder JA, Zhang X, Zhou L, Bestor TH, Cheng X. 2001. Structure of human DNMT2, an enigmatic DNA methyltransferase homolog that displays denaturant-resistant binding to DNA. *Nucleic Acids Res 29*:439-448.

Droogmans L, Roovers M, Bujnicki JM, Tricot C, Hartsch T, Stalon V, Grosjean H. 2003. Cloning and characterization of tRNA (m1A58) methyltransferase (TrmI) from Thermus thermophilus HB27, a protein required for cell growth at extreme temperatures. *Nucleic Acids Res 31*:2148-2156.

Eggermann T, Eggermann K, Schonherr N. 2008. Growth retardation versus overgrowth: Silver-Russell syndrome is genetically opposite to Beckwith-Wiedemann syndrome. *Trends Genet 24*:195-204.

Emmerich B, Zubrod E, Weber H, Maubach PA, Kersten H, Kersten W. 1985. Relationship of queuine-lacking transfer RNA to the grade of malignancy in human leukemias and lymphomas. *Cancer Res 45*:4308-4314.

Ericson JU, Bjork GR. 1986. Pleiotropic effects induced by modification deficiency next to the anticodon of tRNA from Salmonella typhimurium LT2. *J Bacteriol 166*:1013-1021.

Esteller M, Herman JG. 2002. Cancer as an epigenetic disease: DNA methylation and chromatin alterations in human tumours. *J Pathol 196*:1-7.

Fatemi M, Hermann A, Pradhan S, Jeltsch A. 2001. The activity of the murine DNA methyltransferase Dnmt1 is controlled by interaction of the catalytic domain with the N-terminal part of the enzyme leading to an allosteric activation of the enzyme after binding to methylated DNA. *J Mol Biol 309*:1189-1199.

Fechter P, Rudinger J, Giege R, Theobald-Dietrich A. 1998. Ribozyme processed tRNA transcripts with unfriendly internal promoter for T7 RNA polymerase: production and activity. *FEBS Lett 436*:99-103.

Feil R, Khosla S. 1999. Genomic imprinting in mammals: an interplay between chromatin and DNA methylation? *Trends Genet 15*:431-435.

Feinberg AP, Vogelstein B. 1983. Hypomethylation distinguishes genes of some human cancers from their normal counterparts. *Nature 301*:89-92.

Finsterer J. 2007. Genetic, pathogenetic, and phenotypic implications of the mitochondrial A3243G tRNALeu(UUR) mutation. *Acta Neurol Scand 116*:1-14.

Fisher O, Siman-Tov R, Ankri S. 2004. Characterization of cytosine methylated regions and 5-cytosine DNA methyltransferase (Ehmeth) in the protozoan parasite Entamoeba histolytica. *Nucleic Acids Res 32*:287-297.

Fisher O, Siman-Tov R, Ankri S. 2006. Pleiotropic phenotype in Entamoeba histolytica overexpressing DNA methyltransferase (Ehmeth). *Mol Biochem Parasitol 147*:48-54.

Fontecave M, Atta M, Mulliez E. 2004. S-adenosylmethionine: nothing goes to waste. *Trends Biochem Sci 29*:243-249.

Gardiner-Garden M, Frommer M. 1987. CpG islands in vertebrate genomes. *J Mol Biol 196*:261-282.

Garel JP, Keith G. 1977. Nucleotide sequence of Bombyx mori L. tRNA1Gly. *Nature 269*:350-352.

Gaudet F, Rideout WM, 3rd, Meissner A, Dausman J, Leonhardt H, Jaenisch R. 2004. Dnmt1 expression in pre- and postimplantation embryogenesis and the maintenance of IAP silencing. *Mol Cell Biol 24*:1640-1648.

Goll MG, Bestor TH. 2005. Eukaryotic cytosine methyltransferases. *Annu Rev Biochem 74*:481-514.

Goll MG, Kirpekar F, Maggert KA, Yoder JA, Hsieh CL, Zhang X, Golic KG, Jacobsen SE, Bestor TH. 2006. Methylation of tRNAAsp by the DNA methyltransferase homolog Dnmt2. *Science 311*:395-398.

Goto Y, Nonaka I, Horai S. 1990. A mutation in the tRNA(Leu)(UUR) gene associated with the MELAS subgroup of mitochondrial encephalomyopathies. *Nature 348*:651-653.

Gowher H, Leismann O, Jeltsch A. 2000. DNA of Drosophila melanogaster contains 5-methylcytosine. *Embo J 19*:6918-6923.

Gowher H, Loutchanwoot P, Vorobjeva O, Handa V, Jurkowska RZ, Jurkowski TP, Jeltsch A. 2006. Mutational analysis of the catalytic domain of the murine Dnmt3a DNA-(cytosine C5)-methyltransferase. *J Mol Biol 357*:928-941.

Grosjean H. 2005. *Fine-Tuning of RNA Functions by Modification and Editing*: Springer Verlag.

Grosjean H, Benne R. 1998. *Modification and Editing of RNA*: American Society for Microbiology Verlag

Gruenbaum Y, Szyf M, Cedar H, Razin A. 1983. Methylation of replicating and post-replicated mouse L-cell DNA. *Proc Natl Acad Sci U S A 80*:4919-4921.

Hagervall TG, Bjork GR. 1984. Undermodification in the first position of the anticodon of supG-tRNA reduces translational efficiency. *Mol Gen Genet 196*:194-200.

Hall KB, Sampson JR, Uhlenbeck OC, Redfield AG. 1989. Structure of an unmodified tRNA molecule. *Biochemistry 28*:5794-5801.

Hansen RS. 2003. X inactivation-specific methylation of LINE-1 elements by DNMT3B: implications for the Lyon repeat hypothesis. *Hum Mol Genet 12*:2559-2567.

Helm M. 2006. Post-transcriptional nucleotide modification and alternative folding of RNA. *Nucleic Acids Res 34*:721-733.

Hengesbach M, Meusburger M, Lyko F, Helm M. 2008. Use of DNAzymes for site-specific analysis of ribonucleotide modifications. *Rna 14*:180-187.

Hermann A, Gowher H, Jeltsch A. 2004. Biochemistry and biology of mammalian DNA methyltransferases. *Cell Mol Life Sci 61*:2571-2587.

Hermann A, Schmitt S, Jeltsch A. 2003. The human Dnmt2 has residual DNA-(cytosine-C5) methyltransferase activity. *J Biol Chem 278*:31717-31721.

Horie N, Hara-Yokoyama M, Yokoyama S, Watanabe K, Kuchino Y, Nishimura S, Miyazawa T. 1985. Two tRNAIle1 species from an extreme thermophile, Thermus thermophilus HB8: effect of 2-thiolation of ribothymidine on the thermostability of tRNA. *Biochemistry 24*:5711-5715.

Horwich MD, Li C, Matranga C, Vagin V, Farley G, Wang P, Zamore PD. 2007. The Drosophila RNA methyltransferase, DmHen1, modifies germline piRNAs and single-stranded siRNAs in RISC. *Curr Biol 17*:1265-1272.

Hotchkiss RD. 1948. The quantitative separation of purines, pyrimidines and nucleosides by paper chromatography. *J Biol Chem 175*:315 - 332.

Hou YM, Li Z, Gamper H. 2006. Isolation of a site-specifically modified RNA from an unmodified transcript. *Nucleic Acids Res 34*:e21.

Huang BS, Wu RT, Chien KY. 1992. Relationship of the queuine content of transfer ribonucleic acids to histopathological grading and survival in human lung cancer. *Cancer Res 52*:4696-4700.

Hung MS, Karthikeyan N, Huang B, Koo HC, Kiger J, Shen CJ. 1999. Drosophila proteins related to vertebrate DNA (5-cytosine) methyltransferases. *Proc Natl Acad Sci U S A 96*:11940-11945.

Hur S, Stroud RM. 2007. How U38, 39, and 40 of many tRNAs become the targets for pseudouridylation by TruA. *Mol Cell 26*:189-203.

Jeltsch A, Nellen W, Lyko F. 2006. Two substrates are better than one: dual specificities for Dnmt2 methyltransferases. *Trends Biochem Sci 31*:306-308.

Jones PA, Baylin SB. 2002. The fundamental role of epigenetic events in cancer. *Nat Rev Genet 3*:415-428.

Jones PA, Laird PW. 1999. Cancer epigenetics comes of age. *Nat Genet 21*:163-167.

Jurkowski TP, Meusburger M, Phalke S, Helm M, Nellen W, Reuter G, Jeltsch A. 2008. Human DNMT2 methylates tRNAAsp molecules using a DNA methyltransferase-like catalytic mechanism. *Rna*.

Kaneda M, Okano M, Hata K, Sado T, Tsujimoto N, Li E, Sasaki H. 2004. Essential role for de novo DNA methyltransferase Dnmt3a in paternal and maternal imprinting. *Nature 429*:900-903.

Kato Y, Kaneda M, Hata K, Kumaki K, Hisano M, Kohara Y, Okano M, Li E, Nozaki M, Sasaki H. 2007. Role of the Dnmt3 family in de novo methylation of imprinted and repetitive sequences during male germ cell development in the mouse. *Hum Mol Genet 16*:2272-2280.

Katoh M, Curk T, Xu Q, Zupan B, Kuspa A, Shaulsky G. 2006. Developmentally regulated DNA methylation in Dictyostelium discoideum. *Eukaryot Cell 5*:18-25.

Khersonsky O, Roodveldt C, Tawfik DS. 2006. Enzyme promiscuity: evolutionary and mechanistic aspects. *Curr Opin Chem Biol 10*:498-508.

King MY, Redman KL. 2002. RNA methyltransferases utilize two cysteine residues in the formation of 5-methylcytosine. *Biochemistry 41*:11218-11225.

Kirino Y, Mourelatos Z. 2007. 2'-O-methyl modification in mouse piRNAs and its methylase. *Nucleic Acids Symp Ser (Oxf)*:417-418.

Klimasauskas S, Kumar S, Roberts RJ, Cheng X. 1994. HhaI methyltransferase flips its target base out of the DNA helix. *Cell 76*:357-369.

Kowalak JA, Dalluge JJ, McCloskey JA, Stetter KO. 1994. The role of posttranscriptional modification in stabilization of transfer RNA from hyperthermophiles. *Biochemistry 33*:7869-7876.

Kuhlmann M, Borisova BE, Kaller M, Larsson P, Stach D, Na J, Eichinger L, Lyko F, Ambros V, Soderbom F, Hammann C, Nellen W. 2005. Silencing of retrotransposons in Dictyostelium by DNA methylation and RNAi. *Nucleic Acids Res 33*:6405-6417.

Kumar S, Cheng X, Klimasauskas S, Mi S, Posfai J, Roberts RJ, Wilson GG. 1994. The DNA (cytosine-5) methyltransferases. *Nucleic Acids Res 22*:1-10.

Kunert N, Marhold J, Stanke J, Stach D, Lyko F. 2003. A Dnmt2-like protein mediates DNA methylation in Drosophila. *Development 130*:5083-5090.

Kurschat WC, Müller J, Wombacher R, Helm M. 2005. Optimizing splinted ligation of highly structured small RNAs. *Rna 11(12)*: 1909-14.

Larsen F, Gundersen G, Lopez R, Prydz H. 1992. CpG islands as gene markers in the human genome. *Genomics 13*:1095-1107.

Lei H, Oh SP, Okano M, Juttermann R, Goss KA, Jaenisch R, Li E. 1996. De novo DNA cytosine methyltransferase activities in mouse embryonic stem cells. *Development 122*:3195-3205.

Li E, Bestor TH, Jaenisch R. 1992. Targeted mutation of the DNA methyltransferase gene results in embryonic lethality. *Cell 69*:915-926.

Liu Y, Santi DV. 2000. m5C RNA and m5C DNA methyl transferases use different cysteine residues as catalysts. *Proc Natl Acad Sci U S A 97*:8263-8265.

Luciano DJ, Mirsky H, Vendetti NJ, Maas S. 2004. RNA editing of a miRNA precursor. *Rna 10*:1174-1177.

Lustig F, Elias P, Axberg T, Samuelsson T, Tittawella I, Lagerkvist U. 1981. Codon reading and translational error. Reading of the glutamine and lysine codons during protein synthesis in vitro. *J Biol Chem 256*:2635-2643.

Lyko F, Ramsahoye BH, Jaenisch R. 2000a. DNA methylation in Drosophila melanogaster. *Nature 408*:538-540.

Lyko F, Whittaker AJ, Orr-Weaver TL, Jaenisch R. 2000b. The putative Drosophila methyltransferase gene dDnmt2 is contained in a transposon-like element and is expressed specifically in ovaries. *Mech Dev 95*:215-217.

Maas S, Kawahara Y, Tamburro KM, Nishikura K. 2006. A-to-I RNA editing and human disease. *RNA Biol 3*:1-9.

Maden BE, Corbett ME, Heeney PA, Pugh K, Ajuh PM. 1995. Classical and novel approaches to the detection and localization of the numerous modified nucleotides in eukaryotic ribosomal RNA. *Biochimie 77*:22-29.

Maden BE, Hughes JM. 1997. Eukaryotic ribosomal RNA: the recent excitement in the nucleotide modification problem. *Chromosoma 105*:391-400.

Maglott EJ, Deo SS, Przykorska A, Glick GD. 1998. Conformational transitions of an unmodified tRNA: implications for RNA folding. *Biochemistry 37*:16349-16359.

Margot JB, Ehrenhofer-Murray AE, Leonhardt H. 2003. Interactions within the mammalian DNA methyltransferase family. *BMC Mol Biol 4*:7.

Massenet S, Motorin Y, Lafontaine DL, Hurt EC, Grosjean H, Branlant C. 1999. Pseudouridine mapping in the Saccharomyces cerevisiae spliceosomal U small nuclear RNAs (snRNAs) reveals that pseudouridine synthase pus1p exhibits a dual substrate specificity for U2 snRNA and tRNA. *Mol Cell Biol 19*:2142-2154.

Meier F, Suter B, Grosjean H, Keith G, Kubli E. 1985. Queuosine modification of the wobble base in tRNAHis influences 'in vivo' decoding properties. *Embo J 4*:823-827.

Mortusewicz O, Schermelleh L, Walter J, Cardoso MC, Leonhardt H. 2005. Recruitment of DNA methyltransferase I to DNA repair sites. *Proc Natl Acad Sci U S A 102*:8905-8909.

Motorin Y, Grosjean H. 1999. Multisite-specific tRNA:m5C-methyltransferase (Trm4) in yeast Saccharomyces cerevisiae: identification of the gene and substrate specificity of the enzyme. *Rna 5*:1105-1118.

Motorin Y, Keith G, Simon C, Foiret D, Simos G, Hurt E, Grosjean H. 1998. The yeast tRNA:pseudouridine synthase Pus1p displays a multisite substrate specificity. *Rna 4*:856-869.

Murray NE. 2002. 2001 Fred Griffith review lecture. Immigration control of DNA in bacteria: self versus non-self. *Microbiology 148*:3-20.

Nobles KN, Yarian CS, Liu G, Guenther RH, Agris PF. 2002. Highly conserved modified nucleosides influence Mg2+-dependent tRNA folding. *Nucleic Acids Res 30*:4751-4760.

O'Gara M, Horton JR, Roberts RJ, Cheng X. 1998. Structures of HhaI methyltransferase complexed with substrates containing mismatches at the target base. *Nat Struct Biol 5*:872-877.

Okano M, Xie S, Li E. 1998a. Cloning and characterization of a family of novel mammalian DNA (cytosine-5) methyltransferases. *Nat Genet 19*:219-220.

Okano M, Xie S, Li E. 1998b. Dnmt2 is not required for de novo and maintenance methylation of viral DNA in embryonic stem cells. *Nucleic Acids Res 26*:2536-2540.

Panning B, Jaenisch R. 1998. RNA and the epigenetic regulation of X chromosome inactivation. *Cell 93*:305-308.

Patton JR. 1994. Pseudouridine formation in small nuclear RNAs. *Biochimie 76*:1129-1132.

Pradhan S, Bacolla A, Wells RD, Roberts RJ. 1999. Recombinant human DNA (cytosine-5) methyltransferase. I. Expression, purification, and comparison of de novo and maintenance methylation. *J Biol Chem 274*:33002-33010.

Rai K, Chidester S, Zavala CV, Manos EJ, James SR, Karpf AR, Jones DA, Cairns BR. 2007. Dnmt2 functions in the cytoplasm to promote liver, brain, and retina development in zebrafish. *Genes Dev 21*:261-266.

Randerath E, Chia LL, Morris HP, Randerath K. 1974. Transfer RNA base composition studies in Morris hepatomas and rat liver. *Cancer Res 34*:643-653.

Reid R, Greene PJ, Santi DV. 1999. Exposition of a family of RNA m(5)C methyltransferases from searching genomic and proteomic sequences. *Nucleic Acids Res 27*:3138-3145.

Robertson KD, Uzvolgyi E, Liang G, Talmadge C, Sumegi J, Gonzales FA, Jones PA. 1999. The human DNA methyltransferases (DNMTs) 1, 3a and 3b: coordinate mRNA expression in normal tissues and overexpression in tumors. *Nucleic Acids Res 27*:2291-2298.

Rottman FM, Bokar JA, Narayan P, Shambaugh ME, Ludwiczak R. 1994. N6-adenosine methylation in mRNA: substrate specificity and enzyme complexity. *Biochimie 76*:1109-1114.

Rozenski J, Crain PF, McCloskey JA. 1999. The RNA Modification Database: 1999 update. *Nucleic Acids Res 27*:196-197.

Schaefer M, Steringer JP, Lyko F. 2008. The Drosophila Cytosine-5 Methyltransferase Dnmt2 Is Associated with the Nuclear Matrix and Can Access DNA during Mitosis. *PLoS ONE 3*:e1414.

Schermelleh L, Haemmer A, Spada F, Rosing N, Meilinger D, Rothbauer U, Cardoso MC, Leonhardt H. 2007. Dynamics of Dnmt1 interaction with the replication machinery and its role in postreplicative maintenance of DNA methylation. *Nucleic Acids Res 35*:4301-4312.

Shigi N, Suzuki T, Tamakoshi M, Oshima T, Watanabe K. 2002. Conserved bases in the TPsi C loop of tRNA are determinants for thermophile-specific 2-thiouridylation at position 54. *J Biol Chem 277*:39128-39135.

Shoffner JM, Lott MT, Lezza AM, Seibel P, Ballinger SW, Wallace DC. 1990. Myoclonic epilepsy and ragged-red fiber disease (MERRF) is associated with a mitochondrial DNA tRNA(Lys) mutation. *Cell 61*:931-937.

Simos G, Tekotte H, Grosjean H, Segref A, Sharma K, Tollervey D, Hurt EC. 1996. Nuclear pore proteins are involved in the biogenesis of functional tRNA. *Embo J 15*:2270-2284.

Simpson L, Emeson RB. 1996. RNA editing. *Annu Rev Neurosci 19*:27-52.

Sprinzl M, Vassilenko KS. 2005. Compilation of tRNA sequences and sequences of tRNA genes. *Nucleic Acids Res 33*:D139-140.

Suzuki T, Suzuki T, Wada T, Saigo K, Watanabe K. 2002. Taurine as a constituent of mitochondrial tRNAs: new insights into the functions of taurine and human mitochondrial diseases. *Embo J 21*:6581-6589.

Takai D, Jones PA. 2002. Comprehensive analysis of CpG islands in human chromosomes 21 and 22. *Proc Natl Acad Sci U S A 99*:3740-3745.

Thiebe R, Zachau HG. 1968. A specific modification next to the anticodon of phenylalanine transfer ribonucleic acid. *Eur J Biochem 5*:546-555.

Timar E, Groma G, Kiss A, Venetianer P. 2004. Changing the recognition specificity of a DNA-methyltransferase by in vitro evolution. *Nucleic Acids Res 32*:3898-3903.

Tuck MT. 1992. The formation of internal 6-methyladenine residues in eucaryotic messenger RNA. *Int J Biochem 24*:379-386.

Tweedie S, Ng HH, Barlow AL, Turner BM, Hendrich B, Bird A. 1999. Vestiges of a DNA methylation system in Drosophila melanogaster? *Nat Genet 23*:389-390.

Vacher J, Grosjean H, Houssier C, Buckingham RH. 1984. The effect of point mutations affecting Escherichia coli tryptophan tRNA on anticodon-anticodon interactions and on UGA suppression. *J Mol Biol 177*:329-342.

van den Ouweland JM, Lemkes HH, Ruitenbeek W, Sandkuijl LA, de Vijlder MF, Struyvenberg PA, van de Kamp JJ, Maassen JA. 1992. Mutation in mitochondrial tRNA(Leu)(UUR) gene in a large pedigree with maternally transmitted type II diabetes mellitus and deafness. *Nat Genet 1*:368-371.

Walbott H, Auxilien S, Grosjean H, Golinelli-Pimpaneau B. 2007a. The carboxyl-terminal extension of yeast tRNA m5C methyltransferase enhances the catalytic efficiency of the amino-terminal domain. *J Biol Chem 282*:23663-23671.

Walbott H, Husson C, Auxilien S, Golinelli-Pimpaneau B. 2007b. Cysteine of sequence motif VI is essential for nucleophilic catalysis by yeast tRNA m5C methyltransferase. *Rna 13*:967-973.

Walsh CP, Chaillet JR, Bestor TH. 1998. Transcription of IAP endogenous retroviruses is constrained by cytosine methylation. *Nat Genet 20*:116-117.

Wilson AS, Power BE, Molloy PL. 2007. DNA hypomethylation and human diseases. *Biochim Biophys Acta 1775*:138-162.

Wion D, Casadesus J. 2006. N6-methyl-adenine: an epigenetic signal for DNA-protein interactions. *Nat Rev Microbiol 4*:183-192.

Wu JC, Santi DV. 1987. Kinetic and catalytic mechanism of HhaI methyltransferase. *J Biol Chem 262*:4778-4786.

Wyatt GR. 1950. Occurrence of 5-methylcytosine in nucleic acids. *Nature 166*:237-238.

Xie S, Wang Z, Okano M, Nogami M, Li Y, He WW, Okumura K, Li E. 1999. Cloning, expression and chromosome locations of the human DNMT3 gene family. *Gene 236*:87-95.

Yang W, Chendrimada TP, Wang Q, Higuchi M, Seeburg PH, Shiekhattar R, Nishikura K. 2006. Modulation of microRNA processing and expression through RNA editing by ADAR deaminases. *Nat Struct Mol Biol 13*:13-21.

Yoder JA, Bestor TH. 1998. A candidate mammalian DNA methyltransferase related to pmt1p of fission yeast. *Hum Mol Genet 7*:279-284.

Yoder JA, Walsh CP, Bestor TH. 1997. Cytosine methylation and the ecology of intragenomic parasites. *Trends Genet 13*:335-340.

Yu YT, Shu MD, Steitz JA. 1997. A new method for detecting sites of 2'-O-methylation in RNA molecules. *Rna 3*:324-331.

Zeviani M, Muntoni F, Savarese N, Serra G, Tiranti V, Carrara F, Mariotti C, DiDonato S. 1993. A MERRF/MELAS overlap syndrome associated with a new point mutation in the mitochondrial DNA tRNA(Lys) gene. *Eur J Hum Genet 1*:80-87.

Zhao X, Yu YT. 2004. Detection and quantitation of RNA base modifications. *Rna 10*:996-1002.

6 Acknowledgments

I would like to thank

Prof. Dr. Frank Lyko
for the supervision of my thesis, for always valuable and helpful comments on my work, and for the freedom to conduct part of my work at the IPMB in Heidelberg

PD Dr. Mark Helm
for accepting me as a guest in his group, for the great supervision and scientific discussions, and for the tremendous support

Prof. Dr. Christof Niehrs,
my external advisor, for always good counsel

Prof. Dr. Harald Herrmann-Lerdon
for being the referee of my thesis

Martin Hengesbach, Armine Hayrapetyan, and Heike Einberger
for introducing me to the tRNA methods and their great helpfulness concerning all questions

Tanja Musch, Tamara Fries, and Dagmar Wolf
for their assistance and support

Martin Hengesbach, Sascha Feuerhahn, and my mother for helpful comments and patient proof-reading of the manuscript

the lab members of the Division of Epigenetics of the DKFZ and of the AK Jäschke (IPMB Heidelberg) for the pleasant atmosphere at work

most of all, I would like to thank my family, my friends, and Sascha Feuerhahn who have always encouraged and supported me in every respect. Without you, this work would not have been possible.